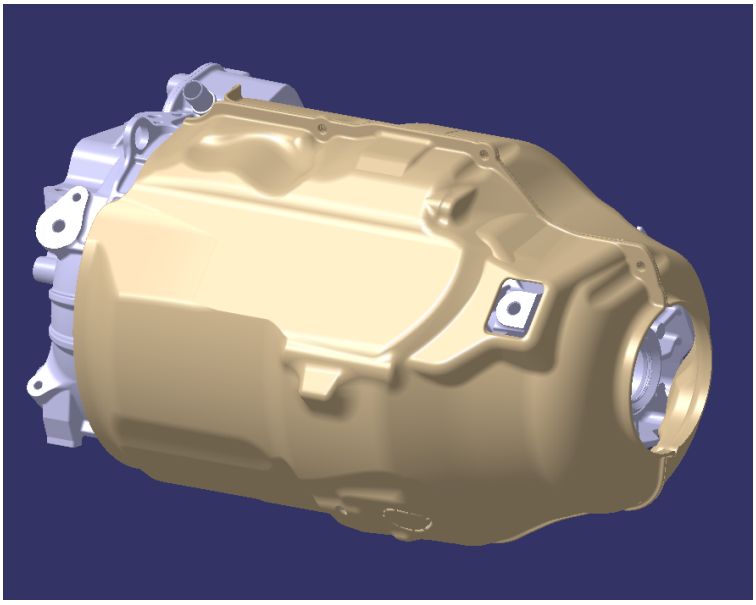

# Optimization of Encapsulation for Electric Drive Units

## An experimental approach to predict Insertion Loss

A thesis work carried out for the master's degree in Sound and Vibration Program by

Piyush Annigeri & Aditya Thombare

Department of Architecture and Civil Engineering, Applied Acoustics
CHALMERS UNIVERSITY OF TECHNOLOGY
Gothenburg, Sweden, 2021

Master's thesis 2021

# Optimization of Encapsulation for Electric Drive Units

Development of an empirical model to predict the Insertion Loss of encapsulations through an experimental approach

PIYUSH ANNIGERI
ADITYA THOMBARE


CHALMERS
UNIVERSITY OF TECHNOLOGY

Department of Architecture and Civil Engineering
*Division of Applied Acoustics*
at
Volvo Car Corporation, Gothenburg, Sweden
Chalmers University of Technology
Gothenburg, Sweden, 2021

Optimization of Encapsulation for Electric Drive Units
Development of an empirical model to predict the Insertion Loss of encapsulations through an experimental approach
PYUSH ANNIGERI
ADITYA THOMBARE



Supervisors: David Lennström, Volvo Car Corporation, Propulsion System NVH & Joel Rådberg, Volvo Car Corporation, Electric Transmission Integration
Examiner: Patrik Höstmad, Docent at Chalmers University of Technology, Division of Applied Acoustics

Master's Thesis 2021
Department of Architecture and Civil Engineering
Division of Applied Acoustics
Volvo Car Corporation
Chalmers University of Technology
SE-412 96 Gothenburg
Telephone +46 31 772 1000

Cover: Electric Drive Unit with an encapsulation

Typeset in LaTeX
Gothenburg, Sweden 2021

**Optimization of Encapsulation for Electric Drive Units**
Development of an empirical model to predict the Insertion Loss of encapsulations through an experimental approach.
PIYUSH ANNIGERI
ADITYA THOMBARE
Division of Applied Acoustics
Department of Architecture and Civil Engineering
Chalmers University of Technology

# Abstract

Considering from the environment stand point and usage, the trend of electric vehicles has been on the rise and is certainly developing as the future of automotive industry. With the increasing customer expectations on the comfort and driving experience, the noise, vibration and harshness (NVH) play an important role in the design and launch of a vehicle. With the advent of electric vehicles, the challenges are different when compared to a conventional internal combustion (IC) engine. The use of Electric Drive Units (EDU) makes the operation less noisy as compared to an IC engine, but it leads to other high frequency noises which are picked up by the human ears inside the cabin of the car. This makes the encapsulation of the EDU, an important part of the electric vehicle's NVH package.

The aim of this thesis is to investigate if, an empirical model can be built to predict the insertion loss by systematic variation of certain control parameters. The parameters considered are sound absorption coefficient ($\alpha$), sound transmission loss (dB) and percentage (%) of coverage of the encapsulation. In the first phase, certain configurations of foam layer, mass layer and carrier layer are built and are called as samples (35 samples). These samples are tested on the impedance tube and characterized for absorption coefficient and transmission loss values. In the second phase, five different encapsulations are built and tested on the EDU for insertion loss (IL) values along with percentage (%) coverage variation. The selection of samples for building the encapsulations from impedance tube results is based on variation of the values (good/average/poor) considering the end goal of model building. A high frequency driver with a hose is used as the noise source which is fed into the EDU exciting it internally. White noise is used to excite all frequency components with equal intensity. As it is an experimental approach, there are measurement uncertainties present and this has been addressed by performing repeatability study in order to achieve confidence and reliability on the results.

The results obtained from the EDU measurements lay the foundation to form an empirical equation through linear regression analysis. This equation will finally be used to predict the insertion loss of the encapsulations. In the future, this work will help to give a prior idea of the encapsulation performance and ensure that the end product is a cost effective and acoustically efficient EDU encapsulation.

**Keywords**: Optimization, Encapsulation, Electric drive unit(EDU), Impedance

tube, Instertion Loss (IL), Linear Regression, Insertion Loss prediction, Repeatability Study.

# Acknowledgements

We would like to thank Volvo Car Corporation (VCC) for giving us this opportunity to work and access the facilities to carry out our thesis work. We would like to thank our supervisors David Lennström and Joel Rådberg for guiding our research at VCC. Special thanks to Anders Ohlson from VCC and the entire NVH team who have supported us in every possible way to reach our goal. A special thanks to Tommy Holmström at VCC's Finmekanisk Verkstad for supporting us in the manufacturing stage of the thesis work. Last but not the least, we would like to express gratitude to our examiner Patrik Höstmad at Chalmers University of Technology for guiding and motivating us at different stages of the work and challenging us to think in all aspects through the entire duration.

Piyush Annigeri & Aditya Thombare, Gothenburg, June 2021.

# Contents

# List of Figures

# List of Tables

# 1
# Introduction

## 1.1 Background

An electric vehicle is powered by a source of energy e.g., a battery or a fuel cell, which converts the fuel to electrical energy powering the electric motors. The engine in an electric vehicle is called an electric drive unit (EDU). It consists of the assembly of the motors, transmission which is the gearbox with drive shafts and inverter which converts the battery's direct current (DC) to alternating current (AC). The power output from EDUs is very high (300 kW). For a plug in hybrid vehicle (PHEV), it is 200 kW which is a lot of electrical power output considering a car body.
As stated earlier, the customer expectations on the driving experience along with the stringent regulations, noise, vibration and harshness (NVH), play an important role in the design and launch of a vehicle. For electric vehicles, the challenges are different when compared to a conventional internal combustion (IC) engine. Acoustically speaking, in the IC engines, masking of high frequency sounds is possible which is not the case in electric vehicles. The EDU operates quieter than an IC engine but the operating RPM is higher when compared to IC engine. This causes the generation of orders in an electric vehicle and some of these orders at high frequency fail to get masked as the masking is majorly from the road and tire noise and not from the engine itself. These high frequency orders are clearly audible to the human ears in the car cabin at passenger and driver ear levels due to direct air borne sound transmission. This makes it an important issue to tackle and paves the way to work directly on the source with encapsulations.

### 1.1.1 Literature Review/Background Study

Based on the defined scope of work, experimental approach was a given. However, to build an understanding and to explore possibilities with simulation and testing, some previous work with the encapsulations both on electric drive-line and internal combustion engines was studied. The idea to try different combinations of materials with different layers was selected from a simulation based work [25]. It helped in conceiving different combinations of samples and to get an idea of the performance of the final encapsulation on insertion loss. To understand the topic in detail, cause of sound radiation in electric motors, SAE research paper [26] was studied. It gave an in depth understanding of the electromagnetic forces acting on the casing of the motor and the reason for their origin. Similarly, a master thesis work [27] was referred to understand air borne noise radiation from electrical machines. Along with this, major inputs were taken from Volvo internal literature [4] and [28] to

understand the existing design, the constraints, things worked on previously and tested before and some target points. This entire study along with the design of experiments technique gave this thesis work an approach which has been shared in detail with experiments.

### 1.1.2 Encapsulation

Encapsulation is a passive noise control layer or a covering added on the source to attenuate the air borne noise radiated by it. In this thesis work, the source is the electric drive unit (EDU). Most encapsulations are composed of the layers namely, the absorption layer, mass layer and/or carrier layer. The absorptive layer is made of foam whose sound absorption capacity is directly proportional to its thickness. The mass layer causes the sound transmission loss depending on the mass law applicable to sound waves and the carrier layer provides the rigidity and structural stiffness to the encapsulation which is added to simplify the process of mounting it on the EDU in the assembly line. Figure 1.1 is an example of one such encapsulation fitted on the EDU in an electric vehicle.

**Figure 1.1:** An existing encapsulation on an EDU [4]

### 1.1.3 Need for an Encapsulation

When compared to the IC engines, most of the low frequency idling and running noise is eliminated in an EDU. However, the motor and transmission together generate some orders of high frequencies in the range of 2 kHz to 5 kHz which bring an unpleasant noise to the driver ear level inside the cabin of the car. To tackle this air borne contribution form the source, one of the best possible approaches is to build an encapsulation around the source which targets the frequencies which lead to the air-borne sound radiation. There are certain limitations in a vehicle considering the thickness and size of the encapsulation. However, to tackle the frequency range in which the problem exists, the maximum thickness of the absorptive layer required for the sound absorption starts from 42 mm to fit a quarter wavelength for the complete absorption of a sound wave at 2 kHz. Similarly, the absorptive layer needs to be just 17 mm to fit a quarter wavelength of 5 kHz. To summarize, an encapsulation around the source makes it the best possible solution to tackle such problems for an electric powered vehicle.

### 1.1.4 Order in Machines

The Figure 1.2 shows a 3D color map which has frequency on the x-axis, RPM or speed on the y-axis and the amplitude of vibration velocity indicated by the color. Two important phenomena can be observed — the resonance and the orders. Resonance is the peak in frequency obtained by performing fast fourier transform (FFT) on the time signal. It remains constant and does not change with increasing speed. Order is the peak in the frequency which shifts linearly with increasing speed. These orders linearly increase with increasing RPM causing some low and high frequency noise radiation. As explained above, the RPM range in an electric vehicle is high and leads to tonal noise.

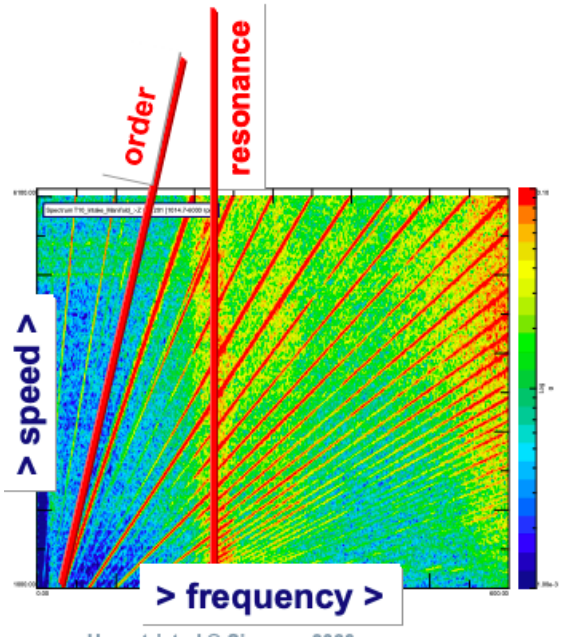


**Figure 1.2:** Order and Resonance [6]

In the Figure 1.3, the 3D color map of an electric vehicle run up is shown with and without encapsulation, which is measured at the driver ear level, hence in this case there is frequency on y-axis, RPM or speed on x-axis and amplitude of sound pressure level is indicated by the color. Here we can clearly notice some of the orders on the left hand side plot for example; order 48, 40, 32 to be exact. There is also the order 13, which comes from the transmission gear whine, which can be seen lightly as it is partially attenuated due to masking by road and wind noise. If compared with the plot on the right hand side, some of these orders are mitigated and also some completely disappear. This helps us to understand better, the significance of encapsulation. Here ERAD stands for electric rear axle drive.

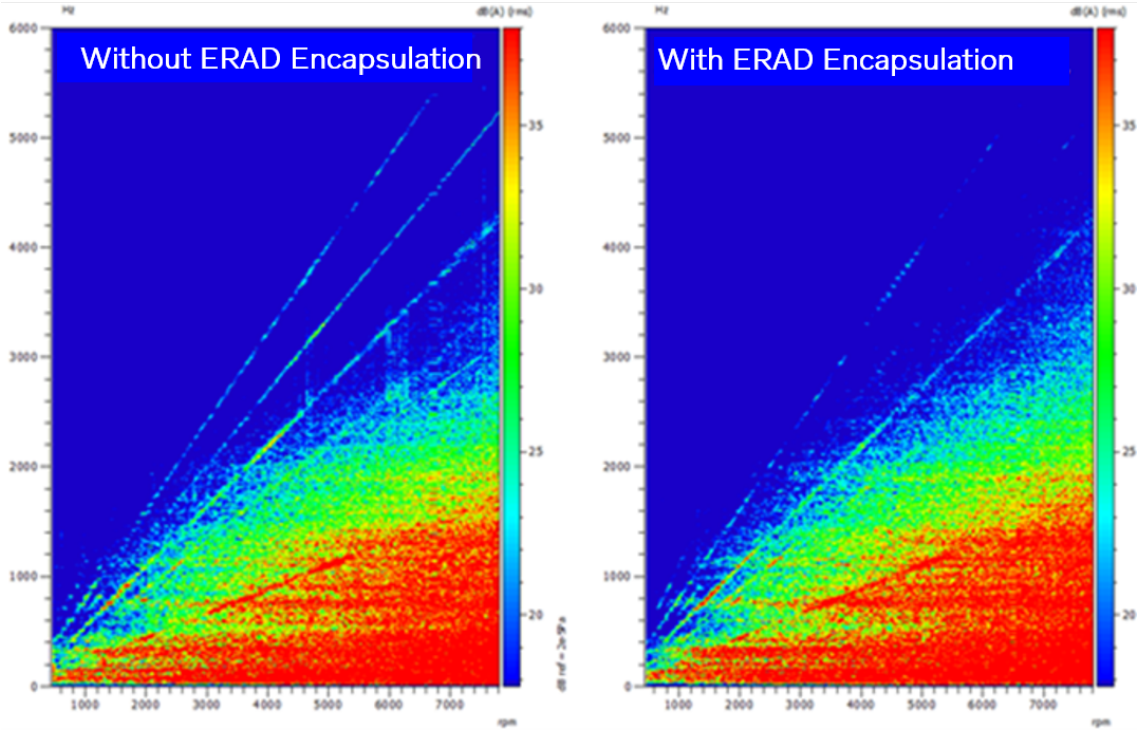


**Figure 1.3:** Effect of Encapsulation on EDU - Spectrogram [4]

In the Figure 1.4, the FFT of order 40 is shown. The blue line indicates shows the noise amplitude of an EDU without any encapsulation. The red line indicates an EDU considered in this work, an electric rear axle drive (ERAD) with an encapsulation. There is a noticeable difference of approximately >=5 dBA from 4 kHz to 7 kHz, again re-iterating the effectiveness of an encapsulation.

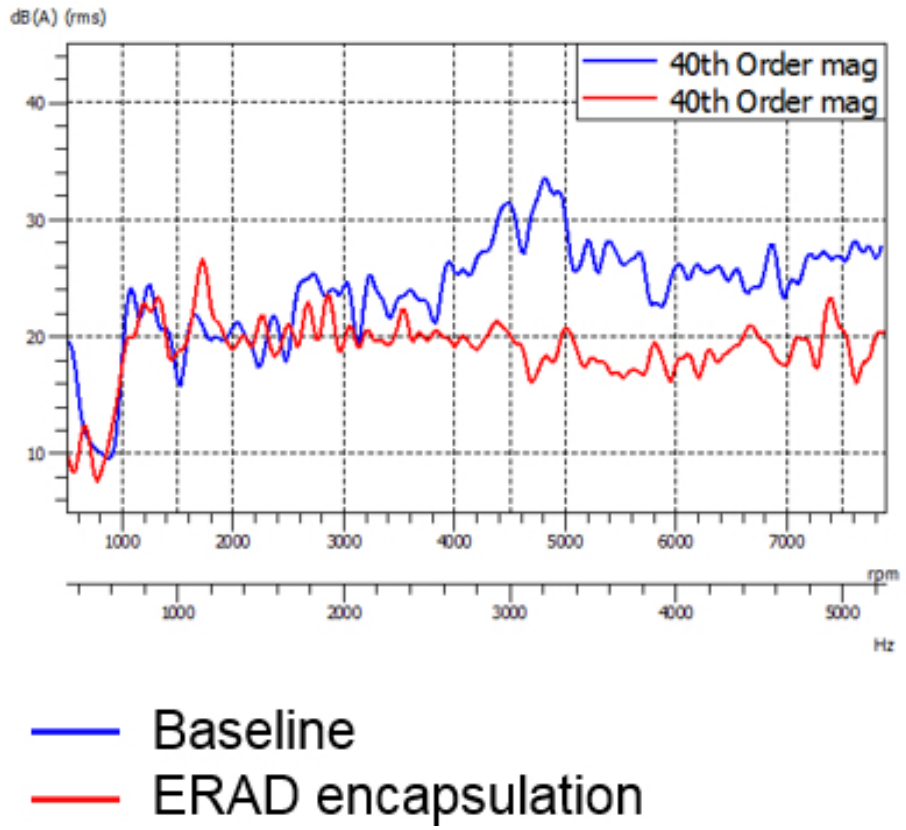


**Figure 1.4:** Effect of a Encapsulation on an EDU at 40th order [4]

## 1.2 Problem Inspection

The investigation will be done on an electric rear axle drive (ERAD). In this thesis work, the stator, rotor and the gear set is disassembled from the EDU casing and it will be excited using an external loudspeaker connected to a hose. The tests carried out will be according to ISO 3745 with 10 microphones in an anechoic environment to evaluate the sound pressure level (SPL) difference in dB(A) and calculate the acoustic transfer functions (ATF) at each microphone position. The frequency range of interest is 2 kHz to 6 kHz however data is generated from 100 Hz to 8 kHz.

### 1.2.1 Aim

In this thesis work, the investigation of the control parameters; absorption coefficient which depends on thickness and material properties, transmission loss which has dependency on mass and percentage of coverage will be evaluated in a systematic study to develop an optimized empirical model to predict insertion loss (IL) offered by an encapsulation. This would help to gain knowledge on how these parameters relate to the acoustic performance of the complete encapsulation and also give an idea on prediction of IL for future projects.

### 1.2.2 Limitations

The main reason for the EDU to be excited using a loudspeaker is to perform repeatability study based on the control parameters. Also, this way it is possible to perform a lot of experiments and also try different theoretical concepts. This would not have been possible if the EDU was run on a test bench connected to a dynamometer, due to limited testing capability in such an environment.

### 1.2.3 Collaboration

This research study is carried out in the anechoic chamber facility at Volvo Car Corporation (VCC), Gothenburg, Sweden. All the instrumentation and accessories needed for the the measurements was provided by VCC - NVH department.

### 1.2.4 Ethical Aspects

In this thesis work, experimental approach is followed to understand the effect of different material combinations used to build an encapsulation and its effect on the insertion loss from the encapsulation. The encapsulation is tested on an actual drive unit of an electric vehicle from Volvo cars. To minimise the risk of harm, the electric drive unit is excited using a loudspeaker connected by a hose pipe. The experimental approach involves handling of tools and to minimise the risk of harm from the handling, special care is taken to abide by the safety rules and take necessary precautions. At all steps during the work, informed advise and consent is taken before taking action. For confidential reasons, the final part of the work is partially disclosed as it remains proprietary to Volvo cars corporation. The methodology and approach taken during the entire work is an inspiration from previous work and internal brainstorming. The content expressed in the report is self generated and where ever necessary citations and links have been hyperlinked to address the authors/ websites.

# 2
# Theory

In this section, the relevant theory related to wave equations, plane and spherical, reflection of plane waves at boundaries, sound absorption and transmission loss and their dependencies. Finally, the concept of insertion loss has been discussed to give a build up for the consecutive sections and understand the methodology with the help of results.

## 2.1 Wave Equations and Solutions

In physics, sound is basically a vibration of particles which travels in the form of a wave through a particular medium like air or water for example. There are two basic types of waves — longitudinal and transverse waves. Sound waves travel in air as longitudinal waves in the form of compressions and rarefactions. While in solids, they also travel in the form of transverse waves. However in solids, for radiation, it is rather bending waves which are a combination of them are of interest. It is characterized by a frequency which has a specific wavelength.
Wave propagation in one dimension space is described by wave equation and is derived from the following 3 basic equations:

Equation of Continuity:

$$\frac{\partial \rho}{\partial t} + \rho_o \frac{\partial u}{\partial x} = 0 \tag{2.1}$$

where first term is the partial derivative of the density $\rho$, and second term is product of density of air and partial spacial derivative of velocity of the mass during the process of flow.
Equation of motion:

$$\rho_o \frac{\partial u}{\partial t} + \frac{\partial p}{\partial x} = 0 \tag{2.2}$$

Where the first term is product of density of air $\rho$ and partial time derivative of the particle velocity, second term is the partial spacial derivative of the pressure experienced by the particle in motion. Both the equations mentioned about talk about conservation and hence the sum of the two terms is equated with a zero.
Gas Equation:

$$\frac{\partial p}{\partial \rho} = \frac{\kappa R T}{M} \tag{2.3}$$

Where the term on left is the partial derivative of pressure with density, second term has the gas constant (R), T is the temperature of the gas, $\kappa$ is the mass of the gas

and M is the molar mass.
Wave Equation:

$$\frac{\partial^2 p}{\partial x^2} - \frac{1}{c^2}\frac{\partial^2 p}{\partial t^2} = 0 \tag{2.4}$$

The wave equation has terms double derivative of the pressure with respect to space as first, second term has the double time derivative of pressure and $1/c^2$ as a constant for proportionality.
where

$$c^2 = \frac{\kappa RT}{M} = \kappa\frac{p_o}{\rho_o} \tag{2.5}$$

### 2.1.1 Plane Wave

There are different solutions for the wave equation and one of the solutions is shown below for a plain wave.

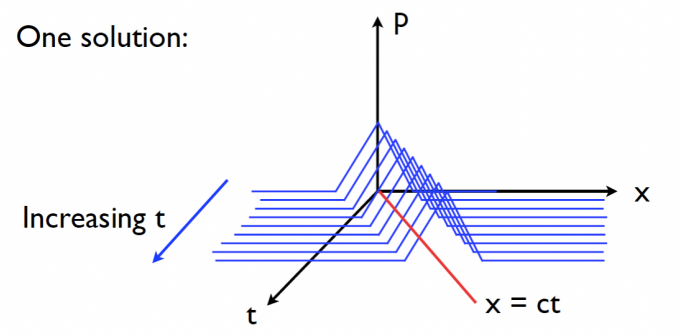


**Figure 2.1:** Solution to 1D wave equation[24]

Plain wave front in 2 dimensions (y,z) and propagating in the third dimension x is given by:

$$p(x,t) = \hat{p}cos(\omega(t \pm \frac{x}{c}) + \phi) = \hat{p}cos(\omega t \pm \frac{\omega}{c}x + \phi) \tag{2.6}$$

Where the equation above shows the pressure at a point in 2D space. Where x represents the spacial condition and t represents the point where the wave is in time. It represented by the magnitude of the particle at that point and phase. $\omega$ is angular frequency given by $2\pi f$, c is the speed of sound in the medium, $\phi$ is the phase.

$$p(x,t) = \hat{p}cos(\omega t \pm kx + \phi) \tag{2.7}$$

where, k is the wave number and is given by,

$$k = \frac{\omega}{c} \tag{2.8}$$

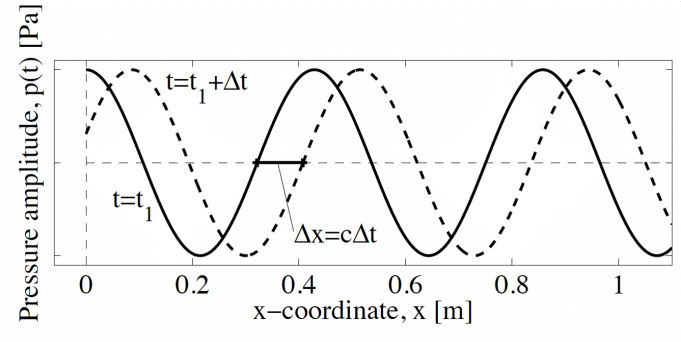


**Figure 2.2:** Solution to 1D wave equation[24]

In complex notations:

$$p(x,t) = Re[\hat{p}e^{j(\omega t \pm kx + \phi)}] = Re[\hat{p}e^{j\phi}e^{j\omega \pm kx}] = Re[\hat{p}e^{j(\omega t \pm kx}] \tag{2.9}$$

Where Re stands for the real part of the wave, which is comprised of sinusoidal behaviour and has some magnitude and phase.

### 2.1.2 Spherical wave

Spherical wave is a 3D presentation of the sound wave which propagates outward in all directions in the form of compressions and rarefactions. It is assumed that each point on the spherical wave surface acts as a source for origination of another wave front. It is represented by the equation:

$$\frac{\partial^2 p}{\partial r^2} + \frac{2}{r}\frac{\partial p}{\partial r} - \frac{1}{c^2}\frac{\partial^2 p}{\partial t^2} = 0 \tag{2.10}$$

It similar to the 2D wave but now the pressure is a variable term with respect to the distance of travel from the source position and that is how it is represented as a 3D wave. Here r is the instantaneous distance from the source.

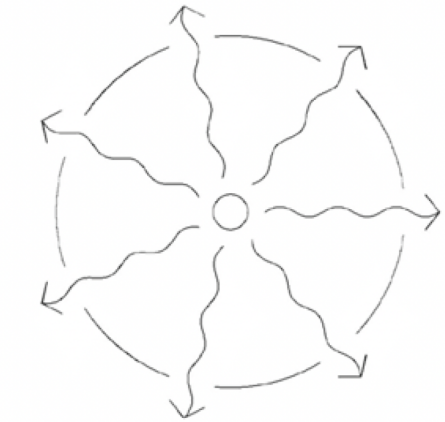

**Figure 2.3:** Spericl Wave Representation [23]

One of the solutions for a spherical wave is given by:

$$p(r,t) = \frac{1}{r} f\left(t \pm \frac{r}{c}\right) \tag{2.11}$$

Harmonic spherical wave only in the out going direction is given by:

$$p(r,t) = \frac{A+}{r} e^{j(\omega t - kr)} \tag{2.12}$$

Where the pressure is dependant on the distance and time and is represented by the amplitude, phase and also inversely dependant on the distance(r) from the source.

## 2.2 Reflection of Plane waves at Boundaries

When a plane wave hits a boundary, there is a change in impedance. As shown in Figure 2.4, there is a boundary at position x = 0 and the 2 separated regions have different impedances Z1 and Z2. When a incident pressure($p_i$) wave travels from medium having impedance Z1 and hits the boundary, part of it reflects ($p_r$) and part of it gets transmitted ($p_t$) into the other medium having impedance Z2. As shown in equation 2.9 the following equations are set-up to represent the waves in Figure 2.4 as follows:

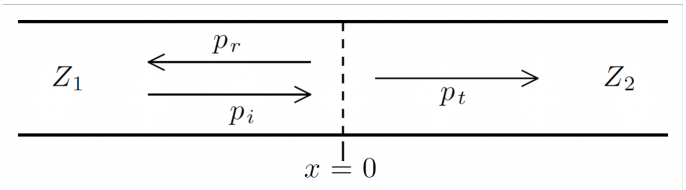


**Figure 2.4:** Plain wave travelling in a medium hitting a boundary [23]

$$p_i(x) = \hat{p}_i e^{-jk_1 x} \tag{2.13}$$

Where $p_i$ is the incident wave in the tube.

$$p_r(x) = \hat{p}_r e^{jk_1 x} \tag{2.14}$$

$p_r$ is the reflected wave in the tube.

$$p_t(x) = \hat{p}_t e^{-jk_2 x} \tag{2.15}$$

$p_t$ is the transmitted wave in the tube. Total field (x<0):

$$p_1(x) = p_i(x) + p_r(x) \tag{2.16}$$

Where, $p_1$ indicated the total pressure field on the left side of the tube.
Total field (x>0):

$$p_2(x) = p_t(x) \tag{2.17}$$

Where, $p_2$ is the total pressure field on the right side of the tube. Continuity condition at x = 0,
p1(x = 0) = p2(x = 0)
u1(x = 0) = u2(x = 0)

which gives the reflection factor '$r$', given by the amplitudes of the sound pressure of the reflected and incident wave [9] represented by the Equation 2.18:

$$r = \frac{\hat{p_r}}{\hat{p_i}} \tag{2.18}$$

The sound absorption coefficient is given by:

$$\alpha = 1 - |r^2| \tag{2.19}$$

Different conditions arise when a plane wave incidents on different boundaries. In Figure 2.5 a plane wave incident on a rigid boundary is shown. The impedance of Z2 of the rigid medium is very high when compared with air. Since $Z_2$»$Z_1$, the wave reflects and over a period of time forms a standing wave. The equations are shown below:

$|\mathrm{Z}_2| >> |\mathrm{Z}_1|; r = 1$

$Z_2$ is the impedance on the right side of the tube and $Z_1$ is the impedance on the left side of the tube. Since it is a rigid wall, the reflection factor is considered to be '$r$' = 1.

Total pressure field is formed at side x < 0:

$$p_1(x) = \hat{p_i}(e^{-jk_1x} + re^{jk_1x}) = \hat{p_i}(e^{-jk_1x} + e^{jk_1x}) = 2\hat{p_i}cos(k_1x) \tag{2.20}$$

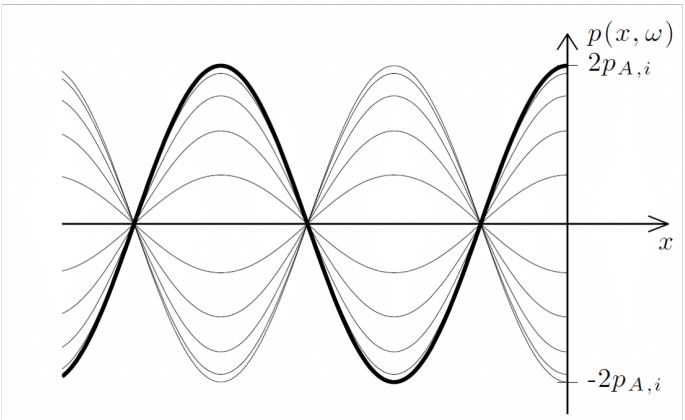


**Figure 2.5:** Plane wave: Normal incidence on Rigid boundary [23]

The second condition is the pressure release condition as shown in Figure 2.6 where the boundary to which the plane wave hits is free or rather open. It is exactly the opposite of being rigid and hence the reflection factor in this case is '$r$' = -1.
$|\mathrm{Z}_2| << |\mathrm{Z}_1|$

Total pressure field (x<0):

$$p_1(x) = \hat{p_i}(e^{-jk_1x} + re^{jk_1x}) = \hat{p_i}(e^{-jk_1x} - e^{jk_1x}) = -2j\hat{p_i}sin(k_1x) \tag{2.21}$$

Looking at the equation, it can be seen that it again forms a standing wave pattern but in a sinusoidal form.

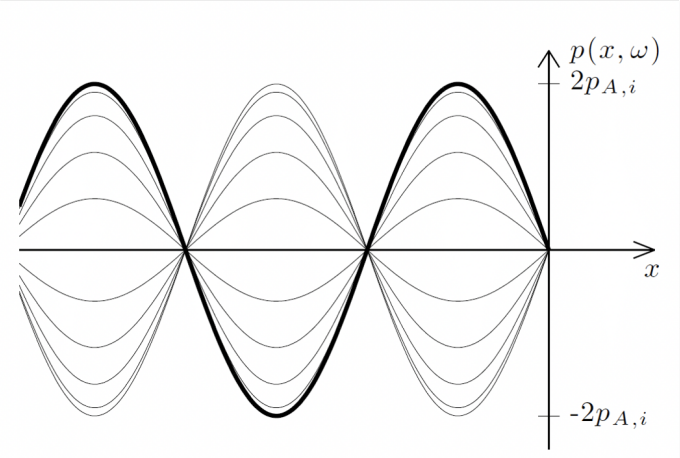


**Figure 2.6:** Plane wave: Normal incidence Pressure release condition [23]

This phenomenon can be observed when the impedance tube is used for measuring the sound absorption coefficient and transmission loss.

## 2.3 Impedance Tube Theory

### 2.3.1 Sound Absorption Coefficient — Two Microphone Transfer Function Method.

The measurements for sound absorption coefficient ('$\alpha$') using two-microphone transfer function method on the Impedance Tube are based upon the ISO 10354-2 and ASTM E1050 -12. The 2D representation of the test setup for each test sample is as shown in the Figure 2.7. The impedance tube for all the tests had an inner diameter '$d$' of 29mm (B&K small tube). The diameter of the tube decides the lower and upper limits of the operating frequency range. The upper limit is given by[17]

$$f_u < \frac{0.58 \cdot c_0}{d} \tag{2.22}$$

the upper limit is also dependant on the distance between the two microphones:

$$f_u < \frac{0.45 \cdot c_0}{s} \tag{2.23}$$

where s is the distance between the microphones.
The lower limit depends on the wavelength which are so long that the pressure at both microphones are quite similar, it is given by:

$$f_l > \frac{0.05 \cdot c_0}{s} \tag{2.24}$$

where '$c_0$' is the speed of sound [9]. The reason to use 29mm diameter tube was to have a wide operating frequency range of measurement from 500 Hz to 6.4kHz [7].

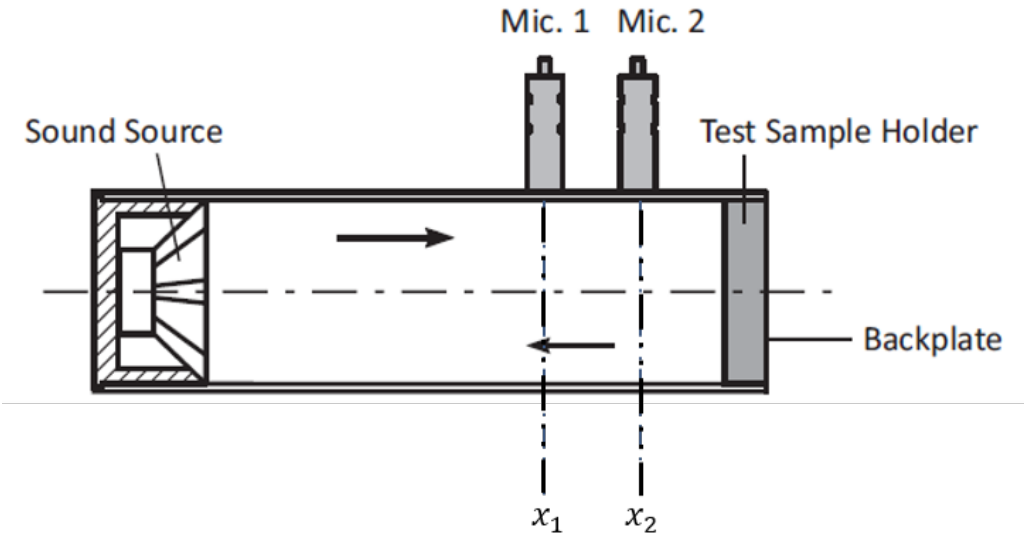


**Figure 2.7:** Microphone and Test Sample setup for Sound Absorption Coefficient measurements [7].

The sound source is located at one end of the tube and the test sample is placed on the opposite side of the tube backed by a rigid plate. White broad band noise was the sound source used for all the tests which generated stationary random sound waves. These waves propagate in the form of plane waves within the tube and hit the test sample and reflect. The end effect of the propagation, contact and reflection of these waves is a standing wave interference pattern. As explained earlier, this is due to the superposition of forward and backward travelling waves within the tube. This movement of the sound waves is monitored by the B&K LabShop software which is connected to the front end during the measurement. The two microphones on the tube measure the sound pressure and the software calculates the complex transfer function using a two-channel digital frequency analyzer which leads to the determination of the sound absorption, complex reflection coefficients and the normal acoustic impedance of the test sample. The sound absorption coefficient is a unitless quantity and always ranges between 0 and 1 and sometimes it is also expressed in percentage [7]. The useful frequency range of operation for data analysis in this case was from 500 Hz to 6.4 kHz.
Total sound pressure at any point in the tube is given by[16]:

$$P(x) = Ae^{-jkx} + Be^{jkx} \tag{2.25}$$

Where P(x) is the total sound pressure level at a certain position x, A and B are the amplitudes of the forward and backward travelling wave, $e^{-jkx}$ is forward travelling wave description in complex terms and $e^{jkx}$ is backward travelling wave description also in complex terms.
The transfer function between Mic-1 and Mic-2 is calculated by:

$$H_{12} = \frac{P(x_2)}{P(x_1)} = \frac{Ae^{-jkx_2} + Be^{jkx_2}}{Ae^{-jkx_1} + Be^{jkx_1}} = \frac{e^{-jkx_2} + Re^{jkx_2}}{e^{-jkx_1} + Re^{jkx_1}} \tag{2.26}$$

where,

$$R = \frac{B}{A} \tag{2.27}$$

is the reflection coefficient of the material.
If we solve for R, we get:-

$$R = \frac{e^{-jkx_2} - H_{12}e^{-jkx_1}}{H_{12}e^{jkx_1} - e^{jkx_2}} \tag{2.28}$$

Where $x_1$ is the distance from center of Mic.1 in figure 2.7 till the beginning of the test sample and $x_2$ is the center distance from Mic.2 till the beginning of the test sample. From this the sound absorption coefficient is calculated using equation 2.19.

### 2.3.2 Sound Transmission Loss — Four Microphone Transfer Matrix Method.

The calculation of Sound Transmission Loss (STL) is done by the four microphone transfer function method in the B&K Impedance Tube setup. It is based on the procedure described in ASTM E2611 - 17. The 2D representation of the test setup for each test sample is as shown in the Figure 2.8. The same tube type was used with an inner diameter of 29mm for all the tests which meant that the operating frequency range was from 500 Hz to 6.4kHz as discussed earlier[7].

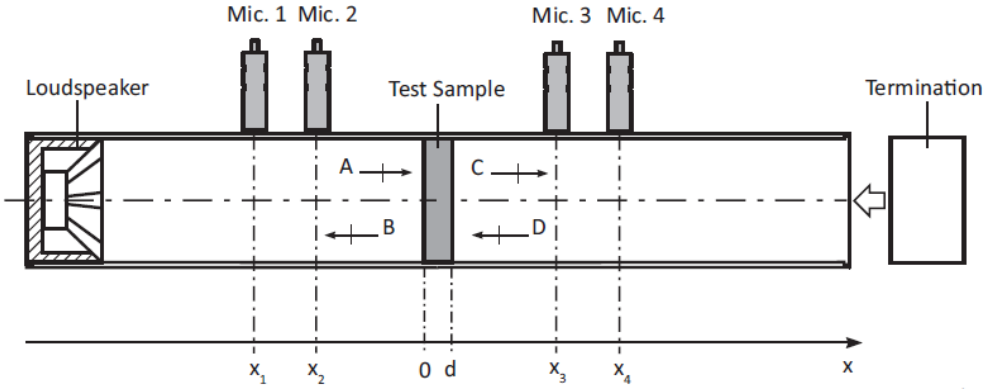


**Figure 2.8:** Microphone and Test Sample setup for Sound Transmission Loss measurements[7].

For the STL measurements, the sound source is the same loudspeaker as for sound absorption coefficient tests. The tube setup slightly changes as the tube now gets extended to introduce the two different boundary conditions for the sound waves in the tube which is necessary for STL tests. The Figure 2.8 shows the boundary conditions labelled as 'Termination'. In this case, the test sample is positioned in between the four microphones with the help of a holder. This holder divides the whole tube into two parts. The part with the loudspeaker is the source tube and the

other one is the receiving tube. The loudspeaker generates broadband, stationary plane waves which propagate as plane waves. These plane waves hit the test sample and some waves are reflected back into the source tube, some are absorbed by the test sample and some get transmitted through the test sample into the receiving tube. The transmitted waves are then incident on the tube termination where some get reflected and some exit the tube. Out of the four microphones, two are located in the source tube and the other two are in the receiving tube. These microphones measure the sound pressure and the B &K LabShop software calculates the complex transfer function using a four channel digital frequency analyzer which finally gives the transmission loss of the test sample [7].
From the transfer matrix method [18] both absorption coefficient and transmission loss of the material can be calculated. To do so, we use four microphones instead of two, and hence we need two load cases which forms a transfer matrix dependant on the load case for each side of the tube a forward and backward travelling wave is equations are setup as follows, which gives the pressure and velocity at the two ends of the sample as seen in figure 2.8.
To set up simply:

$$\begin{Bmatrix} p_1 \\ u_1 \end{Bmatrix} = \begin{Bmatrix} T_{11} & T_{12} \\ T_{21} & T_{22} \end{Bmatrix} \cdot \begin{Bmatrix} p_2 \\ u_2 \end{Bmatrix} \tag{2.29}$$

Where $p_1$, $u_1$ is the pressure and velocity to the left side of the tube and $p_2$ and $u_2$ is the pressure and velocity at the right side of the tube and the matrix with T elements is the transfer matrix which when solved gives the values for transmission loss and absorption coefficient.
Now there will be two load cases and for each load the equations of forward and backward travelling wave at each side of the test sample is given by A, B, C, D:

$$A = j \cdot \frac{H_{1,ref}e^{-jkl1} - H_{2,ref}e^{-jk(l1+s1)}}{2 \cdot \sin k \cdot s1} \tag{2.30}$$

where $H_1$ and $H_2$ are the transfer functions at point 1 and 2, k is the wave number give by

$$k = \frac{\omega}{c} \tag{2.31}$$

$l_1$ is distance between point $x_2$ and 0 marking in figure 2.8, $s_1$ is the distance between the Mic1 and Mic2.

$$B = j \cdot \frac{H_{2,ref}e^{jk(l1+s1)} - H_{1,ref}e^{jkl1}}{2 \cdot \sin k \cdot s1} \tag{2.32}$$

$$C = j \cdot \frac{H_{3,ref}e^{jk(l2+s2)} - H_{4,ref}e^{jkl2}}{2 \cdot \sin k \cdot s2} \tag{2.33}$$

where $H_3$ and $H_4$ are the transfer functions at point 3 and 4, $l_2$ is distance between point $x_3$ and 0 marking in figure 2.8, $s_2$ is the distance between the Mic3 and Mic4.

$$D = j \cdot \frac{H_{4,ref}e^{-jkl2} - H_{3,ref}e^{-jk(l2+s2)}}{2 \cdot \sin k \cdot s2} \tag{2.34}$$

Now, pressures and particle velocities at the two ends of the test sample is given by:

$$p_0 = A + B \tag{2.35}$$

$$u_0 = \frac{(A - B)}{\rho \cdot c} \tag{2.36}$$

$$p_d = C \cdot e^{-jkd} + D \cdot e^{jkd} \tag{2.37}$$

$$u_d = \frac{(C \cdot e^{-jkd} + D \cdot e^{jkd})}{\rho \cdot c} \tag{2.38}$$

Where $p_0$, $u_0$ are the pressure and particle velocities to the left of the test sample, before the 0 marking in the figure 2.8. And $p_d$ and $u_d$ are the pressure and particle velocities to the right side of the test sample after the point d marking in the 2.8. d is the thickness of the test sample.
Now the four pole matrix for calculation of the unknown variables is given by:

$$T = \begin{bmatrix} \frac{p_{0a} \cdot u_{db} - p_{0b} \cdot u_{da}}{p_{da} \cdot u_{db} - p_{db} \cdot u_{da}} & \frac{p_{0b} \cdot u_{da} - p_{0a} \cdot u_{db}}{p_{da} \cdot u_{db} - p_{db} \cdot u_{da}} \\ \frac{u_{0a} \cdot u_{db} - u_{0b} \cdot u_{da}}{p_{da} \cdot u_{db} - p_{db} \cdot u_{da}} & \frac{p_{da} \cdot u_{0b} - p_{db} \cdot u_{0a}}{p_{da} \cdot u_{db} - p_{db} \cdot u_{da}} \end{bmatrix} \tag{2.39}$$

Where subscripts a and b indicate the 2 load cases.
From this the transmission loss of the test sample is calculated by:

$$TL = 20 \cdot \log \left| \frac{1}{2} \cdot (T_{11} + \frac{T_{12}}{\rho c} + \rho c \cdot T_{21} + T_{22}) \right| \tag{2.40}$$

## 2.4 Effect of individual measurement parameters

The parameters used in the study are — thickness, mass, absorption coefficient ($\alpha$) transmission loss (TL) and percentage of coverage. Out of these parameters mass has a direct effect on the transmission loss character and thickness has a direct effect on the absorption coefficient. Hence these 4 parameters are clubbed into 2 parameters i.e. $\alpha$ and TL in which the mass and thickness is characterized in an experimental manner in a impedance tube to get the final combinations for our measurements. Percentage of coverage is one of the parameters which is tested in the later stages of the experiment directly on the test object.

### 2.4.1 Sound Absorption Coefficient

There are different types of absorbers that play an important role in sound absorption. Typically, the types are porous absorbers and Helmholtz resonators.
To achieve a high sound absorption, the sound field in the absorber should be subjected to high losses and the impedance of the absorber has to be as close as possible to the incident sound field.

There are some naturally available absorbers but some are built specifically based on the application. In this thesis work, experimentation was done with an existing inventory of porous absorbing materials - polyurethane foam (PU) and felt materials of different thicknesses keeping in mind the practical constraints.
In the Figure 2.9, the effect of increasing foam thickness has been demonstrated in which foam '$a$' has minimum thickness and foam '$c$' has maximum thickness. It can be seen that as the thickness increases, the absorption in the low and mid frequency region increases drastically. It is clear that the thickness has a direct relation to the sound absorption. A thicker foam has a better performance over a wider frequency range.

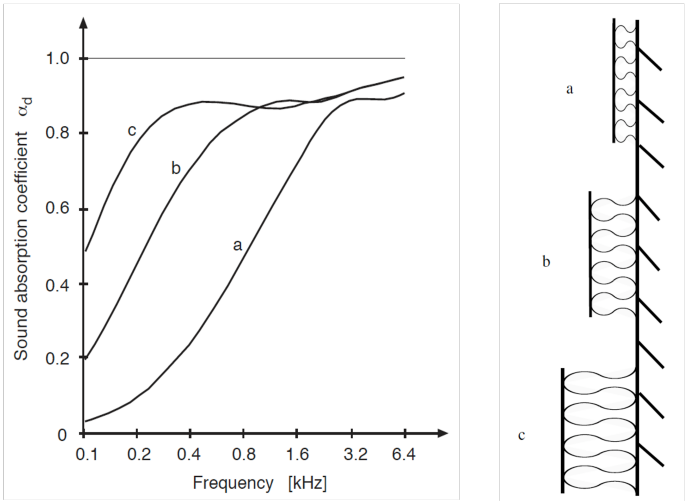


**Figure 2.9:** Effect of Thickness on Absorption [21]

This concept is further elaborated by Figure 2.10. It can be said that if a quarter wavelength of a particular frequency can be absorbed by the absorbing material, then all the frequencies above that frequency are absorbed completely and below that frequency, the absorption gets lower. Figure 2.10 shows reflection from wall and how standing wave pattern is formed, also it shows frequencies of different wavelength and what a quarter wavelength means.

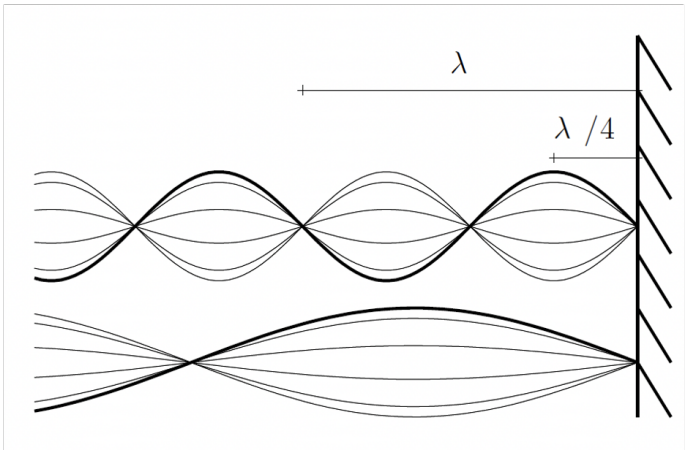


**Figure 2.10:** Reflection of different frequencies from a rigid surface [21]

In the Figure 2.11, the effect of increasing air flow resistivity of the material is shown on its sound absorption coefficient. Air flow resistivity is defined as the resistance to the air flow through the material and defines the permeability through any porous material. Higher the air flow resistance, lesser the air permeability and hence sound waves cannot enter which makes the sound absorption lower. But, the sound absorption increases to a certain extent when air flow resistance is increased as seen in the Figure 2.11. It is seen that it limits after a certain point and is almost constant at higher frequencies above 1.6 kHz. In general, there are open and closed cell PU foams which have a defined set of air flow resistivity making them good absorbers. In this thesis, experimentation was done with both open and closed cell foam. However, for typical absorption requirements, an open cell foam is preferred than a closed cell foam as it gives better air flow resistance. a, b, c, d, e, f are absorbing materials against a rigid wall having same area and thickness but different air flow resistances in increasing order from a to e.

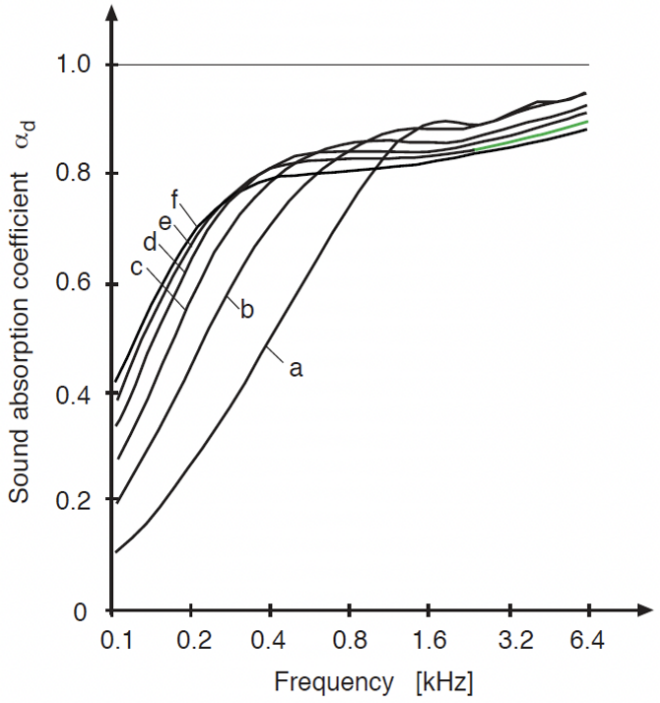


**Figure 2.11:** Effect of Air Flow resistivity on Absorption [21]

### 2.4.2 Sound Transmission Loss

Sound Transmission loss is basically the reduction of energy of a sound wave when it passes through a medium or a boundary which is quantified as the transmitted wave. The higher the value of the sound transmission loss coefficient, the better is the effectiveness of a particular boundary. It is given by the equation:

$$TL = 10 \log \left( \frac{W_i}{W_t} \right) \tag{2.41}$$

It is expressed in decibels (dB), where $W_i$ is the incident power and $W_t$ is the transmitted power.

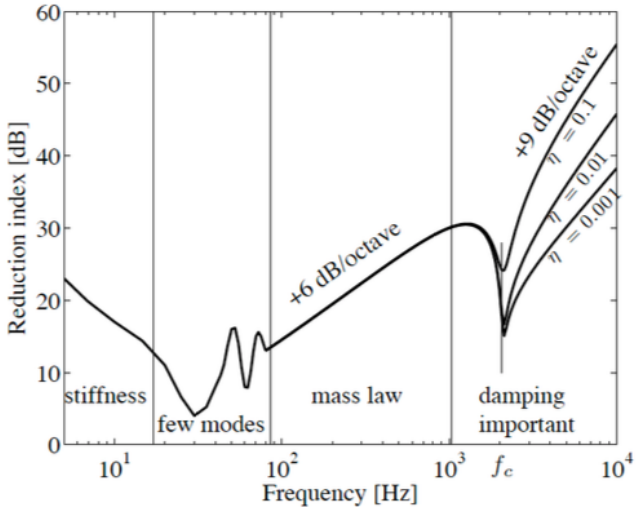


**Figure 2.12:** Effect of mass on Transmission Loss from a single wall or in general any material.[22]

Figure 2.12 shows a typical behaviour of a partition when air borne sound travels across it. It is characterized by different regions. The first one is the stiffness region, where the behaviour of the wall is governed by the stiffness of the wall imagining it to be a mass-spring system. The next region is the resonance region, where usually the natural frequencies of the wall match with the frequency of the incoming sound wave and it radiates sound or vibrates which results in poor transmission loss (TL) represented by the dips in the Figure 2.12. The dips are usually in the low frequency region and hence the sound waves are transmitted as vibrations. The next is the mass region, where the wall shows good TL character and the TL increases by 6 dB per doubling of mass. However, there are some cases where some materials do not behave this law and they are considered to be exceptions and studied carefully at the time of application [14]. The TL increases till the critical frequency of the wall is reached where the speed of sound in air is equal to the speed of sound in the structure. At this frequency, the structure again radiates sound and hence a dip can be seen. This usually happens in the high frequency region and depends on the Young's modulus, partition thickness and density of the partition material. Critical frequency is given by:

$$f_c = \frac{c_o^2}{2\pi}\sqrt{\frac{m''}{B}} = 6.4.10^4 \frac{1}{h}\sqrt{\frac{\rho}{E}} \tag{2.42}$$

Where m" is mass per unit length of the partition, and B is the bending stiffness and is given by

$$B = E.I = E.\frac{bh^3}{12} \tag{2.43}$$

Above the critical frequency the TL behaviour of the partition improves and we can see a 9 dB increase in the TL per doubling of mass.

### 2.4.3 Area of Percentage Coverage

This parameter is more general and is straight-forward considering the understanding or effect. In the Figure 2.13, y-axis on the right shows the percentage open area, y-axis on the left side shows the effective sound reduction in dB and x-axis shows the sound reduction of the encapsulation in dB. x-axis shows the absolute reduction from the encapsulation and y-axis on the left side gives the actual or effective reduction on the actual electric f=drive unit. It is clearly seen that, the lesser the percentage of open area, the better is the effective sound reduction.

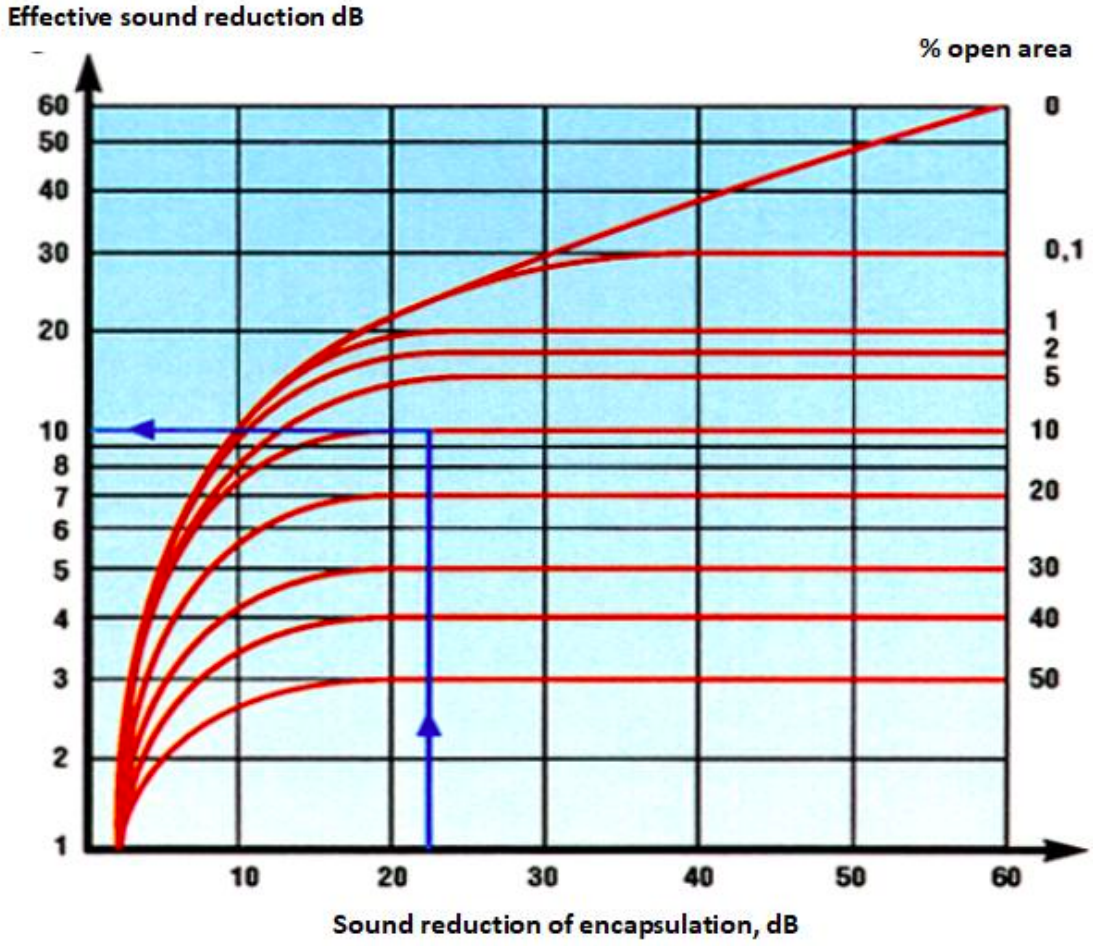


**Figure 2.13:** Effect of percentage(%) of coverage [4]

In the electric drive unit considered for this thesis work, there are some mandatory openings which have to be considered for the heat exchanger ducts and electric wire harness. However, in this study, a 100% coverage covers the entire object and then there are some modifications done on the encapsulation to study and verify the effect and take it into consideration for the model building process.

## 2.5 Concept of Insertion Loss

Theoretically insertion loss is the ratio of transmitted power with isolation and transmitted power without isolation [20]. Given by:-

$$IL = 10 \cdot \log\left(\frac{P_T}{P_R}\right) \tag{2.44}$$

Where $P_T$ is the transmitted power with isolation and $P_R$ is the transmitted power without isolation.

However in our case, instead of calculating the power, we are taking the average pressure of 10 microphones used to get single value, with and without the encapsulation, and then simply taking the difference as shown below:

$$IL = SPL_{withoutencapsulation} - SPL_{withencapsulation} \tag{2.45}$$

Absolute insertion loss value will be calculated using the measurement data.
To verify the theoretical calculations of insertion, calculation of sound power in anechoic conditions is important. This is given by:

$$L_W = L_P + 10 \cdot log\frac{S_1}{S_0} + C_1 + C_2 + C_3 \tag{2.46}$$

Where, $L_P$ is the time averaged sound pressure level for the noise source under test in decibels. $S_1$ is the area of the spherical measurement surface in square meters and $S_0$ is 1 square meters. $C_1$ is the reference quantity correction, in decibels, to account for the different reference quantities used to calculate decibel sound pressure level and decibel sound power level, and is a function of the characteristic acoustic impedance of the air under the meteorological conditions at the time and place of the measurements. $C_2$ is the acoustic radiation impedance correction, in decibels, to change the actual sound power relevant for the meteorological conditions at the time and place of the measurement into the sound power under reference meteorological conditions. $C_3$ is the correction for air absorption, in decibels, at specific frequencies. This is taken from the ISO 3745:2012(E) measurement standard [29]. The formula's for the constants can be looked up in standard for finally evaluating the sound power level from the EDU with and without encapsulation. This ratio is further evaluated to get the insertion loss values.

# 3
# Methods

## 3.1 Design of Experiments

The term "Design of Experiments" or "DoE" is broadly defined as a systematic statistical approach to a particular challenge by planning, performing and analyzing the experimental results by closely observing the relation that lies among the critical parameters that govern the process [10]. Simply put, the factors that control the experiments are evaluated. There are various approaches under DoE and in this report, the Factorial and the Taguchi methods are discussed.
In order to understand the Taguchi method, it is important to know the Factorial approach from which the Taguchi method is derived and modified to give more efficient results with an elegant methodology.

### 3.1.1 Factorial Method

The Factorial method was introduced by the British statistician Ronald Fisher. He came up with this approach and applied in the agricultural field in order to study the effects of the different factors which affected the production of the best crop[12]. For example, in this thesis work, the way to achieve a significant insertion loss is with the help of an encapsulation on the EDU. The Insertion loss is governed mainly by the absorption coefficient of the foam or felt layers, transmission loss of the mass layer and the percentage of coverage of the total encapsulation. So, there are three parameters which determine the Insertion loss. These three parameters again have three levels in their magnitude which cause the variance in the final insertion loss. So, for each type of combination of foam, mass and percentage coverage, the factorial method suggests to carry out $3^3$ tests, i.e, 27 tests. The base '3' represents the three factors governing the insertion loss and the power '3' represents the three magnitude levels of the three factors. The power will increase as the number of magnitude levels increase depending on different experiments. For the tests in this thesis work, it was decided that all the 27 tests for a combination of encapsulation were not critical depending on the levels of magnitude and hence the attention turned towards using the Taguchi method.

### 3.1.2 Taguchi Method

The Taguchi method is a fractional factorial method which considers the critical experiments among the given set of governing factors. This method considers the

interactions related to the selected design parameters and focuses more on the absolutely critical experiments or trials to be performed [11]. It introduces a concept of orthogonal array which helps in deciding the combinations of the selected design parameters for the critical experiments. This array is designed such that for each level of a particular parameter, all the other levels of the remaining parameters are tested at least once [12]. The design of the orthogonal array depends on the number of parameters and their levels. The way to obtain the orthogonal array for an experiment is given by the formula [13]

$$N = L \cdot M \tag{3.1}$$

where 'N' is the number of experiments, 'L' is the number of levels and 'M' is the number of times each level of each parameter tested.
In this thesis work, as there are three levels for the design or governing parameters and they are intended to be tested at least once for the remaining parameters, L = 3 and M = 3 will give the total experiments to be equal to 9 [13]. This approach was not fully satisfactory for this thesis work as the material combinations to be used in the experiments demanded a different way of designing the experiments with a touch of Taguchi method to it and the method adopted for the final experiments is explained in the next section.

## 3.2 Adopted Design of Experiments

As it was mentioned earlier, the foam or felt layers will be responsible for the sound absorption and the mass layer for the sound transmission loss, it was important to carry out the experiments which made sure that each type of foam or felt is tested for all the other types of mass layers and this was the approach that was adapted to carry out the experiments with the material bank available.

### 3.2.1 Material Bank

The materials used in this thesis work for determining one or more efficient combinations for significant Insertion Loss properties are listed in the below tables.

**Table 3.1:** Types of Foam.

| Types of Foam | |
|---|---|
| Type/Make | Mass per unit area)kg/m$^2$ |
| Sundquist LF301DX | 0.30 |
| Sundquist LF301DX | 0.36 |
| Sundquist LF301DX | 0.50 |
| Nitto EPDM Foam | 0.99 |
| Felt | 0.80 |
| Felt | 1.17 |

**Table 3.2:** Types of Mass Layers.

| Types of Mass Layers | |
|---|---|
| Type/Make | Mass per unit area)kg/m$^2$ |
| Antiphon | 1.81 |
| EPDM | 0.94(lowest) |
| EPDM | 1.50 |
| EPDM | 2.27 |
| Acublok | 5.40(highest) |

**Table 3.3:** Pre-built Foam+Mass Layers.

| Pre-built Foam+Mass | | | |
|---|---|---|---|
| Foam Thickness | Mass Layer Thickness | Total Thickness | Mass per unit area)kg/m$^2$ |
| 10mm | 2mm | 12mm | 4.80 |
| 20mm | 1.2mm | 21.2mm | 5.20 |

The Carrier layer having a mass per unit area of 2.56 kg/m$^2$, is the outermost layer for all the material combinations. It provides the structural stiffness and shape to the final encapsulations to be built. In most of the practical scenarios, the carrier is used as it has a relatively high area weight. It is 3D printed using polypropylene as it is considered to be light, water-tight and durable. Polypropylene also eases the process of manufacturing the complex shapes and curvatures.

Using all the above listed materials, the total number of test samples turned out to be 32 with all the possible material combinations. The sequence of the materials arranged in a test sample was based on a simple concept. When an encapsulation is mounted on an EDU in real scenarios, the foam or felt is always facing the surface of the EDU and hence, the test samples also had their first layer as the foam or felt, then comes the mass layer and then the outermost layer which is the carrier. The noise source for the test samples in the Impedance Tube was white noise. The Impedance tube used had a tube diameter of 29mm and all the test samples too had to have a diameter of approximately 29mm. In fact, all the test samples had a diameter of nearly 28.8mm. The 0.2mm difference showed up because the samples had to be sand grinded after they were produced in order to ensure proper fit with the circumference of the impedance tube. The testing methods follow in the upcoming sections. A test sample is shown in the Figure 3.1 .

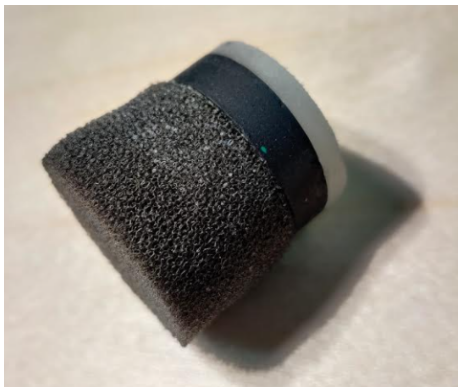

**Figure 3.1:** A Test Sample.

The test samples along with their material configuration are as shown in the Figure 3.2.

| Sample Number | 1 | 2 | 3 | 4 | 5 |
|---|---|---|---|---|---|
| Absorptive Layer | LF301DX-5mm | LF301DX-5mm | LF301DX-5mm | LF301DX-5mm | LF301DX-5mm |
| Mass Layer | antiphon-3mm | 0.8mm EPDM | 1mm EPDM | 2mm EPDM | acublok-2.5mm |
| Carrier Layer | carrier -3.2mm | carrier -3.2mm | carrier -3.2mm | carrier -3.2mm | carrier -3.2mm |
| | | | | | |
| Sample Number | 6 | 7 | 8 | 9 | 10 |
| Absorptive Layer | LF301DX-10mm | LF301DX-10mm | LF301DX-10mm | LF301DX-10mm | LF301DX-10mm |
| Mass Layer | antiphon-3mm | 0.8mm EPDM | 1mm EPDM | 2mm EPDM | acublok-2.5mm |
| Carrier Layer | carrier -3.2mm | carrier -3.2mm | carrier -3.2mm | carrier -3.2mm | carrier -3.2mm |
| | | | | | |
| Sample Number | 11 | 12 | 13 | 14 | 15 |
| Absorptive Layer | LF301DX-15mm | LF301DX-15mm | LF301DX-15mm | LF301DX-15mm | LF301DX-15mm |
| Mass Layer | antiphon-3mm | 0.8mm EPDM | 1mm EPDM | 2mm EPDM | acublok-2.5mm |
| Carrier Layer | carrier -3.2mm | carrier -3.2mm | carrier -3.2mm | carrier -3.2mm | carrier -3.2mm |
| | | | | | |
| Sample Number | 16 | 17 | 18 | 19 | 20 |
| Absorptive Layer | Nitto EE-1000~ 9mm | Nitto EE-1000~ 9mm | Nitto EE-1000~ 9mm | Nitto EE-1000~ 9mm | Nitto EE-1000~ 9mm |
| Mass Layer | antiphon-3mm | 0.8mm EPDM | 1mm EPDM | 2mm EPDM | acublok-2.5mm |
| Carrier Layer | carrier -3.2mm | carrier -3.2mm | carrier -3.2mm | carrier -3.2mm | carrier -3.2mm |
| | | | | | |
| Sample Number | 21 | 22 | 23 | 24 | 25 |
| Absorptive Layer | Felt - 10mm | Felt - 10mm | Felt - 10mm | Felt - 10mm | Felt - 10mm |
| Mass Layer | antiphon-3mm | 0.8mm EPDM | 1mm EPDM | 2mm EPDM | acublok-2.5mm |
| Carrier Layer | carrier -3.2mm | carrier -3.2mm | carrier -3.2mm | carrier -3.2mm | carrier -3.2mm |
| | | | | | |
| Sample Number | 26 | 27 | 28 | 29 | 30 |
| Absorptive Layer | Felt - 15mm | Felt - 15mm | Felt - 15mm | Felt - 15mm | Felt - 15mm |
| Mass Layer | antiphon-3mm | 0.8mm EPDM | 1mm EPDM | 2mm EPDM | acublok-2.5mm |
| Carrier Layer | carrier -3.2mm | carrier -3.2mm | carrier -3.2mm | carrier -3.2mm | carrier -3.2mm |
| | | | | | |
| Sample Number | 31 | 32 | | | |
| Foam+Mass Layer | Foam+Mass-12mm | Foam+Mass-12mm | | | |
| Carrier Layer | carrier -3.2mm | carrier -3.2mm | | | |

**Figure 3.2:** Test Samples with Material Configuration.

The 32 test samples were produced with a strong support from Finmekanisk Verkstad at VCC and they are shown in the Figure 3.3.

**Figure 3.3:** 32 Test Samples.

These 32 samples were divided into groups based on the type of foam layer that they were configured of and they are shown in the Figure 3.4.

| Group | Absorptive Layer | Mass Layer | Carrier Layer |
|---|---|---|---|
| 1 | Sundquist 5mm Foam | Antiphon 3mm | Carrier 3.2mm |
| | | EPDM 0.8mm | |
| | | EPDM 1mm | |
| | | EPDM 2mm | |
| | | Acublok 2.5mm | |
| 2 | Sundquist 10mm Foam | Antiphon 3mm | |
| | | EPDM 0.8mm | |
| | | EPDM 1mm | |
| | | EPDM 2mm | |
| | | Acublok 2.5mm | |
| 3 | Sundquist 15mm Foam | Antiphon 3mm | |
| | | EPDM 0.8mm | |
| | | EPDM 1mm | |
| | | EPDM 2mm | |
| | | Acublok 2.5mm | |
| 4 | Nitto 9mm Foam | Antiphon 3mm | |
| | | EPDM 0.8mm | |
| | | EPDM 1mm | |
| | | EPDM 2mm | |
| | | Acublok 2.5mm | |
| 5 | Felt 10mm | Antiphon 3mm | |
| | | EPDM 0.8mm | |
| | | EPDM 1mm | |
| | | EPDM 2mm | |
| | | Acublok 2.5mm | |
| 6 | Felt 15mm | Antiphon 3mm | |
| | | EPDM 0.8mm | |
| | | EPDM 1mm | |
| | | EPDM 2mm | |
| | | Acublok 2.5mm | |

**Figure 3.4:** Sample Groups.

**NOTE: All Sundquist Foams in the above figure and in the entire report are LF301DX.**
The two pre-built layers of foam and mass were put separately in Group 7.

The foam, felt, mass layers and the carrier layers were weighed individually to understand the weight variation in the individual samples. The weight of each layer is shown in the Tables 3.4 and 3.5.

**Table 3.4:** Absorptive Layers.

| Absorptive Layers | | |
|---|---|---|
| Type | Thickness(mm) | Weight in grams(g) |
| Sundquist LF301DX | 5mm | 0.2g |
| Sundquist LF301DX | 10mm | 0.24g |
| Sundquist LF301DX | 15mm | 0.33g |
| Nitto EPDM Foam | 9mm | 0.66g |
| Felt | 10mm | 0.53g |
| Felt | 15mm | 0.77g |

**Table 3.5:** Mass Layers.

| Mass Layers | | |
|---|---|---|
| Type | Thickness(mm) | Weight in grams(g) |
| Antiphon | 3mm | 1.2g |
| EPDM | 0.8mm | 0.62g(lightest) |
| EPDM | 1mm | 0.99g |
| EPDM | 2mm | 1.5g |
| Acublok | 2.5mm | 3.57g(heaviest) |

The weight of the carrier layer was measured to be 1.69 grams.

The weight of individual samples are listed in the Tables 3.6 and 3.7.

**Table 3.6:** Weight of Individual Samples 1 to 16.

| Sample Weight in grams(g) | |
|---|---|
| Sample Number | Weight in grams(g) |
| Sample 1 | 3.25g |
| Sample 2 | 2.42g |
| Sample 3 | 2.76g |
| Sample 4 | 3.08g |
| Sample 5 | 5.04g |
| Sample 6 | 3.08g |
| Sample 7 | 2.63g |
| Sample 8 | 2.94g |
| Sample 9 | 3.41g |
| Sample 10 | 5.38g |
| Sample 11 | 3.33g |
| Sample 12 | 2.64g |
| Sample 13 | 2.84g |
| Sample 14 | 3.1g |
| Sample 15 | 5.24g |
| Sample 16 | 3.66g |

**Table 3.7:** Weight of Individual Samples 17 to 32.

| Sample Weight in grams(g) | |
|---|---|
| Sample Number | Weight in grams(g) |
| Sample 17 | 2.69g |
| Sample 18 | 3.23g |
| Sample 19 | 3.68g |
| Sample 20 | 5.8g |
| Sample 21 | 3.29g |
| Sample 22 | 2.74g |
| Sample 23 | 3.22g |
| Sample 24 | 3.66g |
| Sample 25 | 5.8g |
| Sample 26 | 3.65g |
| Sample 27 | 2.94g |
| Sample 28 | 3.45g |
| Sample 29 | 3.96g |
| Sample 30 | 5.67g |
| Sample 31 | 3.17g |
| Sample 32 | 3.43g |

Along with the above mentioned 32 samples, two other samples were prepared with a different material combination in which the mass layer was not included. Only

the absorptive or the foam layers were used along with the carrier layer. These were termed as special samples and there details are shown in the Table 3.8. The idea of the material configuration for these samples was purely based on the individual characteristics of the absorptive layers which led to some interesting results which are explained in the results and conclusion sections.

**Table 3.8:** Special Samples.

| Special Samples | | | |
|---|---|---|---|
| Sample | Layers | Total Thickness(mm) | Weight in grams(g) |
| Special Sample 1(SS-1) | Felt 10mm + Nitto 9mm | 22.2 | 2.59g |
| Special Sample 2(SS-2) | Sundquist 10mm + Nitto 9mm | 22.2 | 2.88g |

## 3.3 Impedance Tube Testing

After the samples were prepared, it was time to study their sound absorption and sound transmission characteristics with the help of an Impedance Tube. At VCC, the test setup consisted of a B&K Impedance Tube Type 4206 and Type 4206-T small tube as shown in the Figure 3.5.

**Figure 3.5:** B&K Pulse - Impedance Tube Setup at Volvo Cars' Facility.

The tube is rigid and made up of opaque material to restrict the sound within the tube along a single direction which is the direction of propagation. The sound propagation in a duct is considered to be stationary plane waves. This simplifies the three dimensional wave equation 2.9 to a one dimensional wave equation. –cite– For the study of sound absorption coefficient, the two microphone transfer function method is followed and for the study of sound transmission loss, the transfer matrix method is used which makes use of four microphones. The setup of the extra two microphones for the sound transmission loss measurements is done using the extended tube arrangement. For all the measurements, white noise was used as the sound source and the B&K type 2735 power amplifier had a gain setting of -6 dB which is shown in the Figure 3.7. The Figure 3.6 shows the B&K front end which

has the information about the sound source, power amplifier and all the microphone channels on the tube setup. This front end is connected to the computer via LAN to visualize the data acquired with the help of B&K Pulse LabShop software and the connection scheme is shown in the Figure 3.8. [7].

**Figure 3.6:** B&K Acoustic Material Test Front-end.

**Figure 3.7:** B&K Power Amplifier.

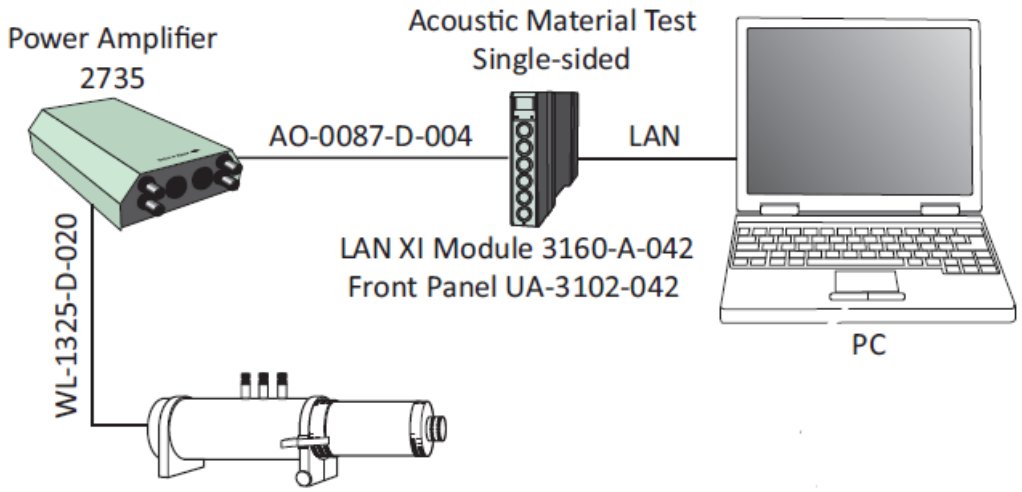


**Figure 3.8:** Impedance Tube Connections [7].

### 3.3.1 Test Methodology

The transfer function methods for both the sound absorption coefficient and sound transmission loss basically explained the physical and mathematical aspects involved

in their calculation. There is one more important aspect and that is the practicality of conducting all the tests on the impedance tube. Because of the above mentioned uncertainties, variations and deviations, the whole process of measurement seemed to be highly sensitive. The foam present in the test sample was wrapped around with an aluminium foil in order to ensure that there is no leakage of sound waves along the circumference of the test sample especially at high frequencies. It is shown in the Figure 3.9.

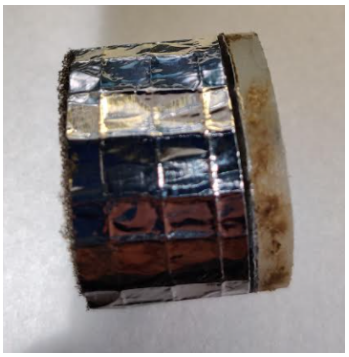

**Figure 3.9:** Aluminium foil wrapped around the foam.

The carrier on the test samples were wrapped around by a thin rubber tape which ensured a sealed surface area between circumference of the test sample and the tube which is shown in the Figure 3.10.

**Figure 3.10:** Rubber tape wrapped around the carrier.

To ensure that all the test samples went through the exact same measurement procedure, a systematic methodology was defined to enhance the robustness and reliability of the end results. The methodology is explained as below:

1. **Visual Inspection** - For every test sample, before it was mounted in the impedance tube, the person carrying out the test checked the sample for any kind of damage or defect which can be due to manufacturing or some other uncertainty. After careful visual inspection, the sample was discarded if it is damaged or else it was taken ahead for testing. A photograph of the sample was taken for documentation.

2. **Test Sample Fit** - In this step, the test sample was introduced into the impedance tube (with the sealing tape wrapped) and the quality of the fit was checked. A quality fit means that there should be no air gaps between the sample and the tube, the foam should not be compressed because of the sealing tape and the rubber tape during STL tests should be as thin as possible to avoid its effects on the test results. If not, then that particular sample was discarded and documented with a photograph.

3. **Testing & Data Acquisition** - For both sound absorption coefficient and sound transmission loss tests, each sample was tested three times by re-mounting it after each run. Because of all the uncertainties present, it was difficult to trust the sample's behaviour in one run. To be confident about this, the data of three runs of each sample were compared to see the magnitude of deviations among them which eventually led to the quality of the repeatability of the test procedure for each test sample. If the deviations were too high or very unsual, the sample was discarded and was not considered for further study.

4. **Data Processing** - The data acquired for three runs of each test sample was then averaged to obtain a single curve which represented the properties of that particular test sample. As a final step, the averaged single values of both sound absorption coefficient and sound transmission loss were calculated between 2kHz and 6kHz which happens to be our frequency range of interest. The samples with poor repeatability were not considered for further study.

### 3.3.2 Limitations and Uncertainties

The measurements performed on the B&K Impedance tube are sensitive to the quality of the sample manufactured, the mounting of the sample in the tube, the small gaps between the sample and the circumference of the tube and the handling of the sample by the operator. The results are bound to have slight variations and uncertainties. These uncertainties introduce a challenge to rely on the output of the measurements. But it is a given that a very minimum variation is always present for each and every measurement and hence it is dealt with by addressing the issues that an operator might face. These uncertainties are a part and parcel of the measurement process which can only be reduced and not completely removed. The uncertainties are as listed below:

1. **Sample Manufacturing** - The test samples used in all the measurements have to be manufactured with great care to maintain the precision of foam cutting, grinding and also the accuracy of their dimensions. Due to their dimension (diameter of 29mm), the foam and the mass layers in the samples are tricky to be sand grinded on a grinding machine. It sometimes happens that either foam or mass layer get an extra grind at some portions which later causes them to have a loose fit in the impedance tube even after using the sealing material. Sometimes the foam is damaged which can cause a deviation in its absorption properties when tested. The three layers (foam, mass layer

and carrier) are glued together to form a test sample. There is a potential chance that the glue might flow inside the foam and harden it again harming its absorption properties. An example for a defective sample is shown in the Figure 3.11 If anyone of these traits was observed in the test samples, it was discarded for measurements.

**Figure 3.11:** Foam damaged around the circumference.

2. **Test Sample Sealing** - As mentioned earlier, the test samples were sealed using aluminium foil and rubber tape for sound absorption and sound transmission loss tests respectively. There is a chance that the portion of these two sealing materials used to cover the test sample might vary depending upon the operator. The pressure applied while wrapping the sealing material around the test samples also varies and if it is high, the foam might get compressed and can cause a loose fit of the test sample in the tube as shown in Figure 3.12.

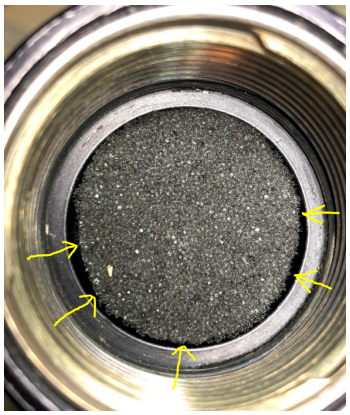

**Figure 3.12:** Loose fit Test Sample.

3. **Variation in 3D Printed Carrier** - For all the test samples, the outermost layer was the carrier. The carrier is a 3D printed thermoplastic and it has its own texture once it is produced. The orientation of the fibres in the carrier also varies from one sample to another. This is a completely 3D printing related aspect and because of this, even though a same sample is tested multiple times, it tends to have minute deviations in the results. As there were 32 samples, the variety in fibre orientation was quite substantial. But this issue was tried to negate as much as possible by performing repeatability tests which is explained further in next sections.

### 3.3.3 Repeatability and Selection of Samples.

The samples tested on the Impedance Tube were mainly filtered and discarded based on the repeatability of their results. The samples with poor repeatability were discarded and only the ones with a good repeatability were retained.

As mentioned earlier, the repeatability tests were carried out on each sample to be confident about the accuracy and reliability of its results. These results played a vital role in deciding the final material combination to build the encapsulation for the EDU. For every sample, these steps were followed:

1. The sample to be tested was installed in the impedance tube.
2. It was tested for both sound absorption '$\alpha$'and STL properties.
3. After the measurements, the sample was removed from the tube and installed back in the tube for the next run.

The above three steps constitute one run for the selected test sample and these steps were repeated three times for every test sample. For example, the Figure 3.13 shows the sound absorption coefficient results for test sample 3.

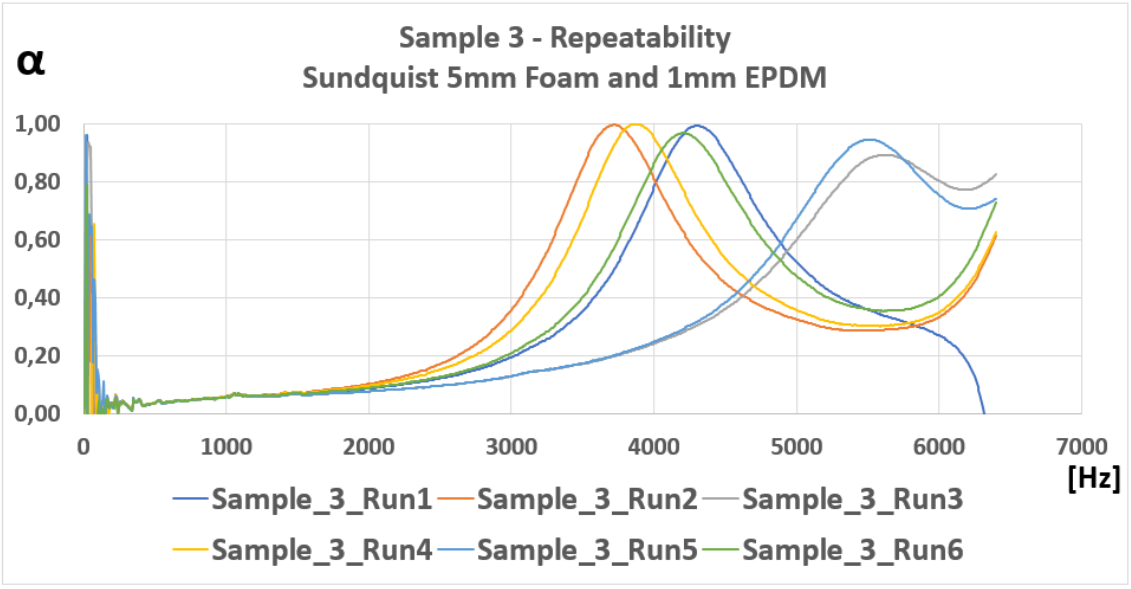


**Figure 3.13:** Sample 3 Repeatability Study - Sound Absorption Coefficient

The curves look highly deviated from one another and even after six runs, they clearly indicate low accuracy and reliability. The reasons for this may be minute defects in the sample not visible to the naked eye or as mentioned earlier, the gluing of the layers in the sample might also be contributing substantially. Hence the samples with similar repeatability results as sample 3, were discarded. On the other hand, Figure 3.14 shows the measurement results for test sample 17 which display a good repeatability for the three runs. The deviations among the three runs are small which indicate reliability and accuracy of the obtained results.

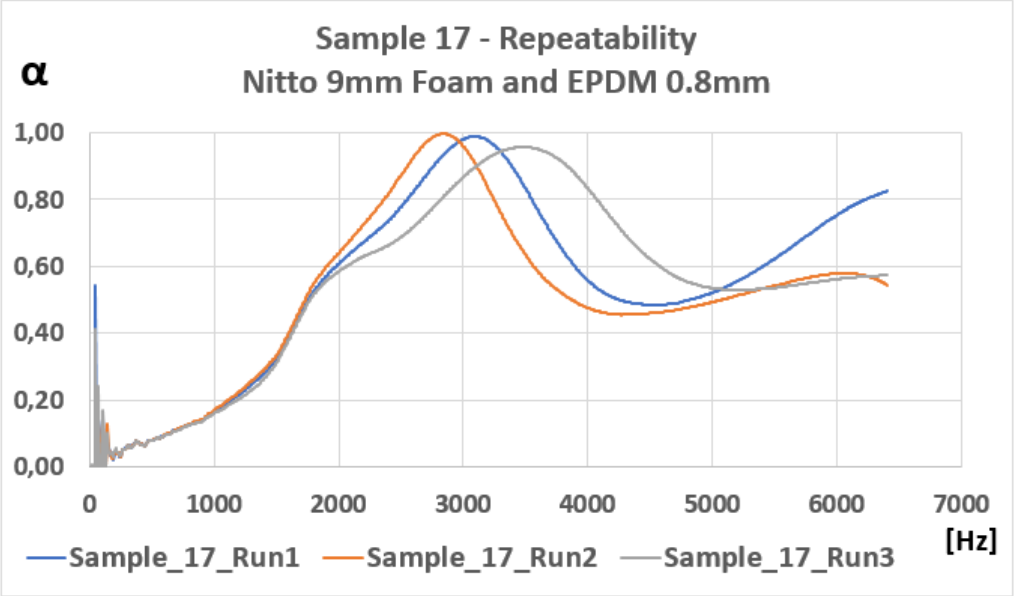


**Figure 3.14:** Sample 17 Repeatability Study - Sound Absorption Coefficient

The repeatability study for the sound transmission loss of sample 7 is shown in the Figure 3.15. The y-axis represents the sound transmission loss in dB scale and the x-axis shows the frequency in Hz. It can be seen that the differences in the results among the three runs is sufficiently large to discard it for further study. The samples with repeatability results similar to that of Sample 7 were rejected.

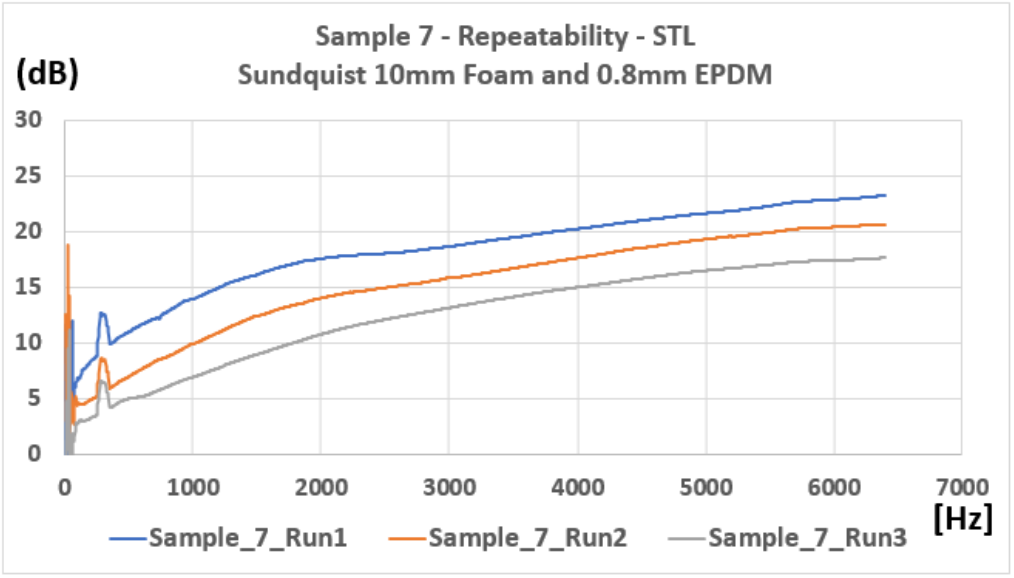


**Figure 3.15:** Sample 7 Repeatability Study - STL

On the other hand, the repeatability of the STL results for Sample 17 are shown in the Figure 3.16 which are acceptable. The samples with repeatability results similar to that of sample 17 were qualified for further study.

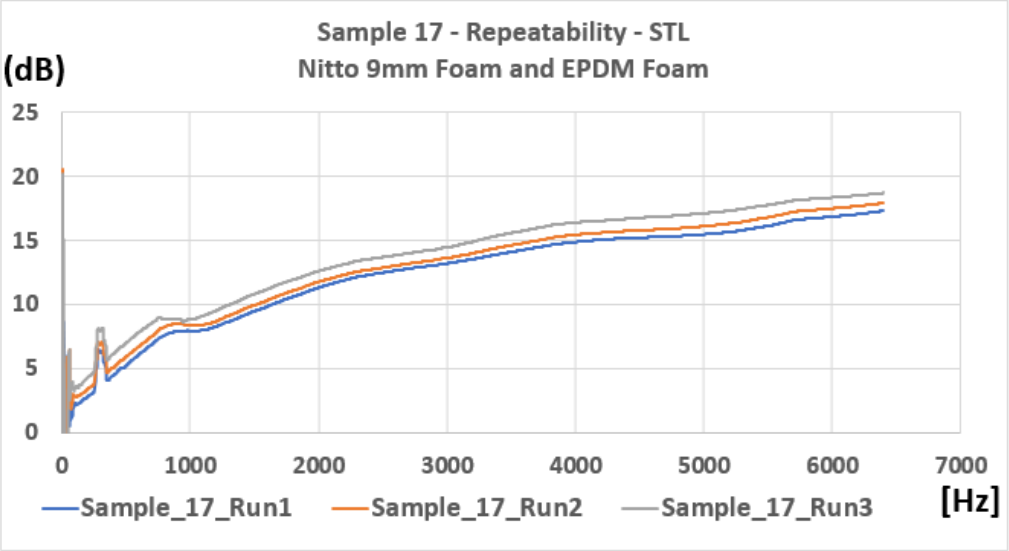


**Figure 3.16:** Sample 17 Repeatability Study - STL

Based on the repeatability studies, 16 samples qualified for further studies out of the total 32 samples. Out of these 16 samples, 5 samples were finally chosen to build the encapsulations for the Insertion Loss measurements. The list of final 5 samples is given in the Table 3.9.

**Table 3.9:** Final Samples to build the Encapsulations.

| List of Final Samples - Averaged from 2 kHz to 6 kHz | | | |
|---|---|---|---|
| Sample | Thickness (mm) | Avg '$\alpha$' | Avg STL(dB) |
| 17 | 13.0 | 0.67 | 15.15 |
| 24 | 15.2 | 0.75 | 21.57 |
| 30 | 20.7 | 0.93 | 21.74 |
| Special Sample 1 | 22.2 | 0.75 | 17.92 |
| Carrier 10 mm Offset | 10.0 | 0.21 | 10.50 |

Samples 17, 24 and 30 were selected as the sound absorption coefficient and sound transmission loss for them were respectively in the order of lowest, moderate and highest. One more reason for their selection was the variety in the material configuration which had different absorptive layers and mass layers. This variety would make the final measurements more interesting and wide ranged for the final empirical model. To add more variety and versatility, special sample 1 and the carrier with 10 mm offset were also chosen among the final samples.

## 3.4 Fabrication of Encapsulations

To build the encapsulations of the shortlisted samples, carrier templates of 10 mm and 20 mm offsets were used which are shown in the Figures 3.17 and 3.18.


**Figure 3.17:** Carrier Templates - 10 mm and 20 mm Offset.


**Figure 3.18:** Carrier Templates - 10 mm and 20 mm Offset.

Surface area of 20 mm offset template is 7066 $cm^2$ and the 10 mm offset template has a surface area of 6292 $cm^2$. Each template has three faces (left, right and bottom) which combine to enclose the EDU which can be visualized in the Figure 3.19.

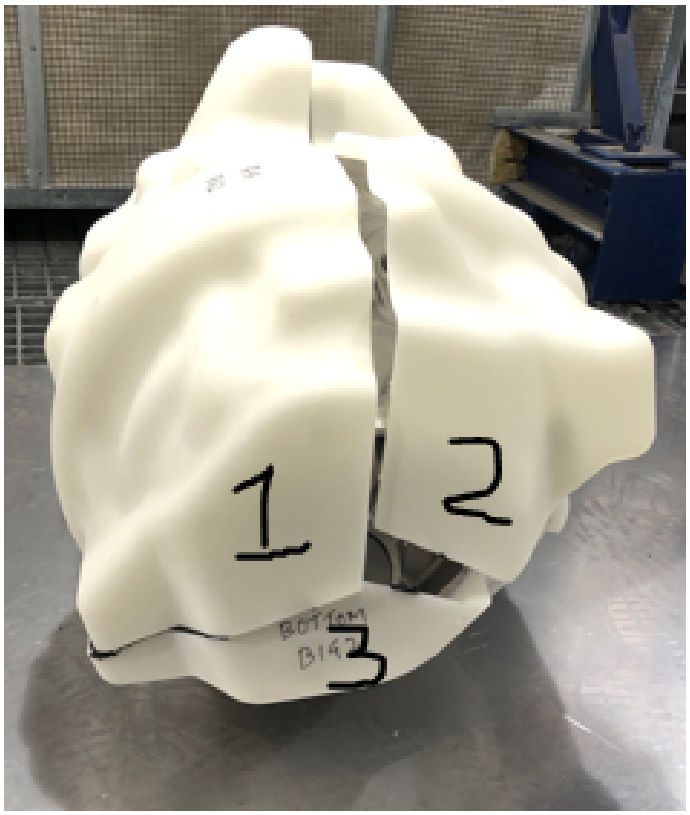


**Figure 3.19:** Three faces of an Encapsulation covering the EDU.

### 3.4.1 Building Encapsulations - Procedure

The steps followed to build the encapsulations for the short listed samples are described as follows:

1. Based upon the total thickness (foam, mass layer and carrier) of the sample, the offset type of the carrier was chosen. This was done to ensure a closed fit of the encapsulation on the EDU during the tests. For example, in the case of sample 17, the 10 mm offset carrier template was chosen as the total thickness was 13 mm. For special sample-1, the 20 mm offset carrier template was chosen as the total thickness for it was 22.2 mm.
2. After the first step, the mass layer is adhered on to the selected carrier template with the help of a strong double sided adhesive tape. The curvature on the templates are handled carefully by sticking patches of the mass layer so that all the small gaps are filled. This is done for on three faces of the carrier template
3. Once the mass layer is completely adhered, the foam/felt layer is adhered on the surface of the mass layer. The foam layer has an adhesive side and requires no external adhesive tapes. However, in some curvatures of the template, the foam is adhered using some spray glue to ensure better adhesion and to cover the gaps.
4. All the three faces of the encapsulation are weighed after the foam layers and mass layers are adhered on the carrier template.

### 3.4.2 Sample 17

The material configuration of sample 17 is,

- Layer 1 - 9 mm Nitto Foam
- Layer 2 - 0.8 mm EPDM Mass Layer
- Layer 3 - 3.2 mm Carrier.

The carrier templates with the 10 mm offset was used to build the encapsulation of sample 17.

#### Coverage Variation

1. **100% Coverage**

   The complete encapsulation for the sample 17 material configuration is shown in the Figure 3.20. The total surface are of the encapsulation is 6292 $cm^2$.

**Figure 3.20:** Encapsulation of Sample 17 - 100% Coverage.

2. **95% Coverage**

   The total surface area was to be reduced by 5% to achieve a total coverage of 95%. To do this, the area had to be reduced uniformly on all the three faces of the encapsulation to maintain an equally distributed change. Instead of selecting squares or any other shapes, it was decided to cut out circles on the encapsulation with hole saw as the chances of maintaining the uniformity in this were more and also had an advantage of the ease in cutting. Based on the total surface area of 6292 $cm^2$, a hole saw with a diameter of 41 mm was chosen to drill 8 holes on each face of the encapsulation to reach 95% coverage which is shown in the Figure 3.21.

**Figure 3.21:** Encapsulation of Sample 17 - 95% Coverage.

Similarly, for both the 90% and 85% coverages, the 41 mm diameter hole saw was used to cut as many holes required to achieve the respective total coverage percentage. The calculation can be seen in the Table

**Table 3.10:** Encapsulation of Sample 17 - Calculation of Percentage Coverage.

| % Coverage Calculation for Sample 17 | | | |
|---|---|---|---|
| % Coverage | Hole Diameter(mm) | No. of Holes on each face | Total Area of holes ($cm^2$) |
| 95 | 41 | 8 | 316.87 |
| 90 | 41 | 15 | 594.13 |
| 85 | 41 | 23 | 910.97 |

Figures 3.22 and 3.23 show the 90% and 85% coverages respectively for sample 17.

3. **90% Coverage**

**Figure 3.22:** Encapsulation of Sample 17 - 90% Coverage.

4. **85% Coverage**

**Figure 3.23:** Encapsulation of Sample 17 - 85% Coverage.

### 3.4.3 Sample 24

The material configuration of sample 24 is,

- Layer 1 - 10 mm Foam

- Layer 2 - 2 mm EPDM Mass Layer
- Layer 3 - 3.2 mm Carrier.

The carrier templates with the 10 mm offset was used to build the encapsulation of sample 24.

### Coverage Variation

1. **100% Coverage**

**Figure 3.24:** Encapsulation of Sample 24 - 100% Coverage.

2. **95% Coverage**

**Figure 3.25:** Encapsulation of Sample 24 - 95% Coverage.

**Table 3.11:** Encapsulation of Sample 24 - Calculation of Percentage Coverage.

| % Coverage Calculation for Sample 24 | | | |
|---|---|---|---|
| % Coverage | Hole Diameter(mm) | No. of Holes on each face | Total Area of holes ($cm^2$) |
| 95 | 60 | 3 | 254.47 |
| 90 | 60 | 7 | 593.75 |
| 85 | 60 | 11 | 933.05 |

3. **90% Coverage**

**Figure 3.26:** Encapsulation of Sample 24 - 90% Coverage.

### 3.4.4 Sample 30

The material configuration of sample 30 is,

- Layer 1 - 15 mm Felt
- Layer 2 - 2.5 mm EPDM Mass Layer
- Layer 3 - 3.2 mm Carrier.

The carrier templates with the 20 mm offset was used to build the encapsulation of sample 30.

**Coverage Variation**

1. **100% Coverage**

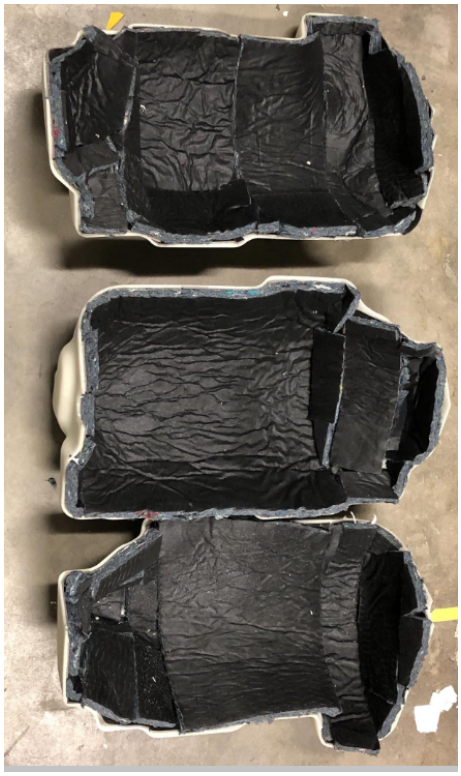

**Figure 3.27:** Encapsulation of Sample 30 - 100% Coverage.

2. **95% Coverage**

   The percentage coverage variation for sample 30 was done in a non-uniform way unlike other samples. The number of holes on each face of the encapsulation is explained below:

**Table 3.12:** Encapsulation of Sample 30 - Calculation of 95% Percentage Coverage.

| 95% Coverage Calculation for Sample 30 | | | |
|---|---|---|---|
| Location of Holes | Hole Diameter(mm) | No. of holes | Total Area of holes ($cm^2$) |
| Right Face | 127 | 1 | 126.68 |
| Left Face | 127 | 1 | 126.68 |
| Bottom Face | 127 | 1 | 126.68 |

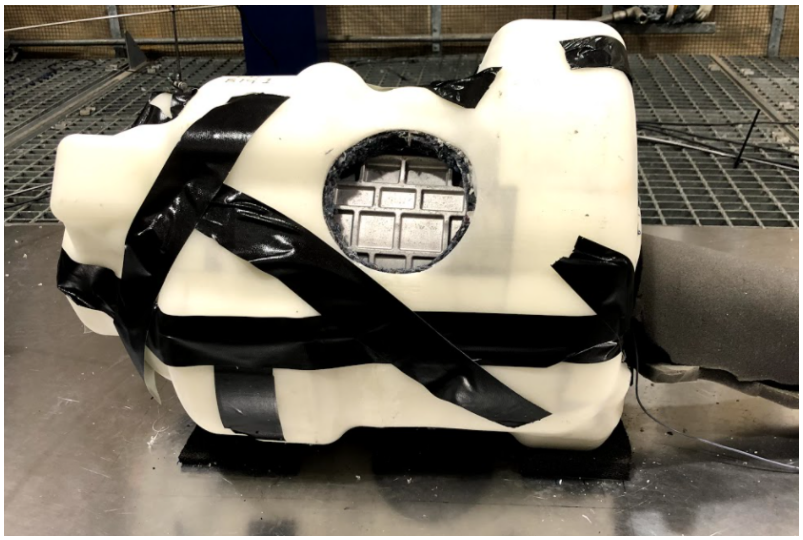

**Figure 3.28:** Encapsulation of Sample 30 - 95% Coverage.

3. **90% Coverage**

**Table 3.13:** Encapsulation of Sample 30 - Calculation of 90% Percentage Coverage.

| 90% Coverage Calculation for Sample 30 | | | |
|---|---|---|---|
| Location of Holes | Hole Diameter(mm) | No. of holes | Total Area of holes ($cm^2$) |
| Right Face | 127 | 1 | 126.68 |
| Right Face | 60 | 4 | 113.096 |
| Left Face | 127 | 1 | 126.68 |
| Bottom Face | 127 | 1 | 126.68 |
| Bottom Face | 60 | 9 | 254.46 |

The total surface area removed by the holes adds up to 747.602 $cm^2$ which is equal to 90% of the total coverage area.

**Figure 3.29:** Encapsulation of Sample 30 - 90% Coverage.

4. **85% Coverage**

**Table 3.14:** Encapsulation of Sample 30 - Calculation of 85% Percentage Coverage.

| 85% Coverage Calculation for Sample 30 | | | |
|---|---|---|---|
| Location of Holes | Hole Diameter(mm) | No. of holes | Total Area of holes ($cm^2$) |
| Right Face | 127 | 1 | 126.68 |
| Right Face | 60 | 5 | 113.096 |
| Left Face | 127 | 1 | 126.68 |
| Left Face | 60 | 5 | 113.096 |
| Bottom Face | 127 | 1 | 126.68 |
| Bottom Face | 60 | 9 | 254.46 |

The total surface area removed by the holes adds up to 717.246 $cm^2$ which is close to 85% of the total coverage area.

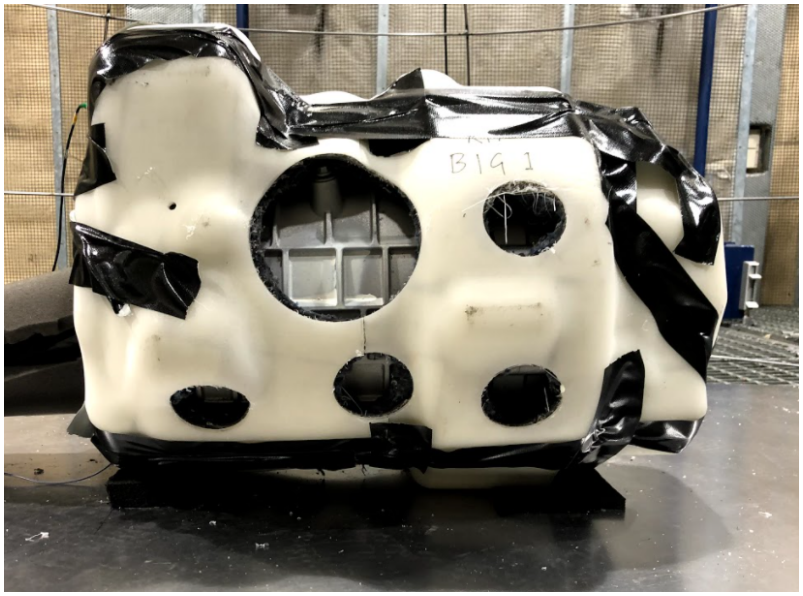


**Figure 3.30:** Encapsulation of Sample 30 - 85% Coverage.

### 3.4.5 Special Sample - 1

The material configuration of sample 30 is,

- Layer 1 - 9 mm Nitto Foam
- Layer 2 - 10 mm Sundquist Foam
- Layer 3 - 3.2 mm Carrier.

The carrier templates with the 20 mm offset was used to build the encapsulation of special sample - 1.

**Coverage Variation**

1. **100% Coverage**

**Figure 3.31:** Encapsulation of Special Sample 1 - 100% Coverage.

2. **95% Coverage**

The percentage coverage calculation for the special sample 1 are shown in the Table 3.15.

**Table 3.15:** Encapsulation of Special Sample 1 - Calculation of Percentage Coverage.

| % Coverage Calculation for Special Sample 1 | | | |
|---|---|---|---|
| % Coverage | Hole Diameter(mm) | No. of Holes on each face | Total Area of holes ($cm^2$) |
| 95 | 60 | 4 | 339.29 |
| 90 | 60 | 8 | 678.58 |
| 85 | 60 | 12 | 1017.86 |

**Figure 3.32:** Encapsulation of Special Sample 1 - 95% Coverage.

3. **90% Coverage**

**Figure 3.33:** Encapsulation of Special Sample 1 - 90% Coverage.

4. **85% Coverage**

### 3.4.6 Carrier

The material configuration of carrier is just a single layer of 3D printed polypropylene with a 3.2 mm thickness. The carrier templates with the 10 mm offset was used in the tests as an encapsulation.

#### Coverage Variation

1. **100% Coverage**
2. **95% Coverage**
   The percentage coverage calculation for the carrier are shown in the Table 3.16.

**Table 3.16:** Encapsulation of Carrier - Calculation of Percentage Coverage.

| % Coverage Calculation for Carrier | | | |
|---|---|---|---|
| % Coverage | Hole Diameter(mm) | No. of Holes on each face | Total Area of holes ($cm^2$) |
| 95 | 60 | 3 | 254.47 |
| 90 | 60 | 7 | 593.75 |
| 85 | 60 | 11 | 933.05 |

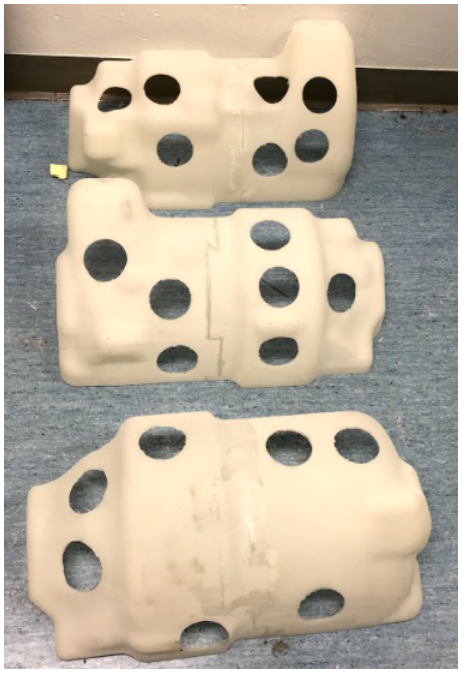

**Figure 3.34:** Encapsulation of Carrier - 95% Coverage.

3. **90% Coverage**

**Figure 3.35:** Encapsulation of Carrier - 90% Coverage.

4. **85% Coverage**

**Figure 3.36:** Encapsulation of Carrier - 85% Coverage.

## 3.5 Insertion Loss Measurement Methodology

In this section the methodology adopted for performing the insertion loss measurements, the reference to the standard used for measurement, implementation, instrumentation, setup and equipment quantification is explained in detail.

### 3.5.1 Procedure — According to ISO 3745

After the initial check of all the requirements in the experimental setup, it is now time to start the system and acquire the data. To check if all the connections and

setup are accurate, two or three pre-tests are run. Pre-tests are especially important to verify another requirement based upon the number of microphones used. The standard ISO 3745:2012(E) states that the number of microphone positions used to capture the data is sufficient if the difference between the highest and the lowest sound pressure level (SPL) in dB, is less than half of the number of microphone positions across all the frequency bands. All the iterations are performed only after this condition is met. Three tests are run in order to ensure that there is good repeatability and averaging for each encapsulation. The steps followed for the pre-tests and all the iterations are as mentioned below:

- White noise is generated using PAK system front-end and the PC audio card is sent to the power amplifier which conditions it and sends it to the loudspeaker hose.
- The loudspeaker hose emits the generated noise and excites all the internal components of the EDU.
- The output of the loudspeaker hose can be varied through the PAK system. Several iterations can be performed based on the requirements.
- The noise radiated by the EDU is captured by all the microphones placed in the hemispherical arrangement.
- The data is recorded for a minimum of 30 seconds and the number of iterations are decided based on the plan of design of experiments.
- The same steps as mentioned above are followed for all the iterations.

#### 3.5.1.1 Implementation

- $L_p$(avg) - Averaged sound pressure level of the EDU when excited by white noise.
- $L_p$(BN) - Averaged background sound pressure level when all the equipment in the test room are turned off.
- $L_p$(max) - highest sound pressure level among the 10 microphones used.
- $L_p$(min) - lowest sound pressure level among the 10 microphones used.
- All the tests were carried out in an Anechoic chamber at VCC.
- Sound pressure - Single level averaged over 10 microphones (A-weighted) for the iterations with and without encapsulations.
- The radius of the hemisphere base of the microphone array should be greater than or equal to double of the characteristic dimension of the noise source or greater than or equal to the triple of the distance between the floor and the acoustic centre of the source (whichever is the larger).
- Criteria for background noise: The result of $L_p$(avg) - $L_p$(BN) has to be 6 dB for all frequency bands and 10 dB for 1/3rd octave bands of mid frequency range from 250 Hz to 5 kHz. Otherwise, the background noise correction factor (K) is applied accordingly.
- Microphone positions - The result of $\Delta = L_p(\text{max}) - L_p(\text{min})$ should be less than or equal to half the number of microphones used. For example, if twenty microphones are used, then the $\Delta$ should be less than 10 dB. In this thesis work, ten microphones were used and the $\Delta$ was verified to be below 5 dB.
- Calibration - The calibration of the microphones was done using B&K microphone calibrator — Type 4231.

#### 3.5.1.2 Instrumentation

1. 12 Channel Mueller BBM PAK system — MKII Front end.
2. 10 ICP type free-field Microphones (PCB Piezotronics) with built-in pre-amplifiers. Refer: A.3 A.4
3. One 1/4" ICP microphone for the reference microphone.
4. 11 BNC to BNC cables (5m length) with extended SMB connectors.
5. Measurement Laptop with the data acquisition software licensed by PAK Müller-BBM for controlling the hardware and signal generator.
6. High frequency driver connected to a PVC hose of length 2.4m with an inner diameter 25 mm and outer diameter 35 mm.
7. ISVR power amplifier.
8. B&K microphone calibrator Type 4231 94 dB SPL at 1 kHz.

#### 3.5.1.3 Experimental Setup

- The EDU, which is the noise source in this case, is positioned at the centre of the hemi-anechoic room.
- The surface on which the EDU is positioned is a completely reflective sheet metal plate so as to obtain a free sound field and get more reflections from the plate.
- The ten free field condenser microphones are calibrated and arranged in a hemispherical manner with the help of a semi circular grid to hold all the microphones to envelope the EDU and this is done according to ISO 3745:2012(E). It is shown in the Figure 3.37.[19]
- The centre of the hemispherical grid is aligned with the acoustic centre of the EDU if it is known or else the geometric centre is considered.
- The radius of the microphone grid is checked for its basic requirements according to the standard mentioned above.
- The input signal for the system is generated by the PAK System interface using the PC audio card. The measurement computer is connected through a 3.5mm audio jack having BNC connector to the power amplifier which conditions the input signal and finally feeds it to the EDU through the PVC hose.
- The EDU casing had steel plates on its surface which were damped by clamping mass layers on their surfaces to decrease their sound radiation.
- The reference microphone is attached by the side of the opening of the loudspeaker hose (Figure 3.39).
- The output of the microphones is connected to the PAK front end through which the data from the microphones is recorded.

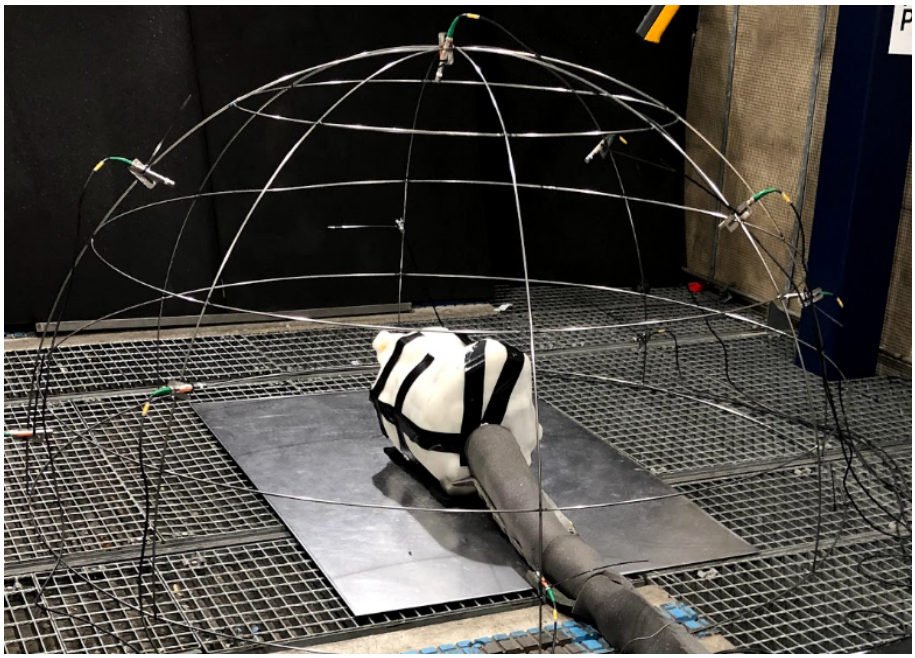

**Figure 3.37:** Setup of the grid and the test object.

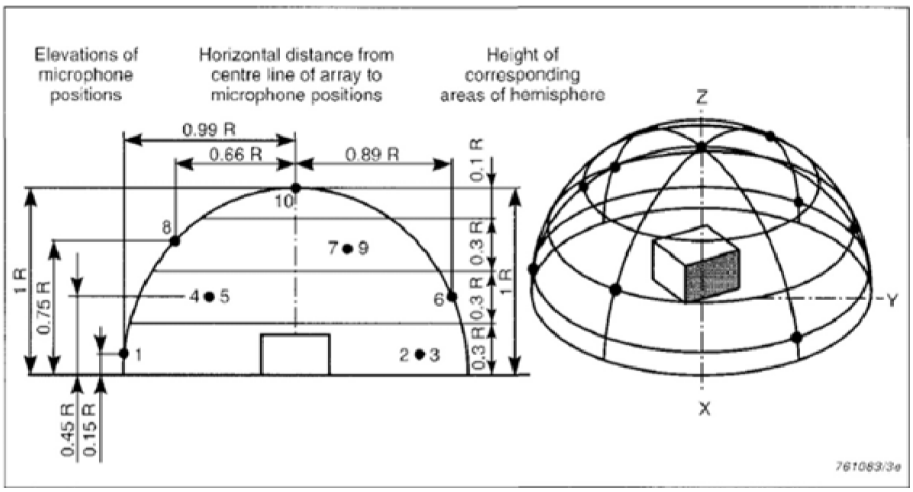


**Figure 3.38:** Hemispherical Microphone Grid enveloping the EDU [19]

### 3.5.2 Loudspeaker and Hose — Noise Quantification

As mentioned earlier, for repeatability and safety reasons,the EDU is powered using a loudspeaker and hose. The design consists of following:

- One co-axial 2" driver unit including passive cross-over filter BMS 4590P. Refer A.7
- MDF wooden box: 2 sides are 20x160x340 mm (D*H*W), 2 sides are 20x160x300 mm, top and bottom are 20x340x340 mm
- One steel piece connecting the driver and hose
- Hose PVC/steel 2.4m length, 25mm inner diameter, 35mm outer diameter

- 1 piece Aluminium for orifice

In figure 3.39 below the driver and its construction box image is shown. Please refer the appendix A.5 and A.6 for high frequency source characterization which is build and characterized in VCC.

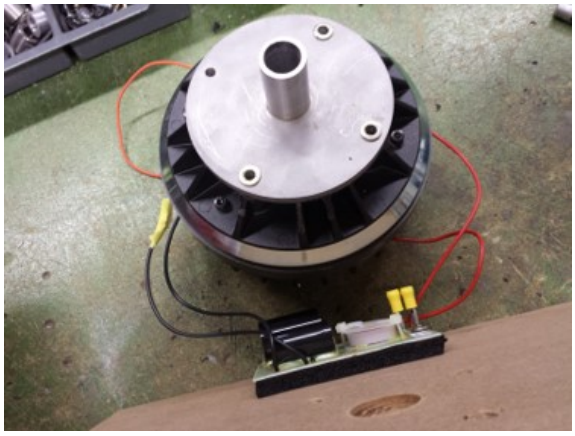

**Figure 3.39:** Driver and Box construction

In the Figure 3.40 below the hose pipe and nozzle can be seen. A quarter inch microphone is taped at the mouth of the nozzle orifice to characterize the source as well have a reference to calcualte the acoustic transfer functions (ATF) later in our work.

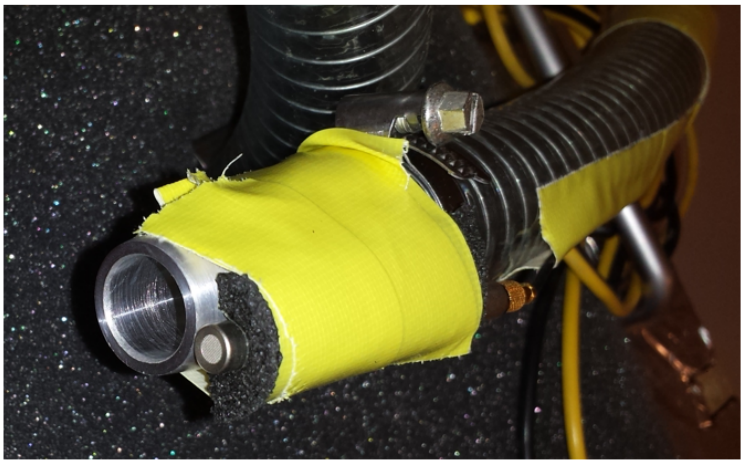

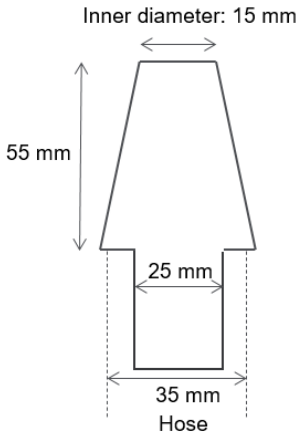


**Figure 3.40:** Hose Pipe, Microphone position and nozzle details

Output at the hose is measured using a microphone and is shown as below 3.41, we can see that it gives a comb filter effect at the output. However the levels are sufficiently high and constant for all measurements which makes it suitable to work with.

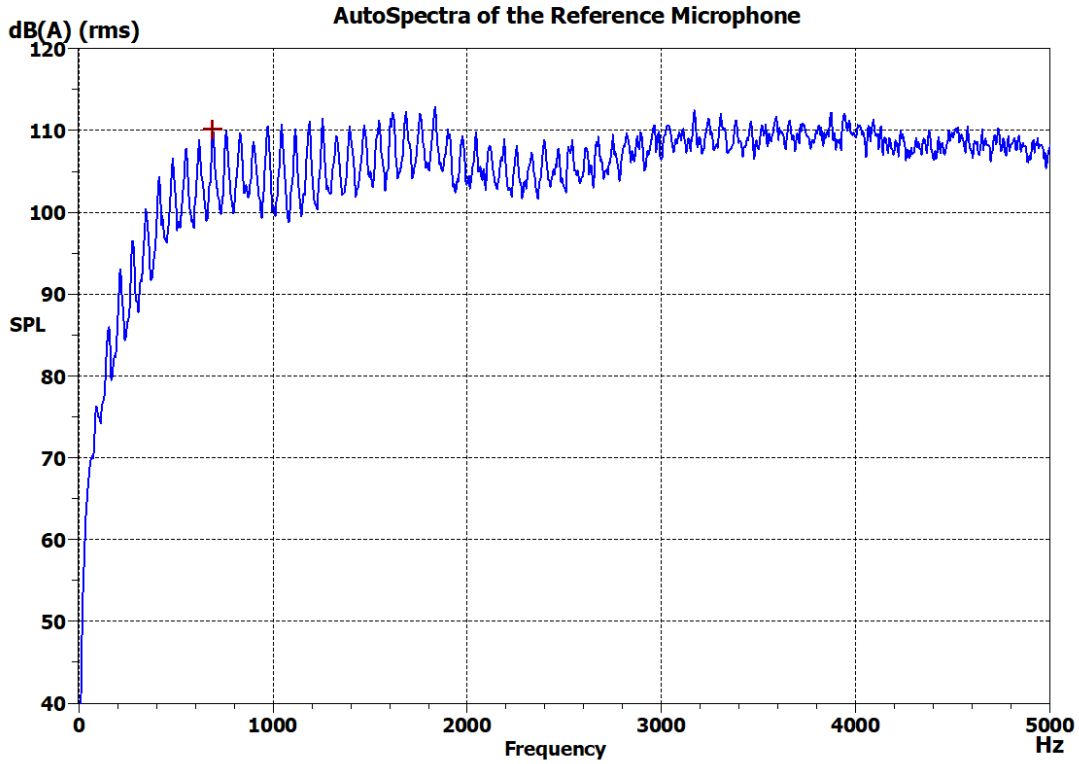


**Figure 3.41:** Auto Spectra for Reference Microphone position

To reduce the noise radiated by the driver box and the hose pipe, it was covered with mass and foam layers as shown in the figure 3.42 and 3.43. The effect of this can be seen in figure 3.45 in which all the samples at 100% coverages were plotted along with without encapsulation data to check how big is the difference in dB. The hose and driver noise contribution was measured by blocking the noise at the outlet of the nozzle by a rubber plug and using the same setup for measurement as seen in figure 3.44.

**Figure 3.42:** 3 layer Covering on the hose pipe 10 mm Foam + 2mm Mass Layer + 10 mm Foam

The driver box was covered using a cardboard box by adding some foam and mass layers of mentioned configuration 3.43. The pipe already had a lesser contribution but however was still covered with a 3 layer configuration as mentioned in figure 3.42.

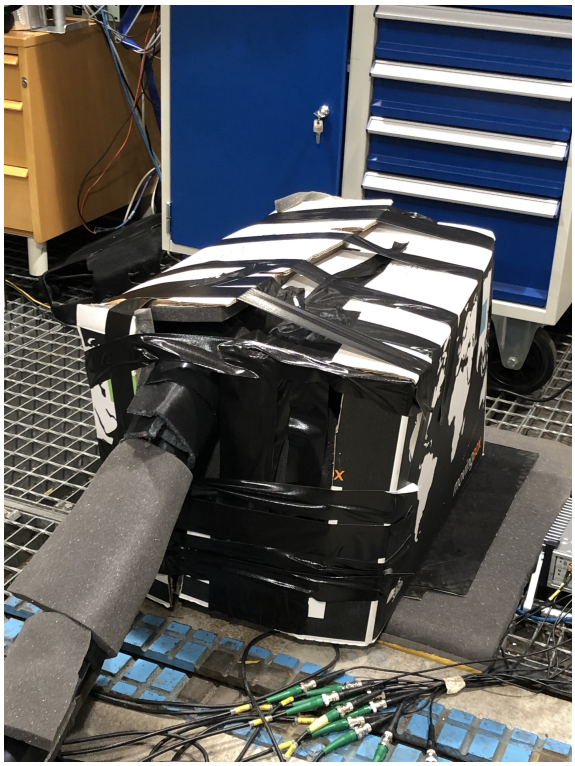

**Figure 3.43:** Encapsulation for Driver - 2 mm Bitumen Mass layer + 15 mm Foam

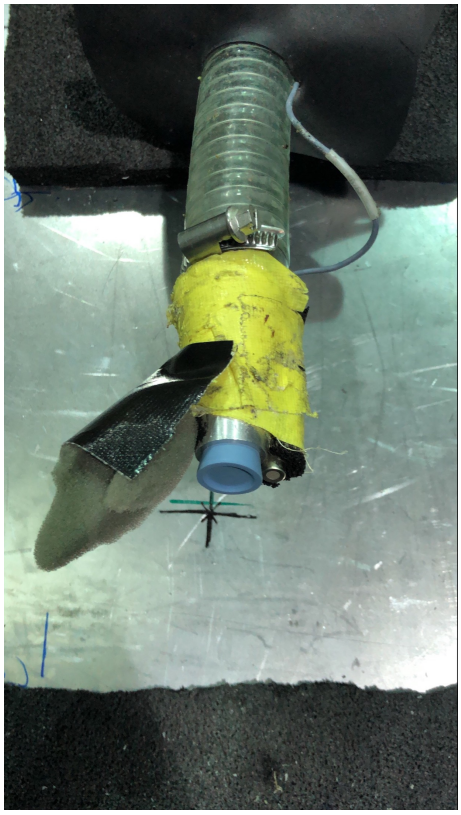

**Figure 3.44:** Hose Plug set-up

From figure 3.45 we can clearly see that there is almost a 10 dB difference at 1 kHz between the samples which could give best insertion loss i.e. with 100% coverage and the hose and driver noise. At 2 kHz and 4 kHz the difference is close to 4 dB. However this was found to be good for our methodology since all test's have fixed setup. Also if standing inside the anechoic room initially one could localize 2 noise sources before treating the hose pipe and driver box. However after treatment this issue was also solved which give a further confirmation.

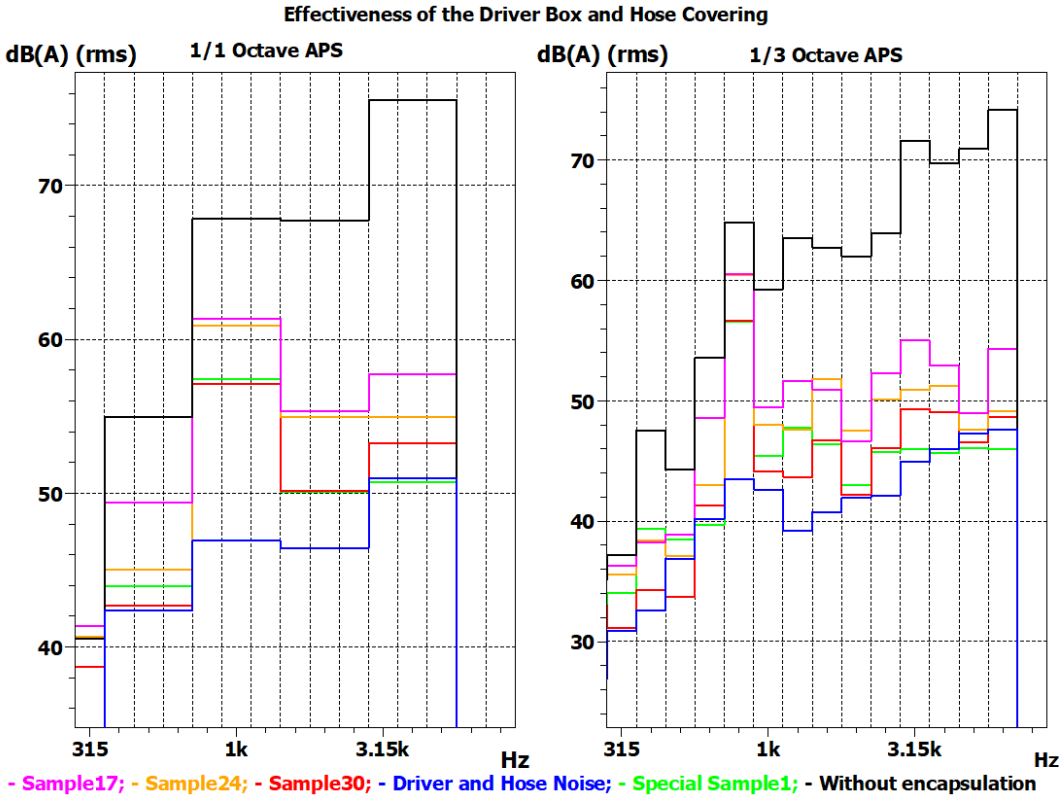


**Figure 3.45:** Quantification of Driver and hose contribution after treatment

Figure 3.46 shows background noise. As expected for an anechoic environment it is quite low at all frequencies. In addition to this, the levels without the encapsulation show that, after passing through the EDU, there is still sufficient excitation across all frequency bands.

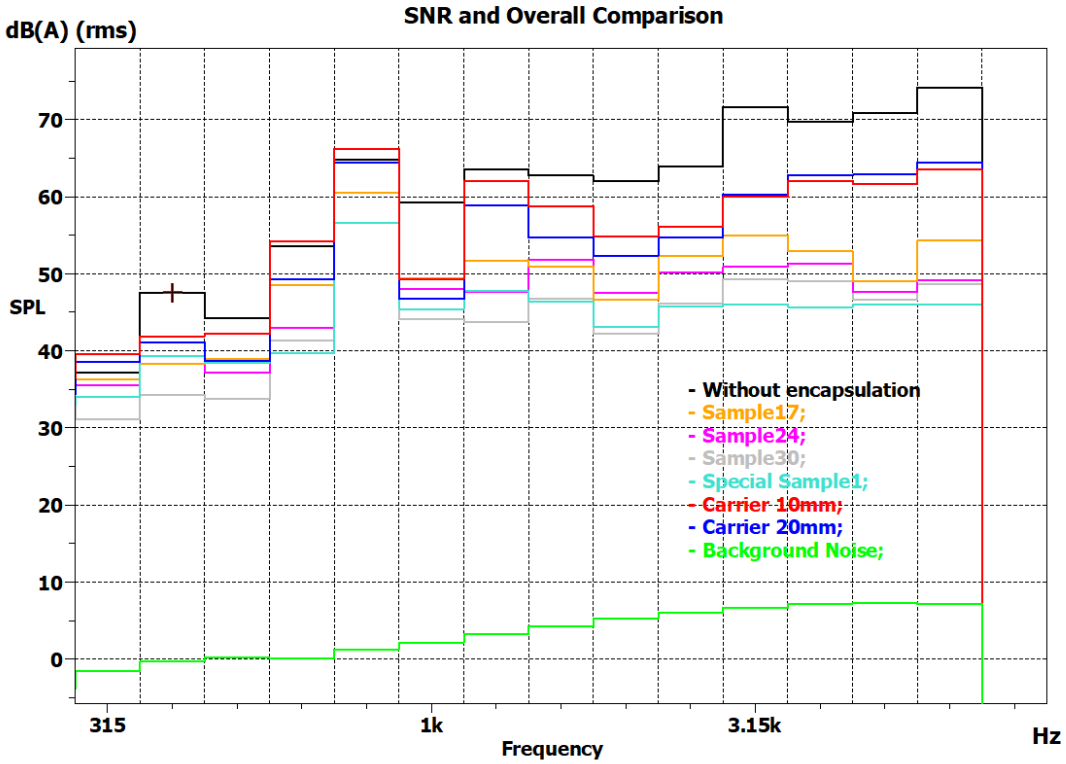


**Figure 3.46:** SNR

# 4

# Results and Discussion

## 4.1 Impedance Tube Measurement Results

In this section, the 16 samples which qualified based on their good repeatability and theoretical trend, are discussed for their sound absorption coefficient and the transmission loss results.

### 4.1.1 Sound Absorption Coefficient - '$\alpha$' - Repeatability Study & Qualified Samples.

As it was mentioned in the earlier sections, the study of the repeatability of the results for each sample was very vital. It was a tool to mitigate and minimize the experimental errors which is very important in characterizing the materials. The samples with good repeatable results were qualified because those results were reliable. Some of the examples for good repeatability out of the qualified samples are shown in the Figures 4.1 and 4.2.

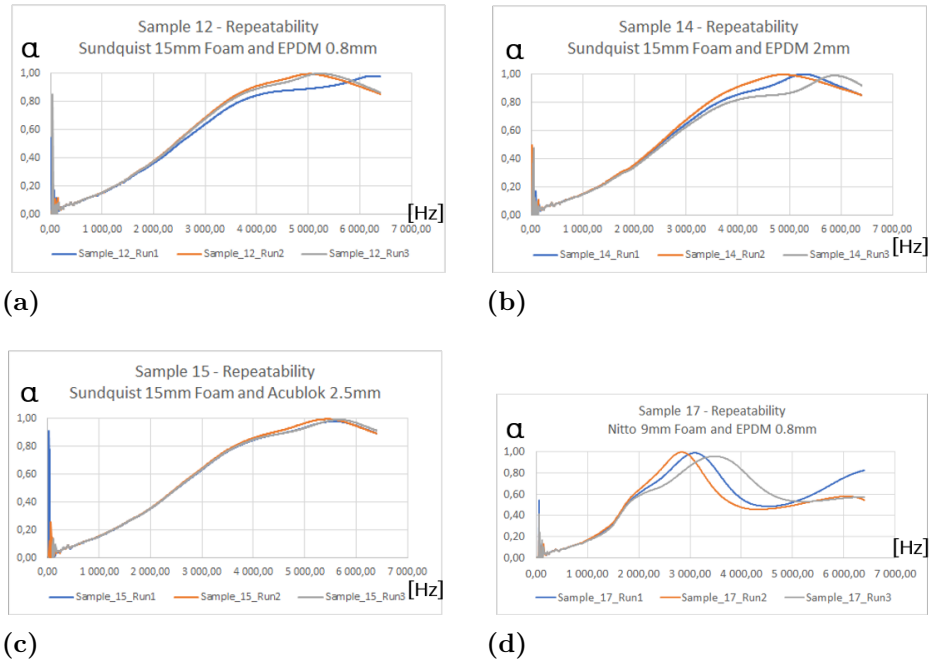


**(a)** **(b)**

**(c)** **(d)**

**Figure 4.1:** Absorption Coefficient Tests - Repeatability - Samples 12,14,15,17.

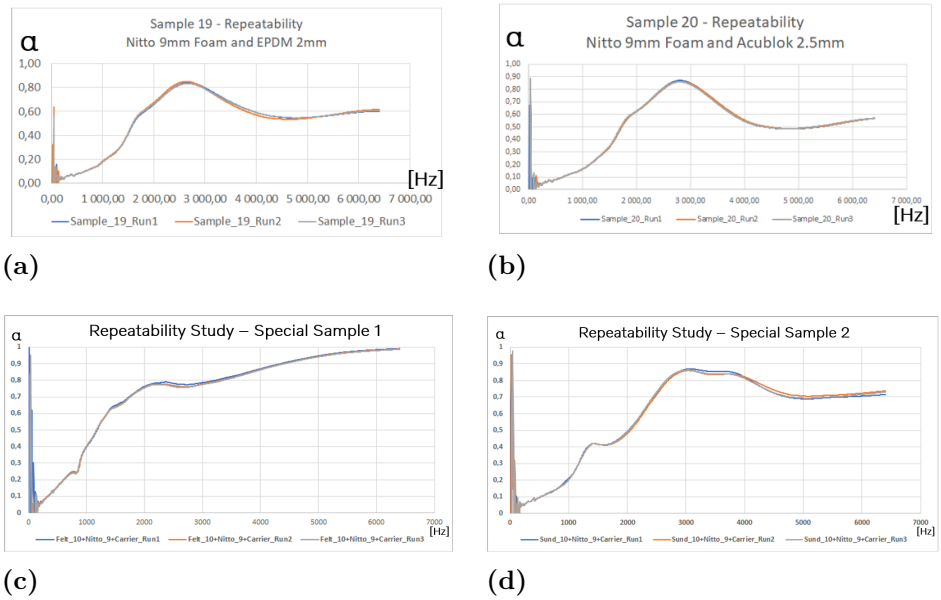


**Figure 4.2:** Absorption Coefficient Tests - Repeatability - Samples 19, 20, Special Samples 12.

Figure 4.3 shows the curves for sound absorption coefficient values for all the qualified samples from all the groups. The curves are mainly divided into three types of lines according to the three mass layers which are EPDM 0.8 mm, EPDM 2 mm and Acublok 2.5 mm. These three mass layers were selected in order to have three levels(low,mid,high) in each sample group. EPDM 0.8 mm is the lightest and Acublok 2.5 mm is the heaviest mass layer.

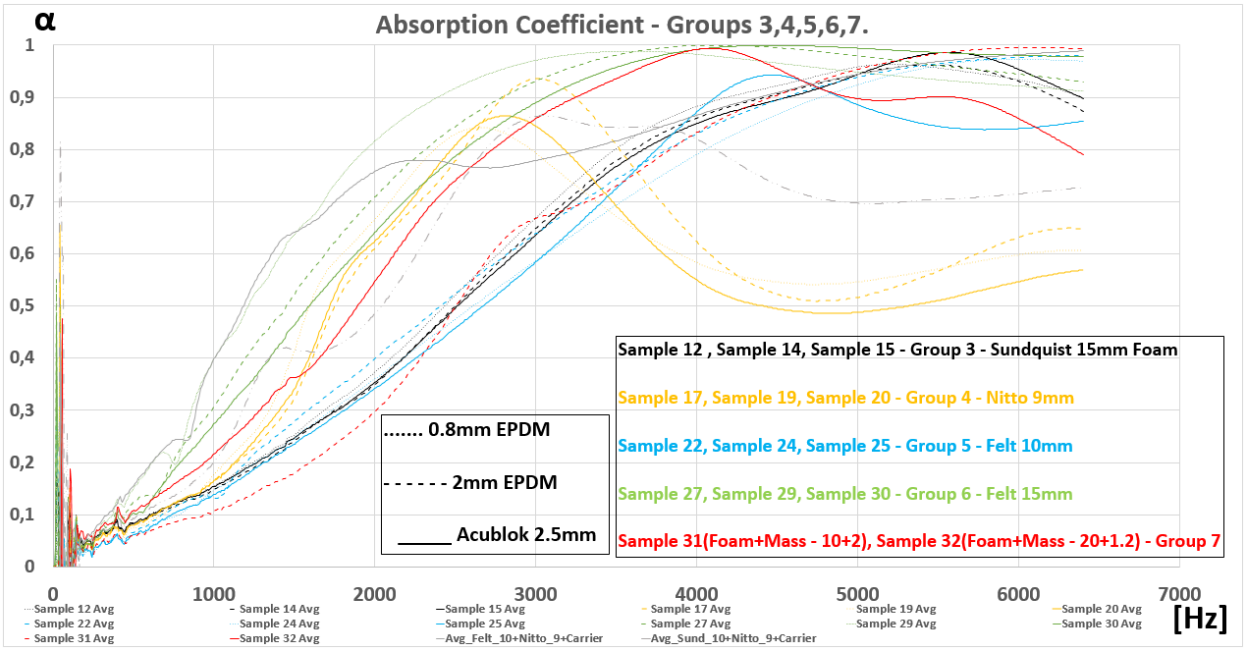


**Figure 4.3:** Sound Absorption Coefficient '$\alpha$' - Qualified Samples

Based on these three levels, the samples were ranked according to their sound absorption coefficient values. The green curves represent the sample group 6 with the absorptive layer of 15 mm felt. All the three curves for this group are clustered above all the other curves and show a strong sound absorbing capacity almost throughout the frequency range starting from 1 kHz. This can be explained mainly by the 15 mm thickness that they have. On the other hand, the yellow curves represent the sample group 4 with the absorptive layer of 9 mm Nitto foam. The Nitto foam is a mixture of foam and EPDM rubber. The curves related to this group have a high sound absorption especially in the range of 1.8 kHz to 3kHz which make this type of foam very unique in this range. Above 3 kHz, the sound absorption for Nitto foam just seems to drop considerably compared to other groups. In an overall way, all the other groups follow the sound absorption capacity based on their respective thicknesses and follow theory aspects.

### 4.1.2 Sound Transmission Loss(STL) - Repeatability & Qualified Samples.

The same repeatability approach was followed even for transmission loss tests and the results for some of the qualified samples with good repeatability is shown in the Figures 4.4 and 4.5. The samples with good repeatable results were qualified because they followed the theoretical mass law with respect to sound transmission.

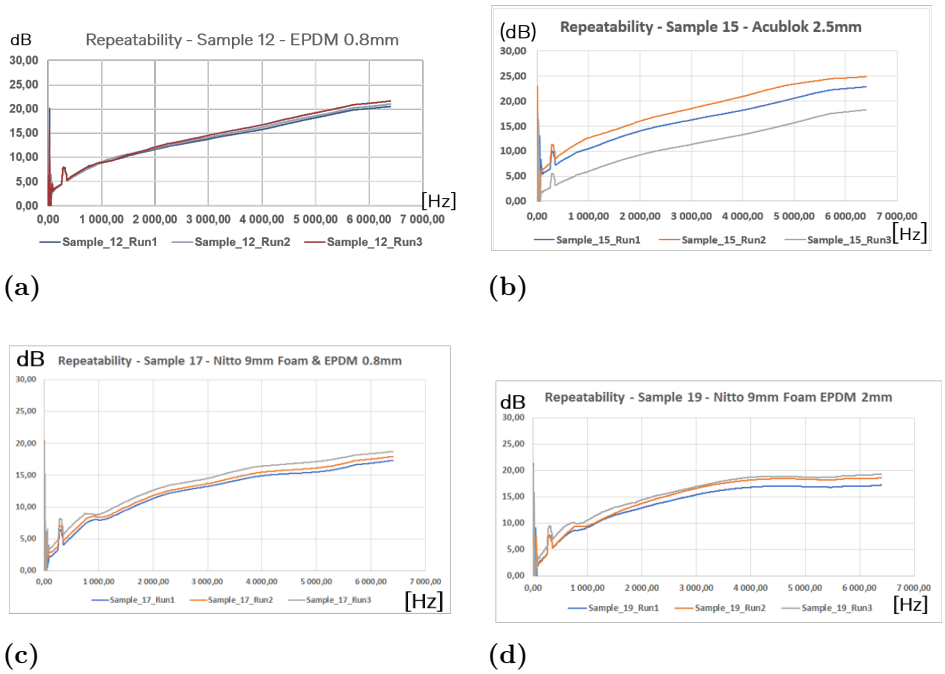


**Figure 4.4:** Transmission Loss Tests - Repeatability - Samples 15,17,19,20.

The Figure 4.6 shows the transmission loss results for the sample groups 4,5 and 6. Similar to sound absorption results, these results are also divided based upon the sample groups and the three mass layers EPDM 0.8 mm, EPDM 2 mm and Acublok 2.5 mm to have low, mid and high levels of STL values. The dotted lines in

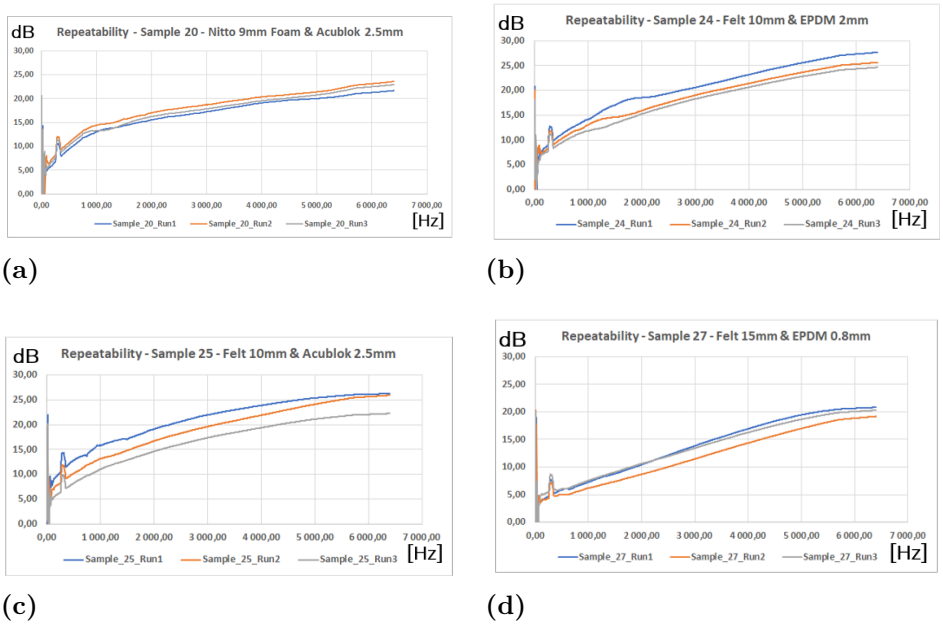


**Figure 4.5:** Transmission Loss Tests - Repeatability - Samples 20,24,25,27.

the Figure 4.6 represent the samples with the mass layer EPDM 0.8 mm which has the least weight. The solid lines represent the samples with the mass layer Acublok 2.5 mm which has the highest weight. Clearly, according to the relation between mass and sound transmission loss, the solid lines with Acublok 2.5 mm are clustered above all the other curves and the dotted lines with EPDM 0.8 mm are right at the bottom below all other curves. The dashed lines with the mass layer EPDM are positioned between these two solid and dotted ones with an exception of Sample 24 which almost equals the STL of sample sample 30 at some points.

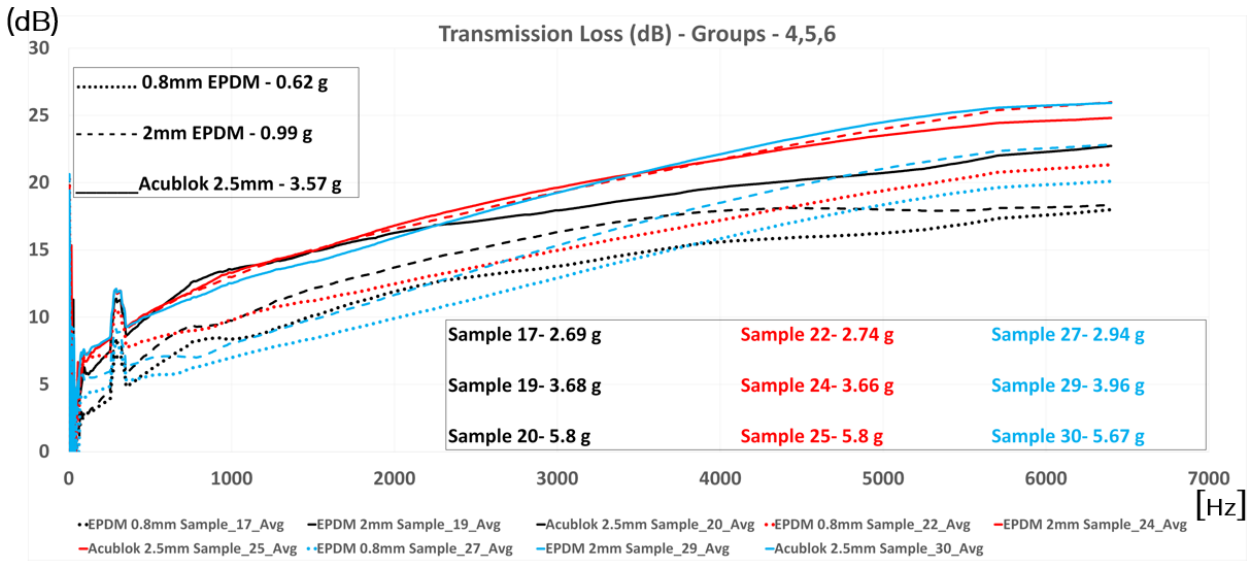


**Figure 4.6:** Sound Transmission Loss - Groups 4,5,6.

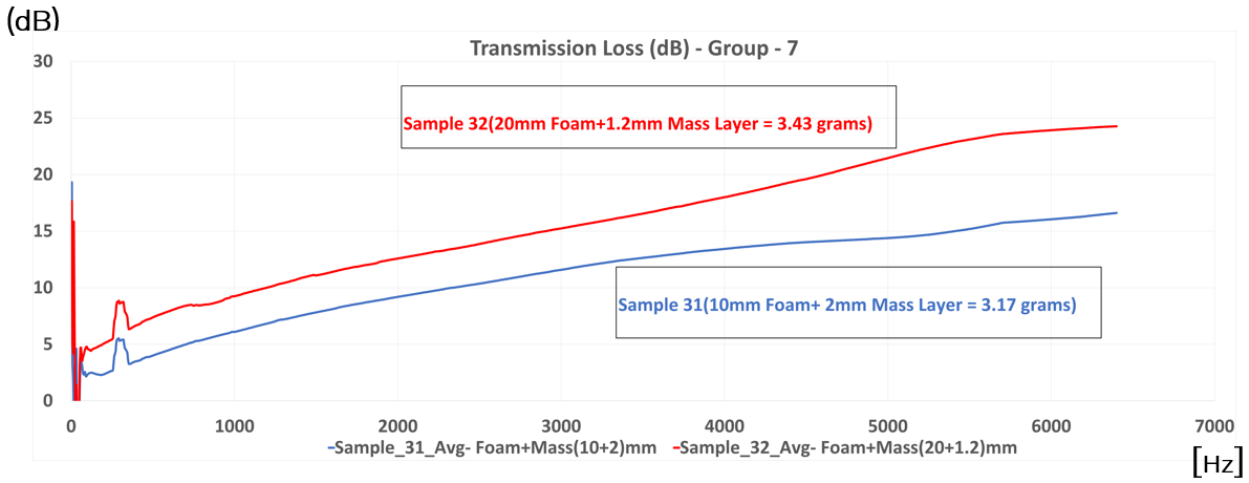


**Figure 4.7:** Sound Transmission Loss - Group 7

The STL values for the samples 31 and 32 of Group 7 are shown below in the Figure 4.7. Sample 32 has higher mass than sample 31 and is quite clear in this figure. However, sample 32 has a thicker foam which also has quite some effect in its higher transmission loss characteristics.

## 4.2 Insertion Loss Measurement Results

In this section results from the insertion loss are discussed. As mentioned above in the methods section, repeatability has played an important role. Hence the section is divided in two subsections. In repeatability section all the shortlisted samples for all the decided coverage is shown. The data is looked in 1/3 octave bands for convenience and also the acoustic transfer function and autospectra of the each results is shown. The reason to show the acoustic transfer function (ATF) is that it is normalized data and hence even if the amplitude of the source changes the ATF data would remain constant, since it is normalized. However for calculation of insertion loss the difference in auto-power spectra (APS) without and with encapsulation is considered. Also for final consideration average of the 3 runs was considered.

### 4.2.1 Repeatability Study

In this section all the shortlisted samples from the impedance tube measurement study are built and tested for repeatability. In this case repeatability means taping and re-taping the encapsulation around the EDU and every coverage. By taping it means that the encapsulation was fixed to the EDU by using tape, as seen in Figure 3.37. We can closely follow trend for each plot however since the main focus is repeatability we can address all of them togheter by saying that the results were repeatable and the deviations between the 3 runs at every coverage was within 6 and 8 dB.

We can also notice some abnormalities happening from 700 Hz to 1200 Hz i.e., the 1 kHz 1/1 Octave band. In this frequency range some of the samples those are

sample 17 and carrier showed some abnormal behaviour at 1 kHz especially at 85% coverage which is seen and investigated in the next section.

An important thing to keep in mind while observing these plots from Figure 4.8 to Figure 4.24 is that the trends for repeatability are to be noticed. There are some uncertainties which are involved due to variation in the taping each time. Along with this, the microphone grid is lifted and placed back which causes the microphone positions to not remain exactly the same.

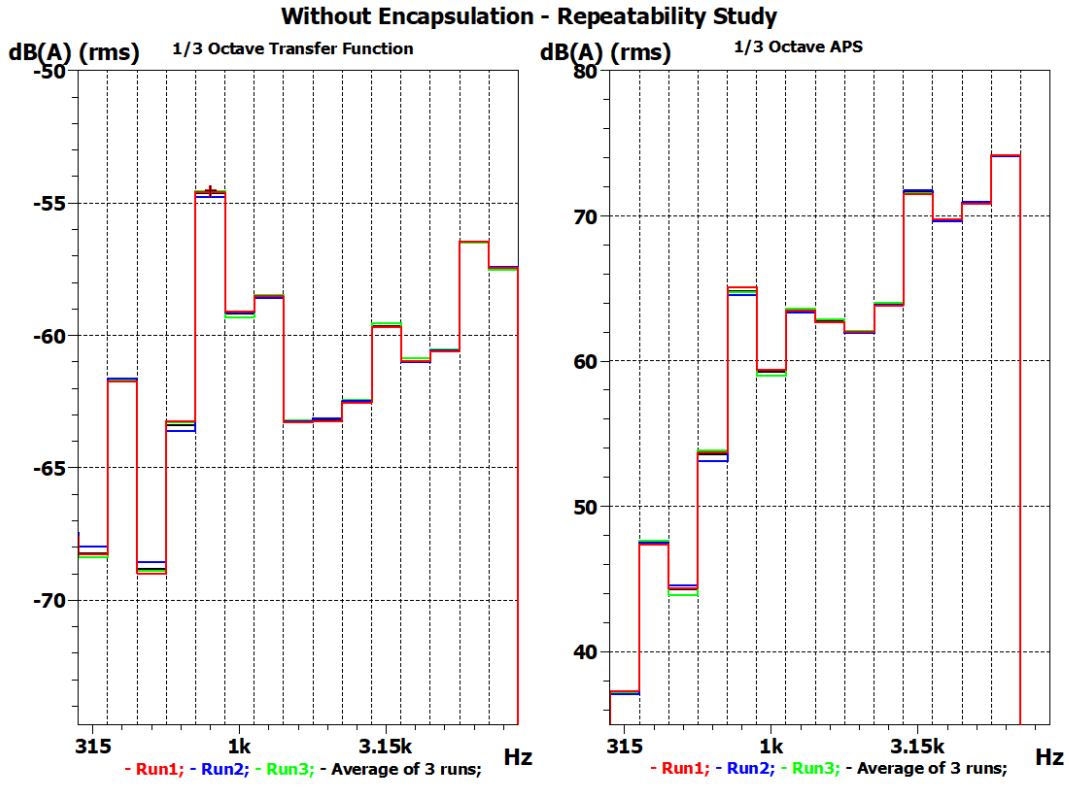


**Figure 4.8:** Repeatability Study of without encapsulation Data - Base Data

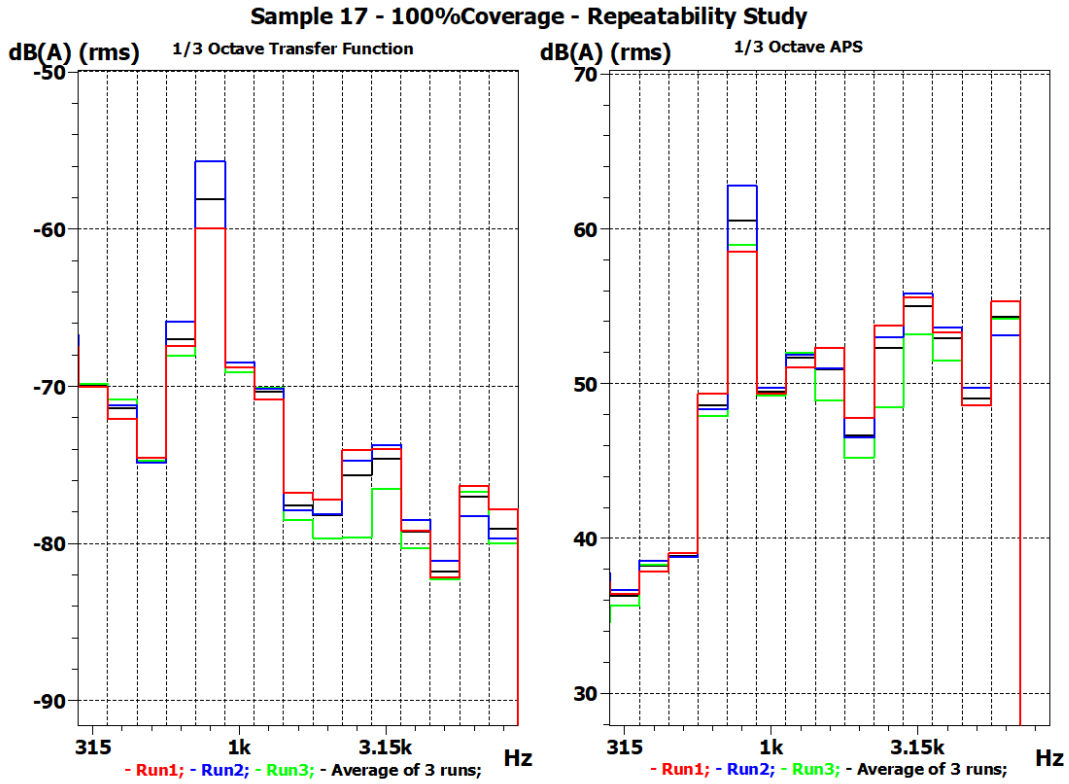


**Figure 4.9:** Repeatability Study of Sample17 at 100% coverage

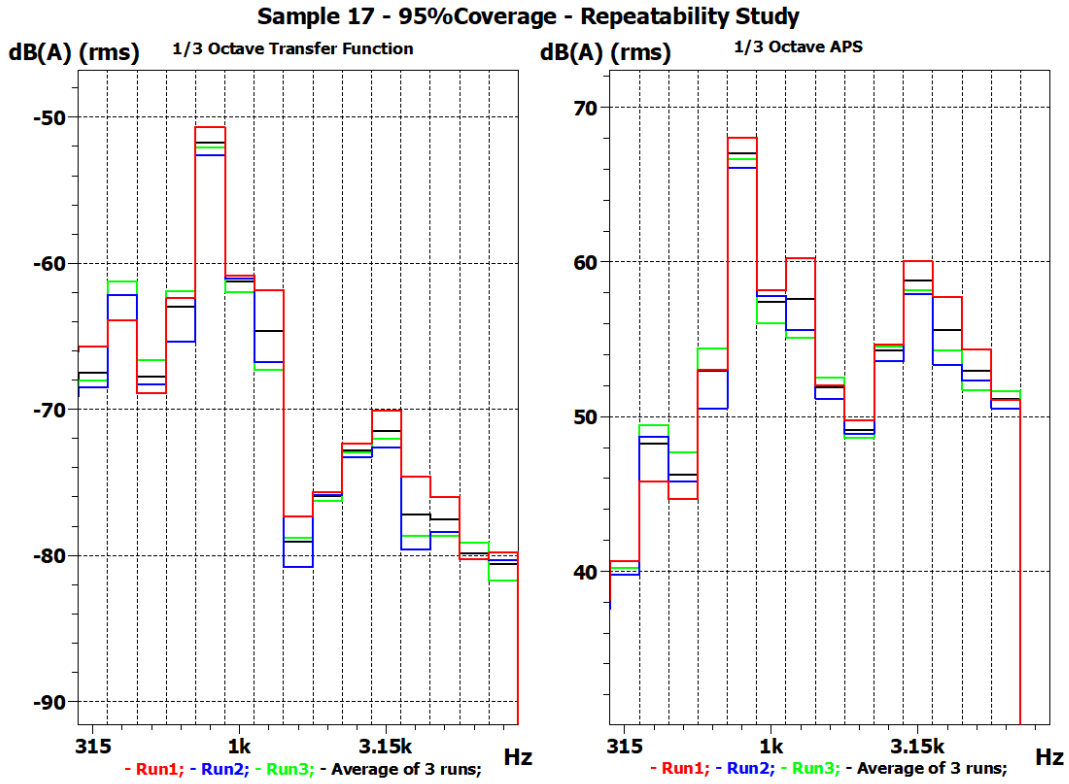


**Figure 4.10:** Repeatability Study of Sample17 at 95% coverage

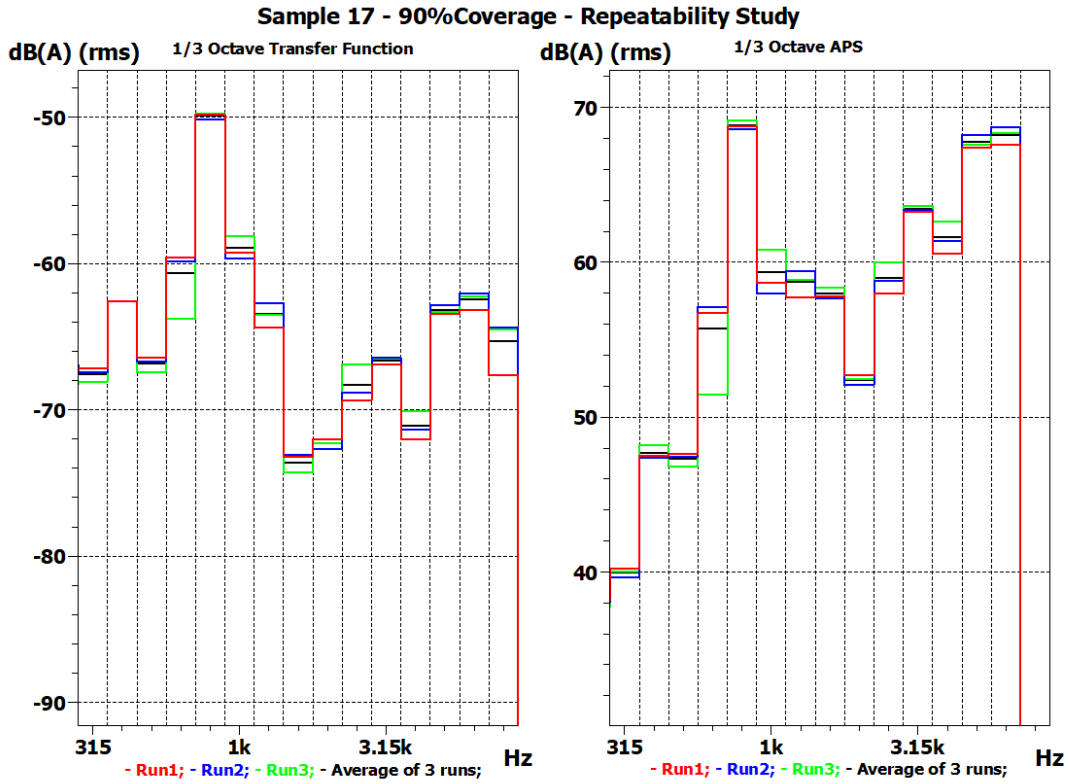


**Figure 4.11:** Repeatability Study of Sample17 at 90% coverage

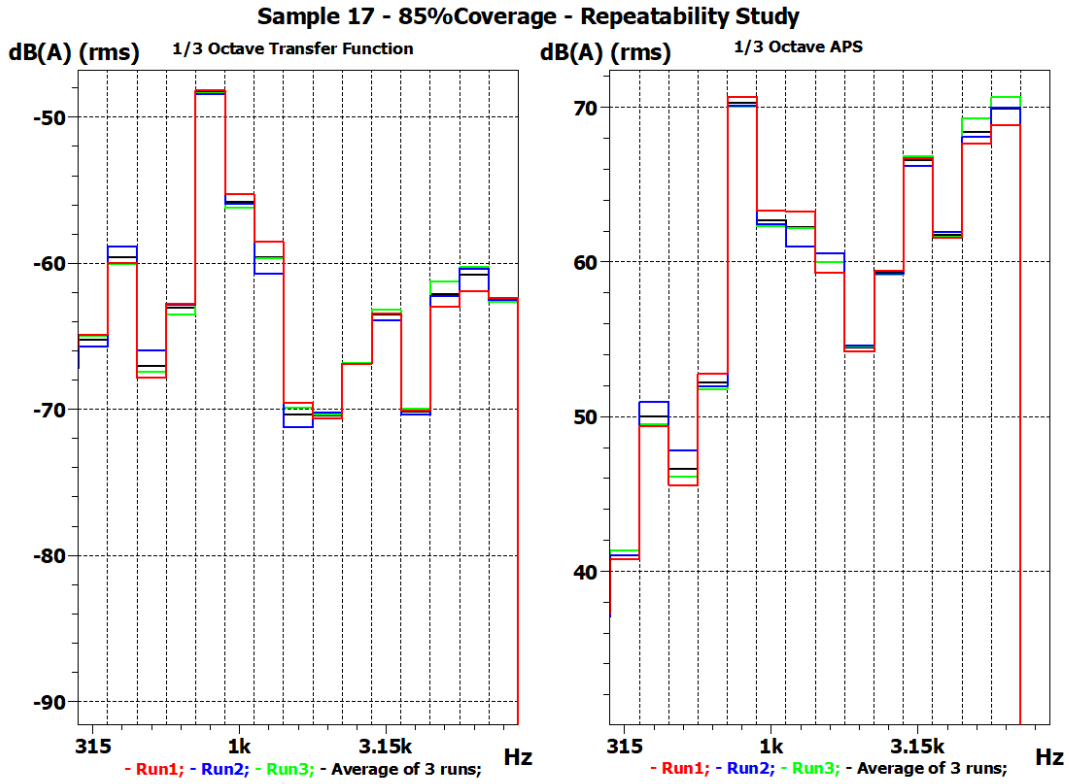


**Figure 4.12:** Repeatability Study of Sample17 at 85% coverage

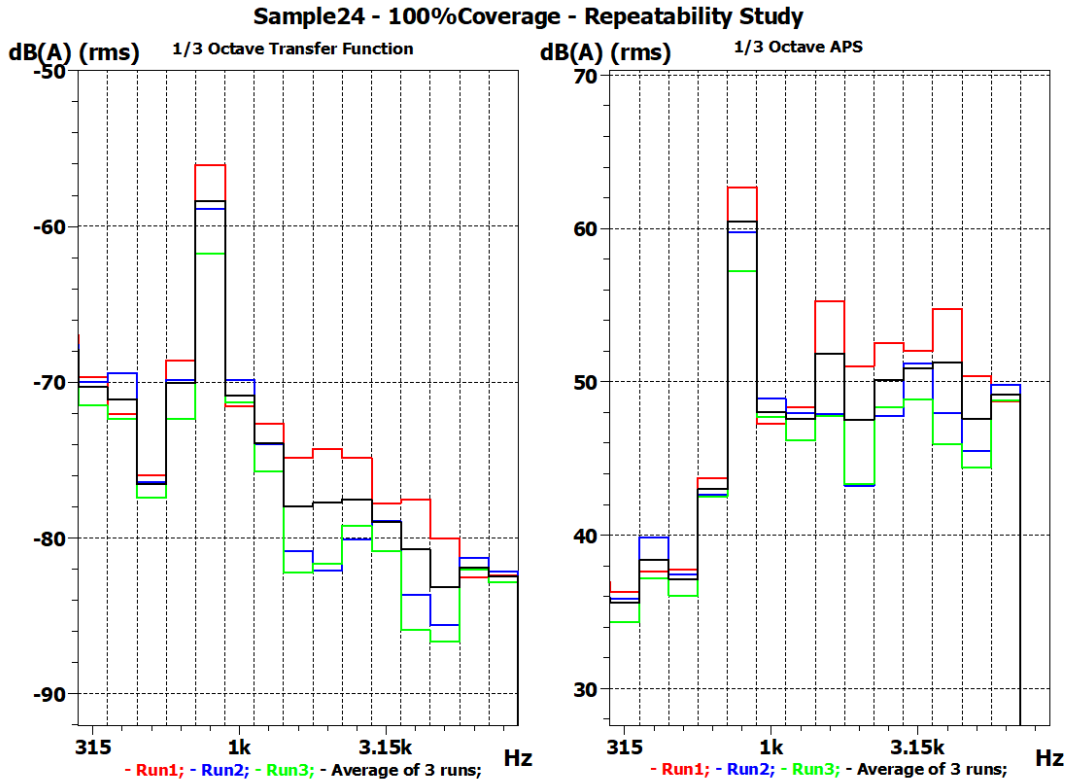


**Figure 4.13:** Repeatability Study of Sample24 at 100% coverage

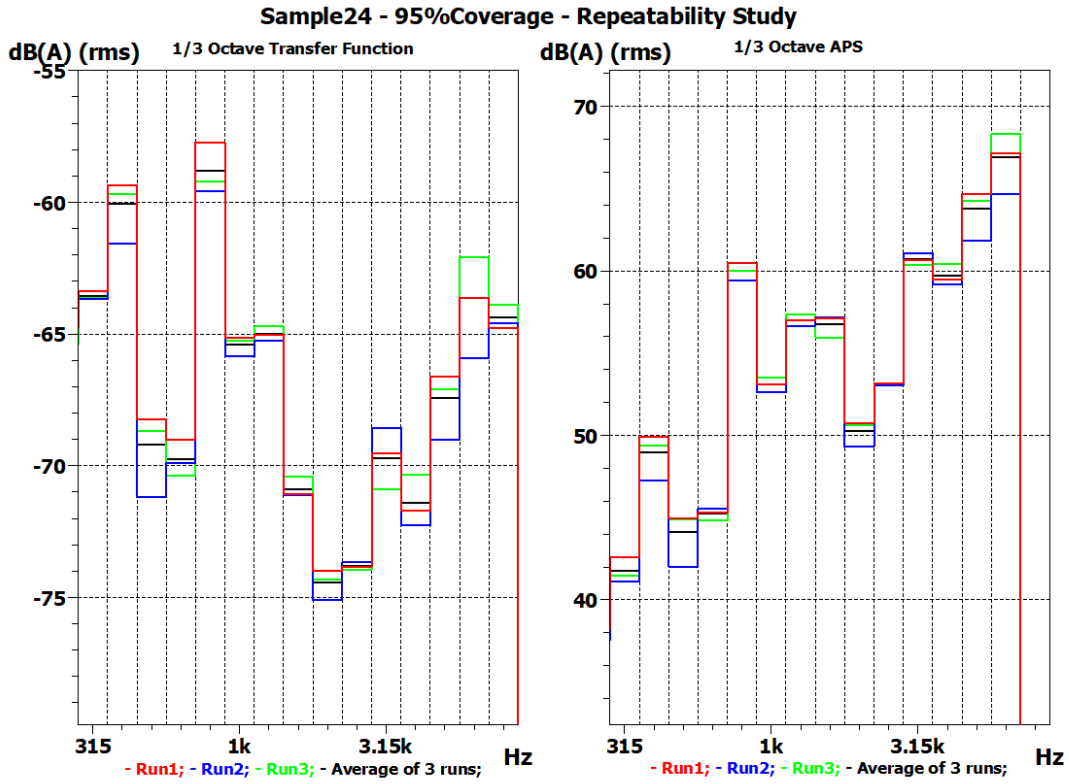


**Figure 4.14:** Repeatability Study of Sample24 at 95% coverage

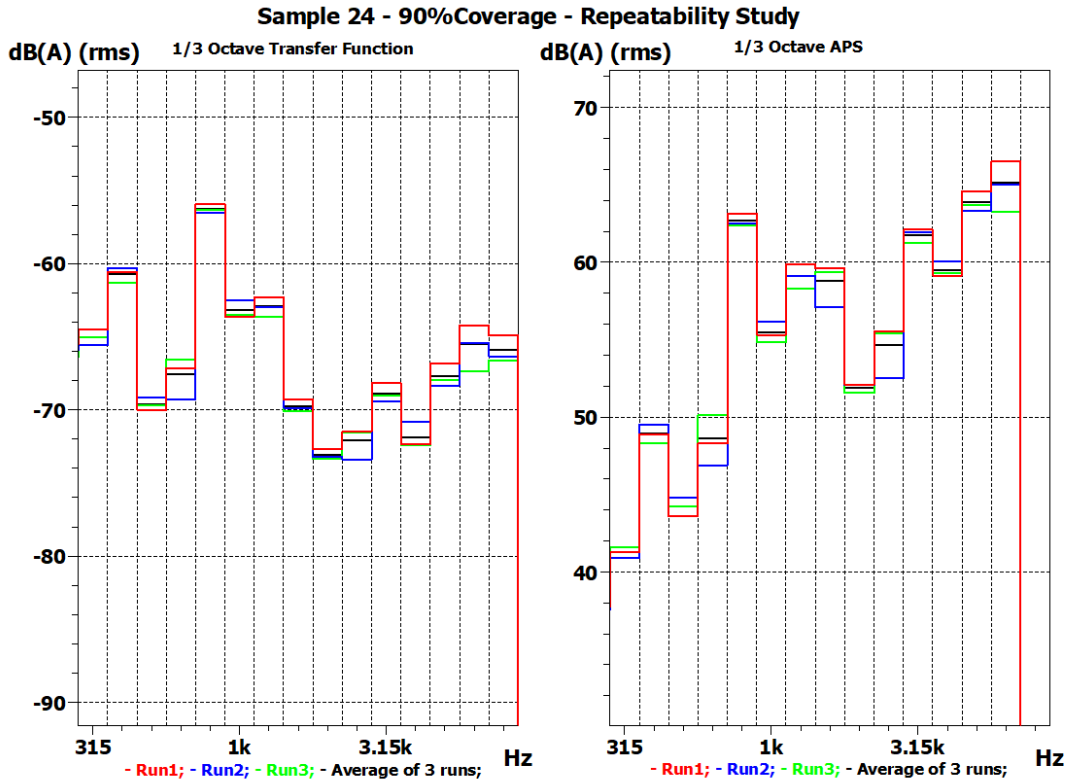


**Figure 4.15:** Repeatability Study of Sample24 at 90% coverage

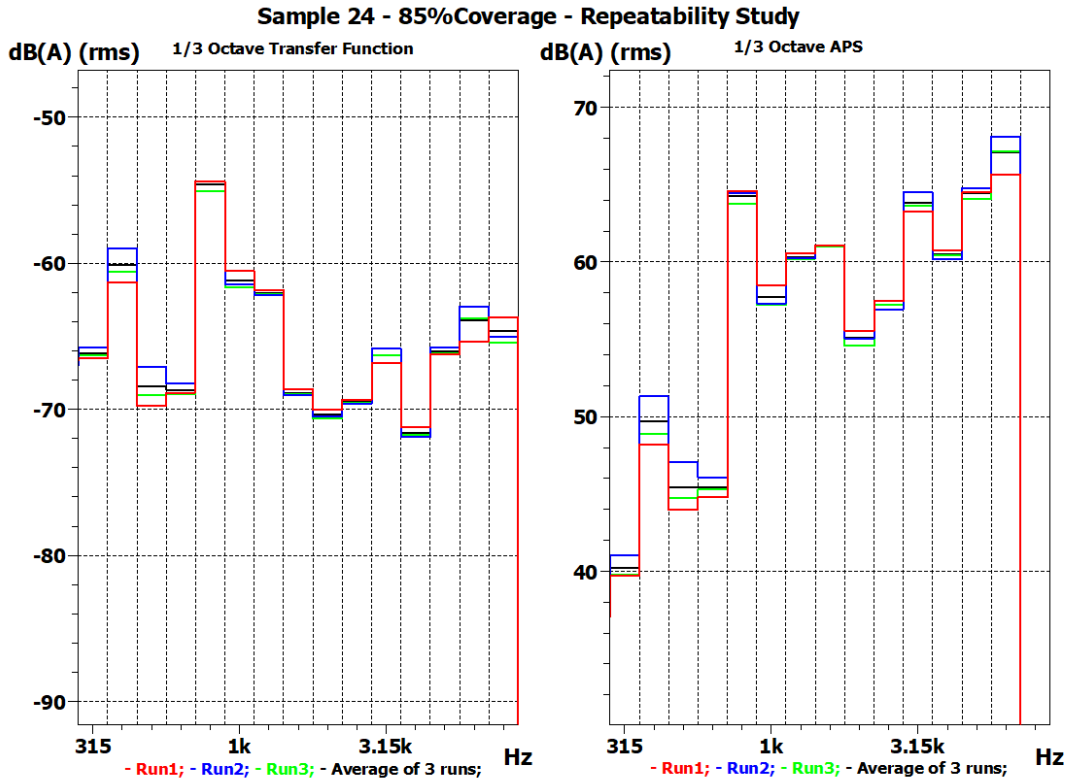


**Figure 4.16:** Repeatability Study of Sample24 at 85% coverage

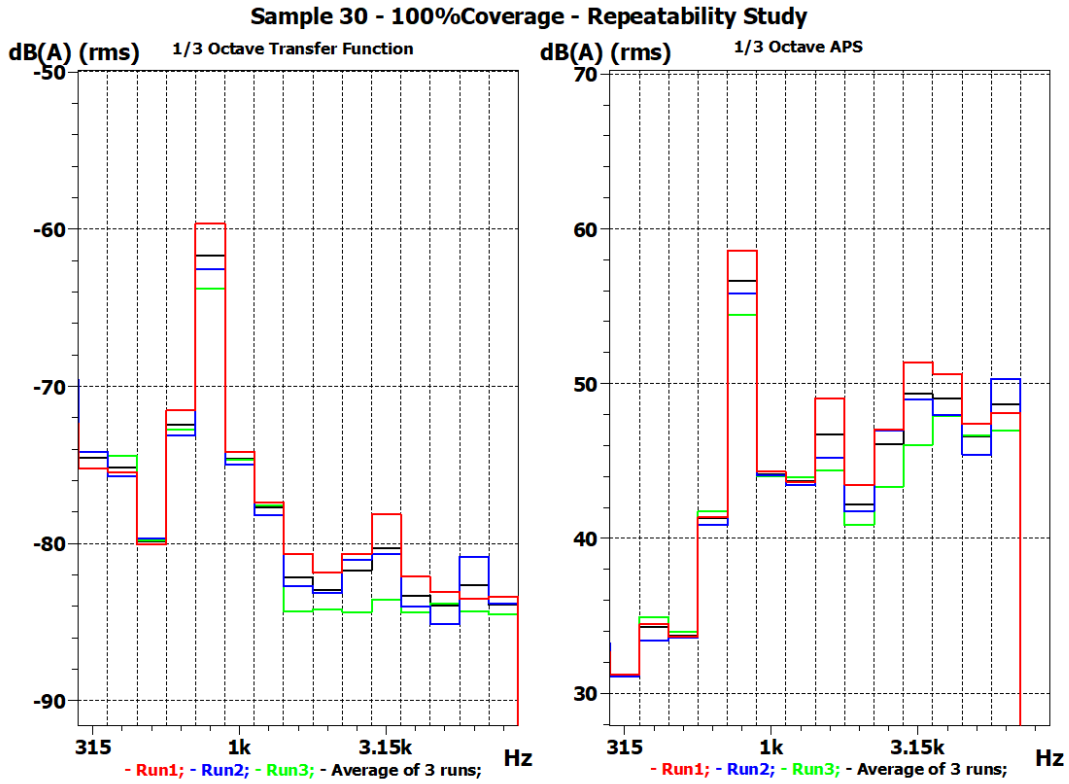


**Figure 4.17:** Repeatability Study of Sample30 at 100% coverage

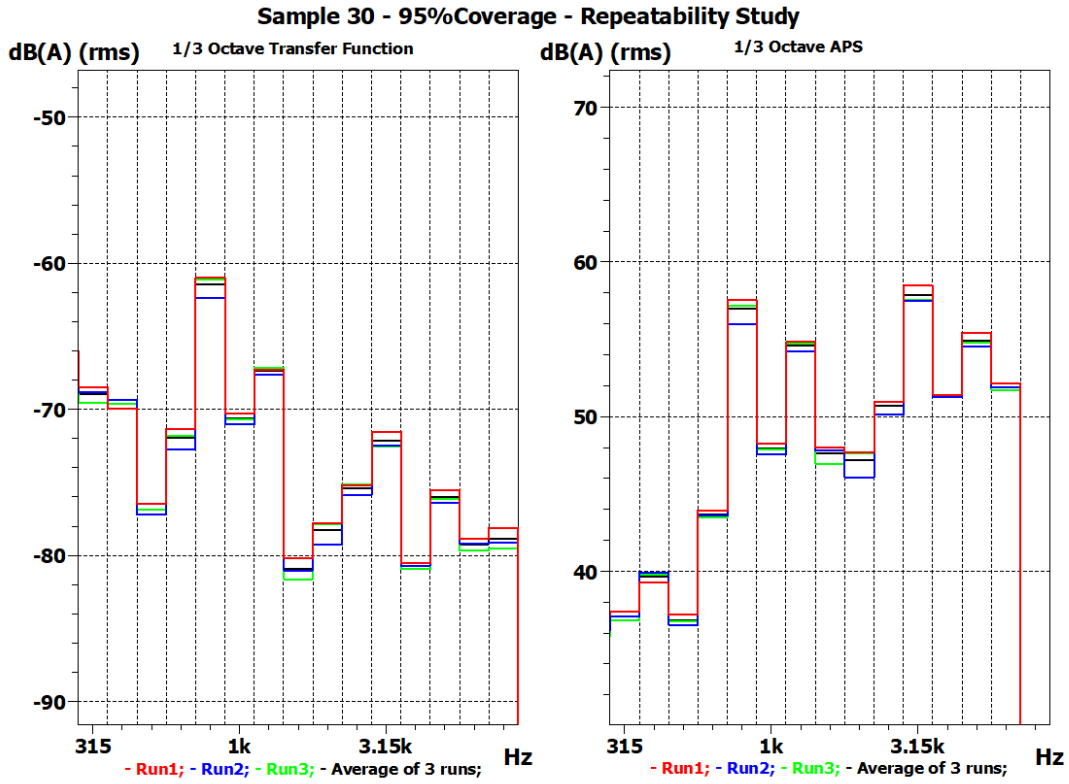


**Figure 4.18:** Repeatability Study of Sample30 at 95% coverage

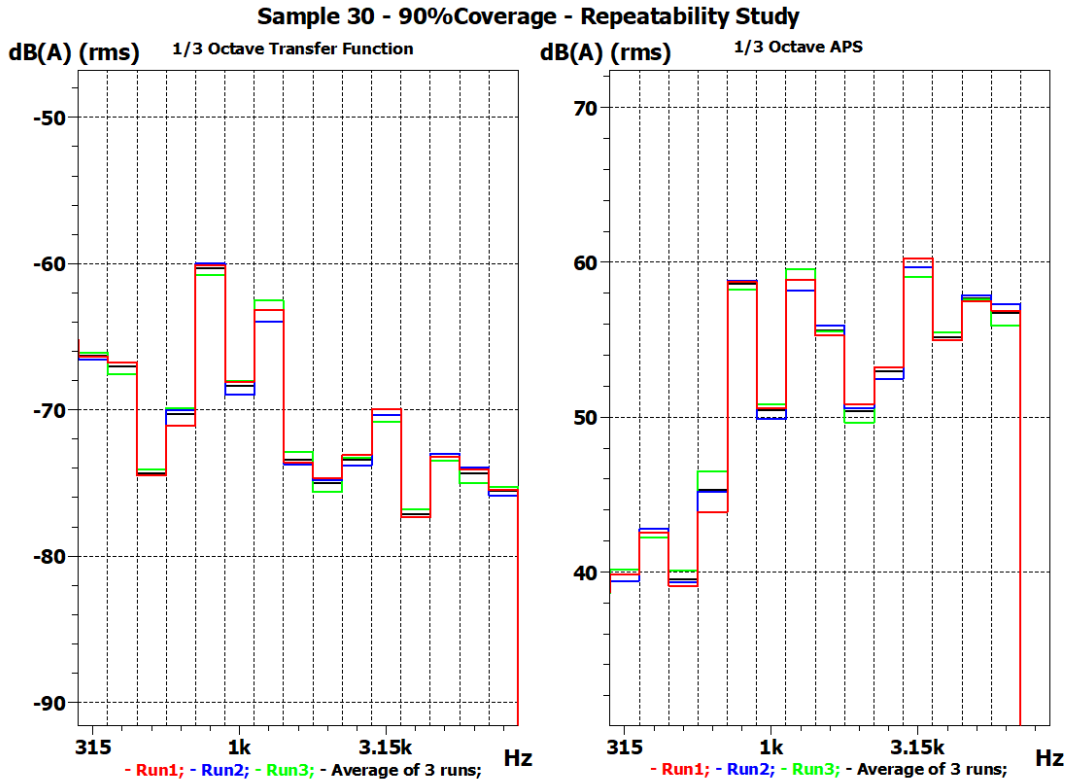


**Figure 4.19:** Repeatability Study of Sample30 at 90% coverage

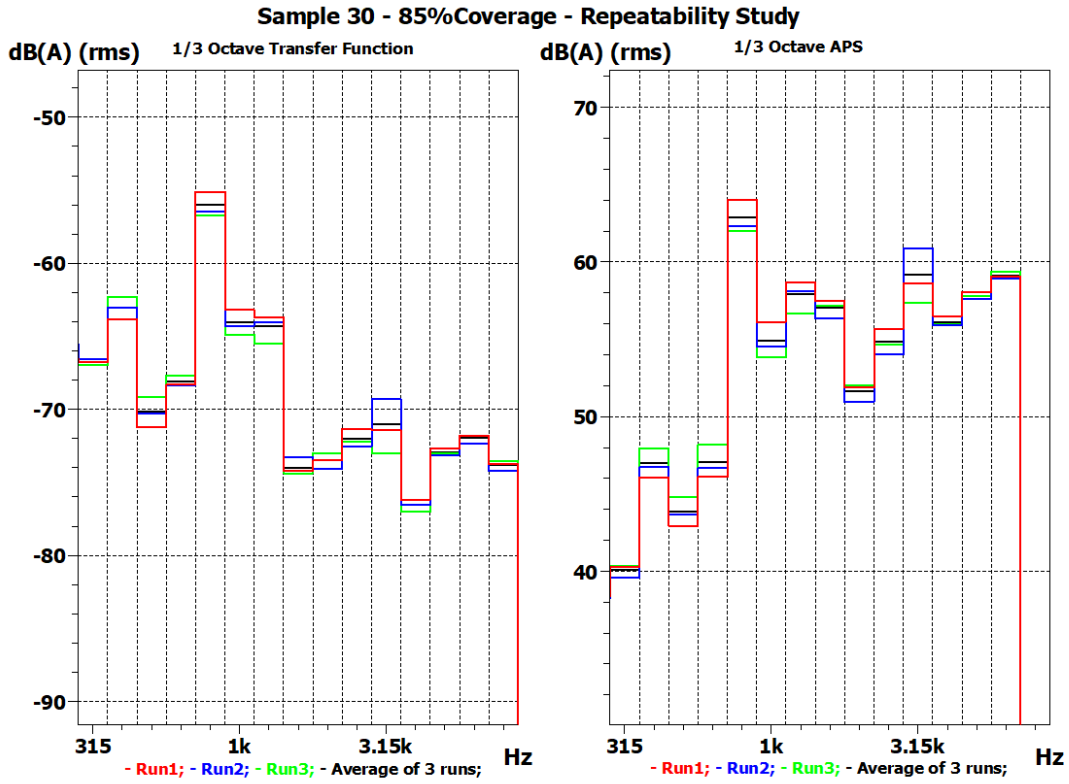


**Figure 4.20:** Repeatability Study of Sample30 at 85% coverage

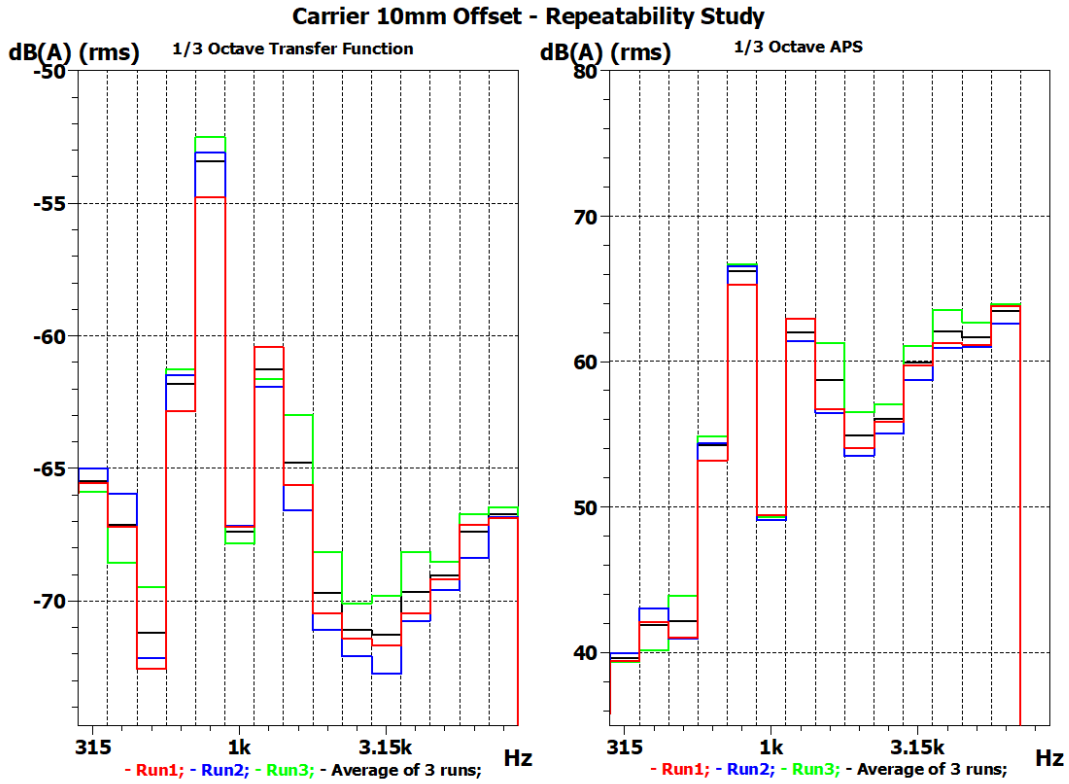


**Figure 4.21:** Repeatability Study of Carrier 10mm offset at 100% coverage

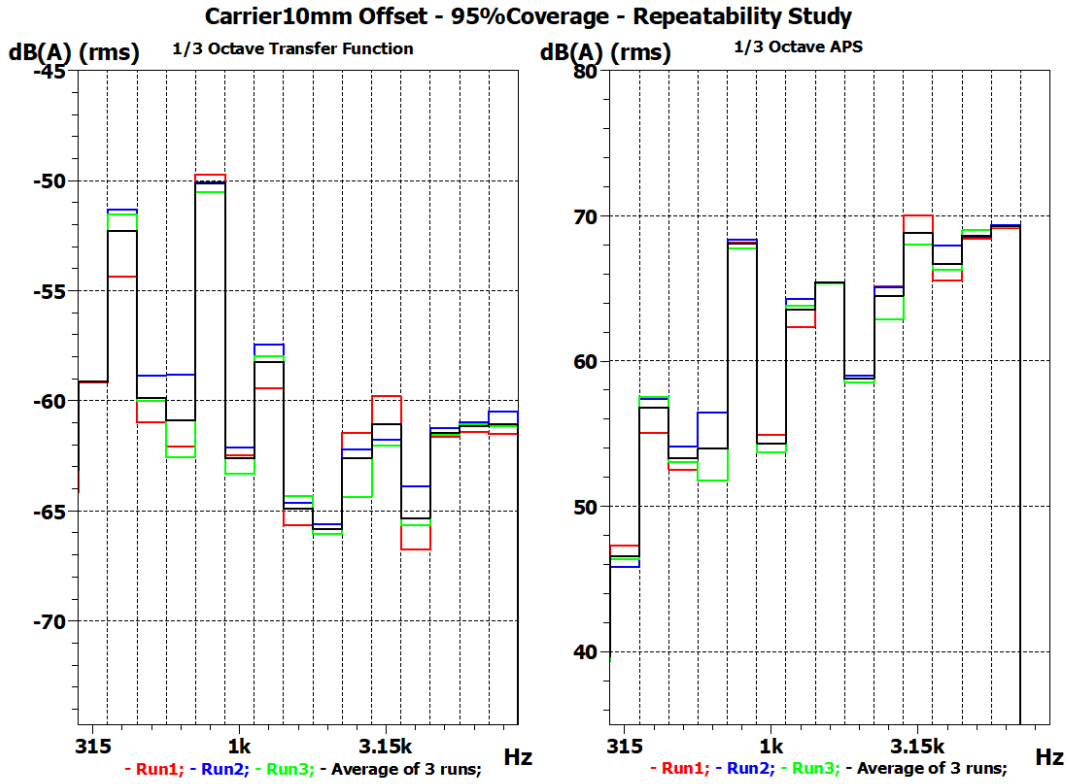


**Figure 4.22:** Repeatability Study of Carrier 10mm offset at 95% coverage

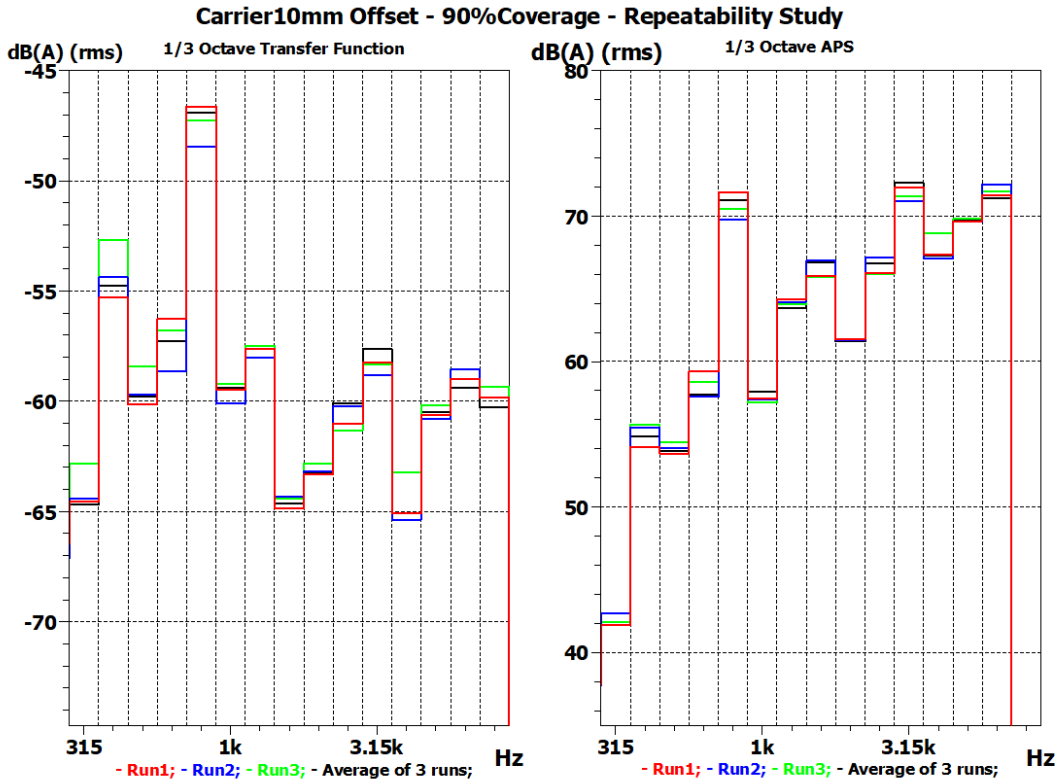


**Figure 4.23:** Repeatability Study of Carrier 10mm offset at 90% coverage

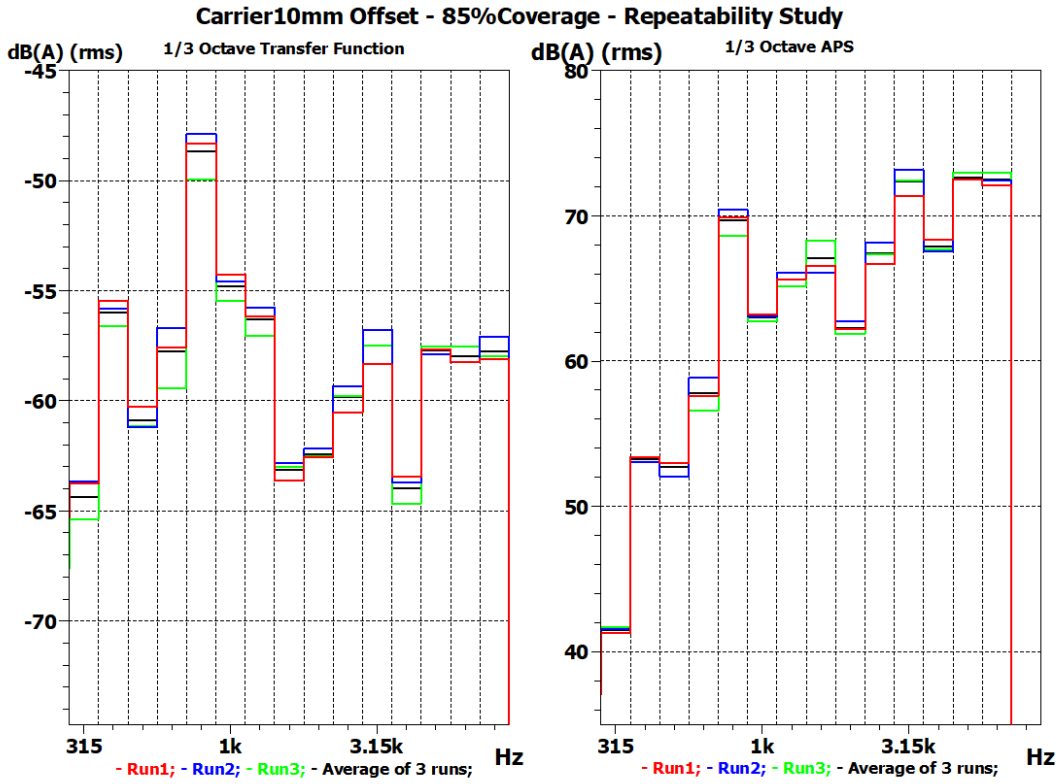


**Figure 4.24:** Repeatability Study of Carrier 10mm offset at 85% coverage

### 4.2.2 Data Visualization in Octave Bands

After the repeatability study of Insertion loss measurements in the 1/3 Octave bands, it was now time to use these measured insertion loss values into building a model for the prediction of Insertion loss. To do this, the 1/3 octave data was further visualized in 1/1 Octave bands to make the process of model building simple yet representing the frequency range of interest. For this, the values of Insertion loss in the 1/1 Octave bands of 1 kHz, 2 kHz and 4 kHz were calculated which broadly represented a frequency range of 700 Hz to 5.7 kHz. The data presented in the next section will be in 1/1 Octave bands.

#### 4.2.2.1 Sample 17

The Figure 4.25 shows the sound pressure level (SPL) for sample 17. The SPL for all the four coverage variations is compared to the SPL without the encapsulation. As it can be seen, the 100% and 95% coverage SPL are well below the without encapsulation SPL and offer a considerable insertion loss at 2 kHz and 4 kHz. However, at 1 kHz, the SPL for 95% coverage line is higher than the without encapsulation SPL by 0.1 dB(A) which shows an amplification.

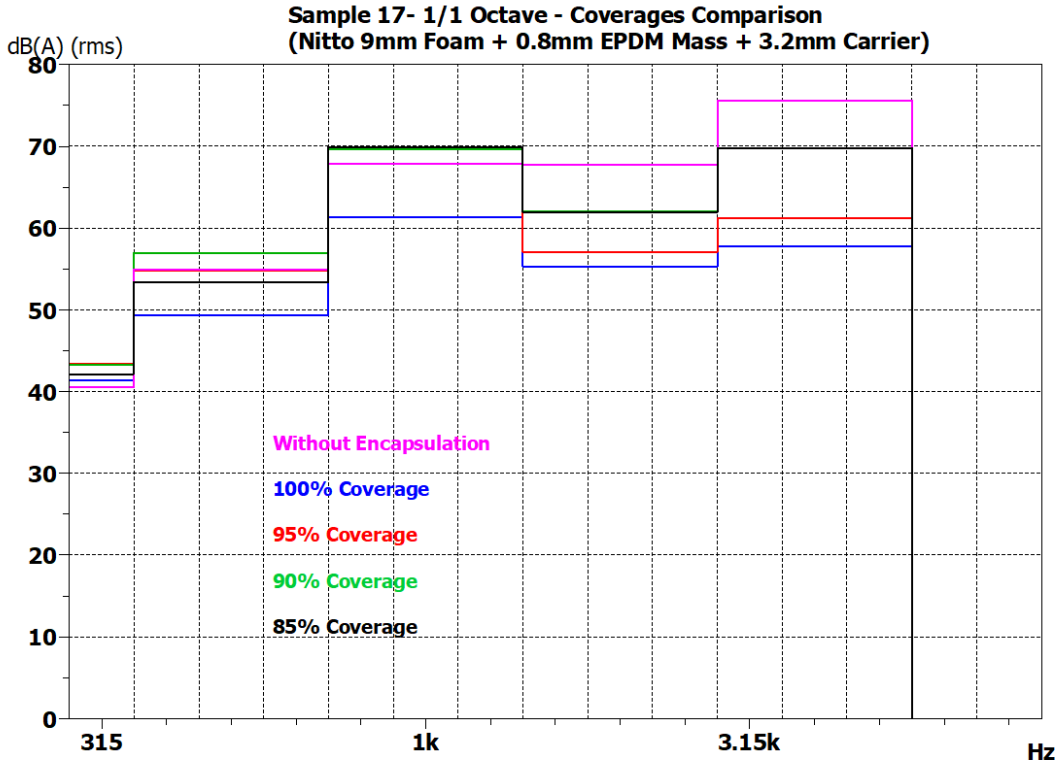


**Figure 4.25:** Sample 17 - All Percentage Coverages

There is a similar amplification of 1.9 dB and 3.7 dB for 90% and 85% coverage SPL respectively at 1 kHz. This amplification might be because of the measurement uncertainties as there was taping and re-taping of the encapsulation on the EDU for repeatability studies. Along with this, the way the holes were drilled on the

encapsulation might have also contributed but however, this is not something which is verifiable with the results obtained.

Never the less, all these kind of uncertainties were observed during the measurements which might alter the results in both ways. They were tried to be minimized as much as possible by focusing on repeatability of th e tests.

#### 4.2.2.2 Sample 24

The Figure 4.26 shows the sound pressure level (SPL) for sample 24. All the percentage coverages offer a significant insertion loss at 1 kHz, 2 kHz and 4 kHz. There is no amplification seen for any type of coverage. If looked closely, the SPL for 90% coverage at 4 kHz is just 0.4 dB(A) than the 95% coverage. However, this is not alarming unless it would have been the other case.

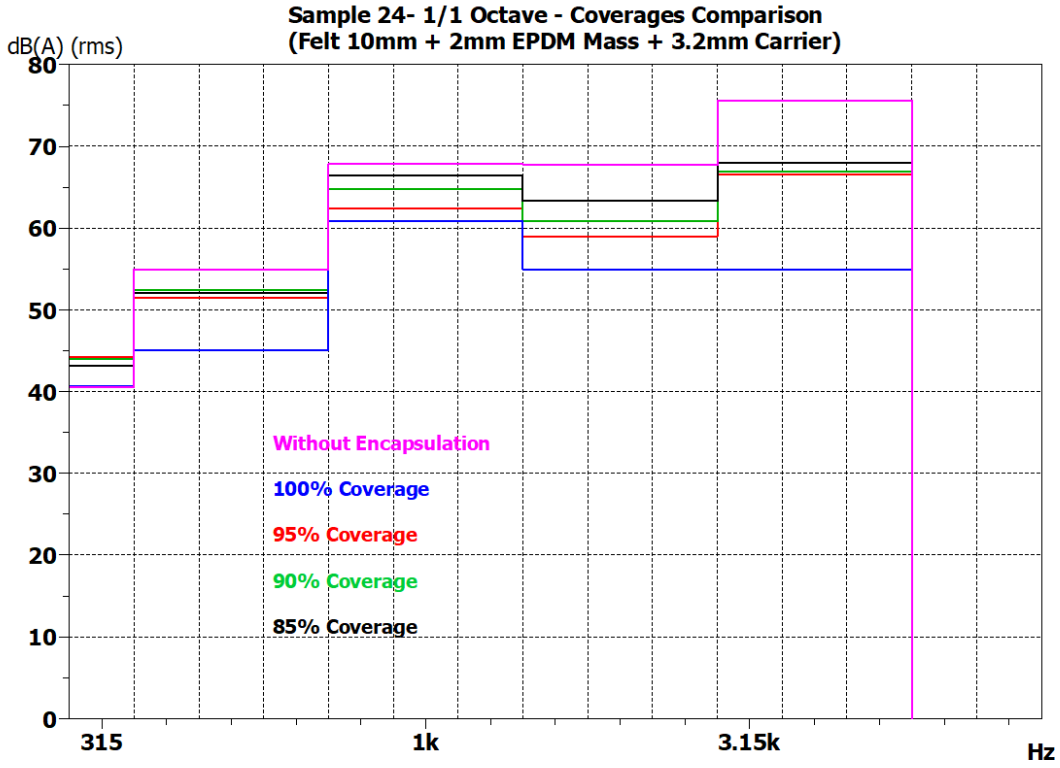


**Figure 4.26:** Sample 24 - All percentage Coverages

#### 4.2.2.3 Sample 30

The Figure 4.27 shows the sound pressure level (SPL) for sample 30. All the percentage coverages offer a significant insertion loss at 1 kHz, 2 kHz and 4 kHz. There is no any kind of amplification for any type of coverage considering the fact that the holes were drilled non-uniformly for this particular sample.

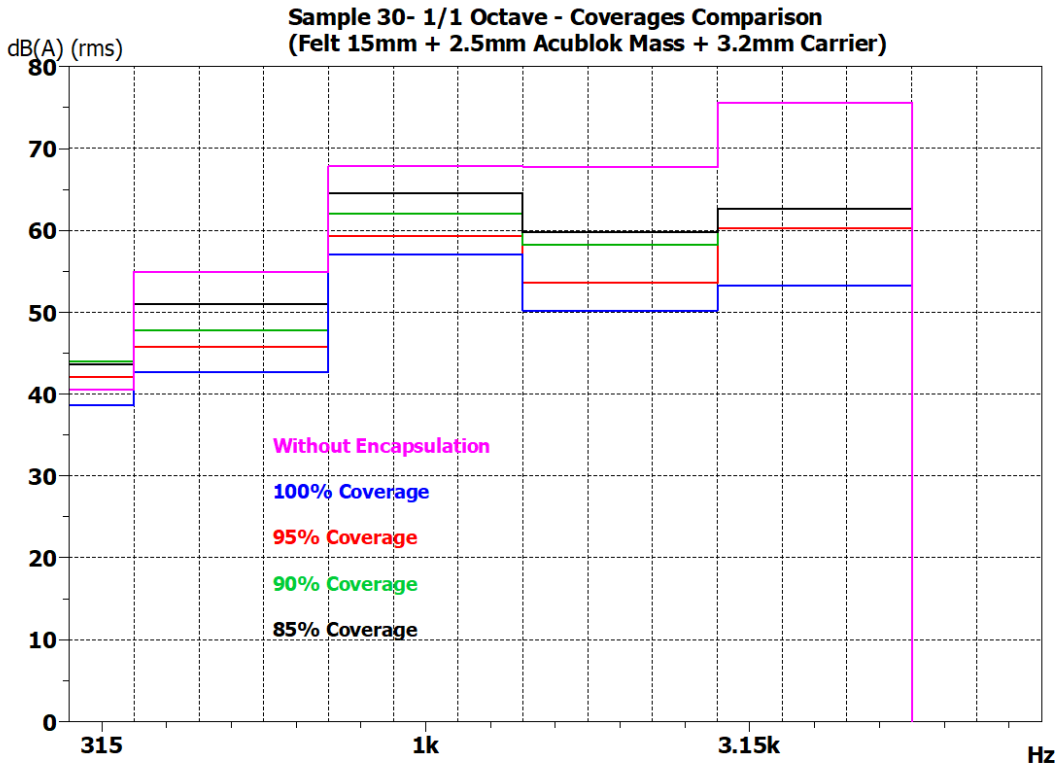


**Figure 4.27:** Sample 30 - All percentage Coverages

But, there is an exception where the SPL for 90% coverage and 85% coverage at 4 kHz is equal to 62.6 dB(A) which might have been caused by the shape of holes drilled or some other measurement uncertainty.

#### 4.2.2.4 Carrier Template

The Figure 4.28 shows the sound pressure level (SPL) for the carrier template. At 1 kHz and 2 kHz, only the 100% coverage gives some insertion loss and all other coverages are either equal or higher than the without encapsulation SPL. This is mainly because of the gaps present between the EDU and the carrier even after taping it well. This gap exists as there are no foam or mass layers to fill them. At 4 kHz, only the 85% coverage has higher SPL than the without encapsulation SPL.

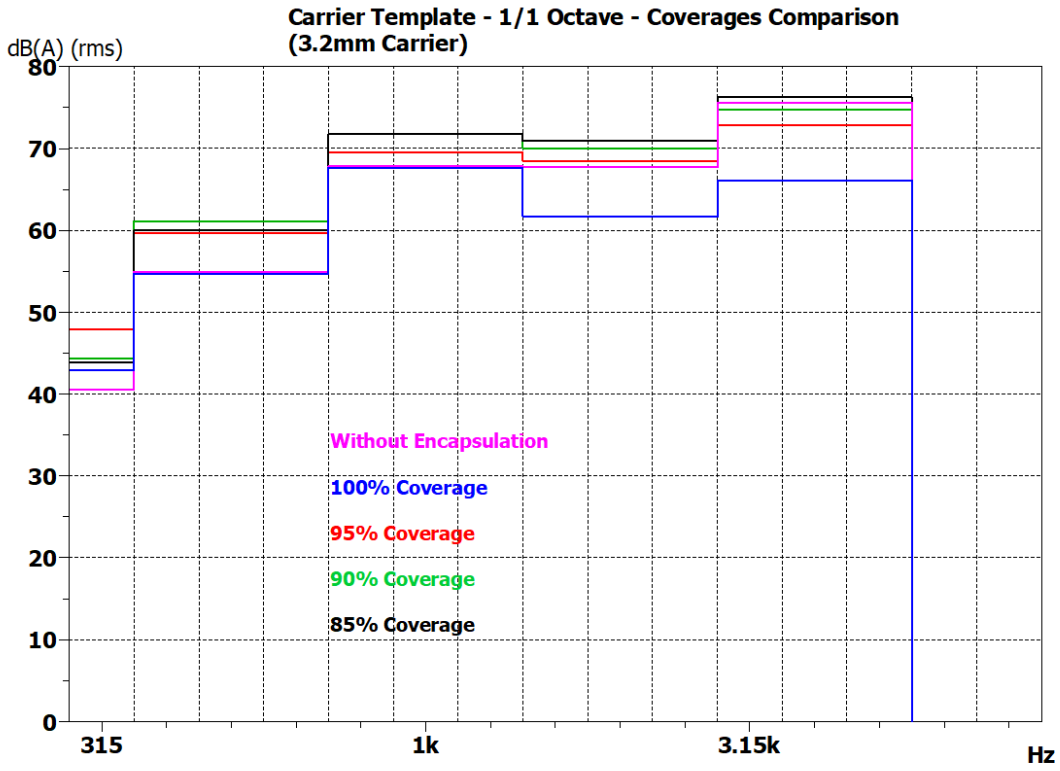


**Figure 4.28:** Carrier - All percentage Coverages

#### 4.2.2.5 Special Sample - 1

The Figure 4.29 shows the sound pressure level (SPL) for the special sample 1. There is significant insertion loss offered at 1 kHz, 2 kHz and 4 kHz in all types of coverage.

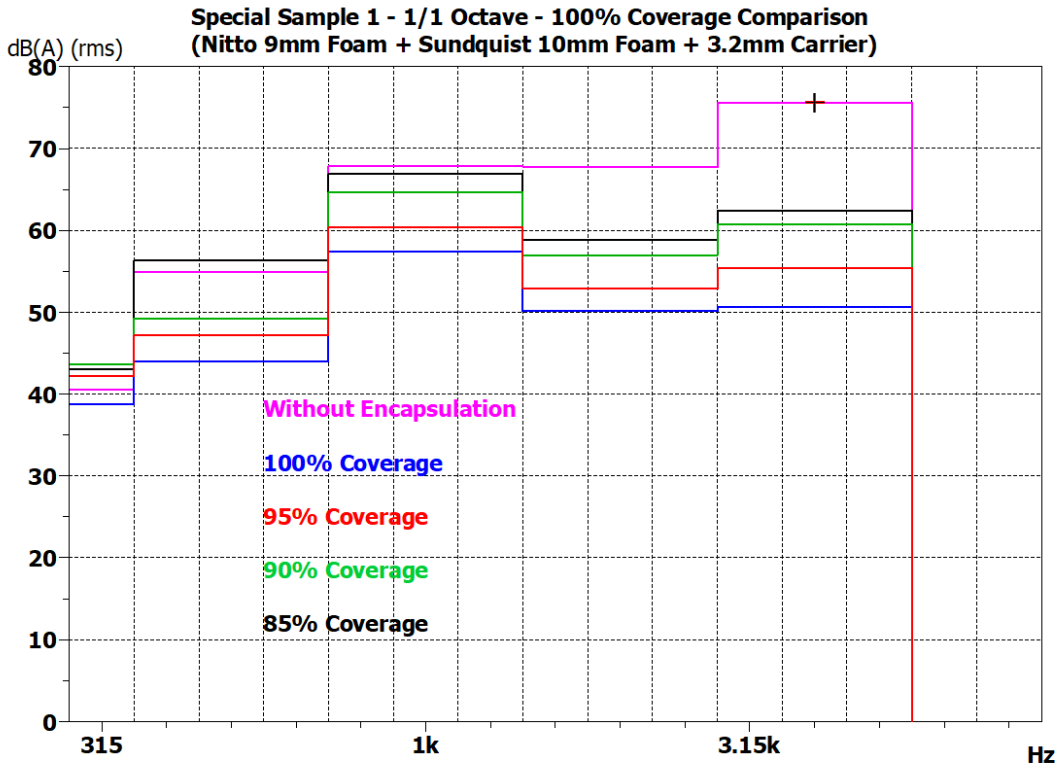


**Figure 4.29:** Special Sample 1 - All percentage Coverages

The amplification which was seen in the Sample 17 and Carrier template at 1kHz in 85% coverage can be further studied in their respective narrow band SPL. In the Figure 4.30, there are three curves representing the three different conditions. Each curve is obtained after the sound pressure levels are averaged over 10 microphones. it can be seen that at 797 Hz, the SPL for both sample 17 and carrier are higher than the without encapsulation SPL. As these peaks appear at the exact same frequency, it is suspected that there is resonance taking place between the EDU casing and these encapsulations. Further, the carrier has higher SPL at 937 Hz which again promises to be some kind of phenomenon, either resonance or diffraction.

**NOTE: The insertion loss measurements for special sample 1 at coverages 95%, 90% and 85% were done only once which means that they did not undergo the repeatability method.**

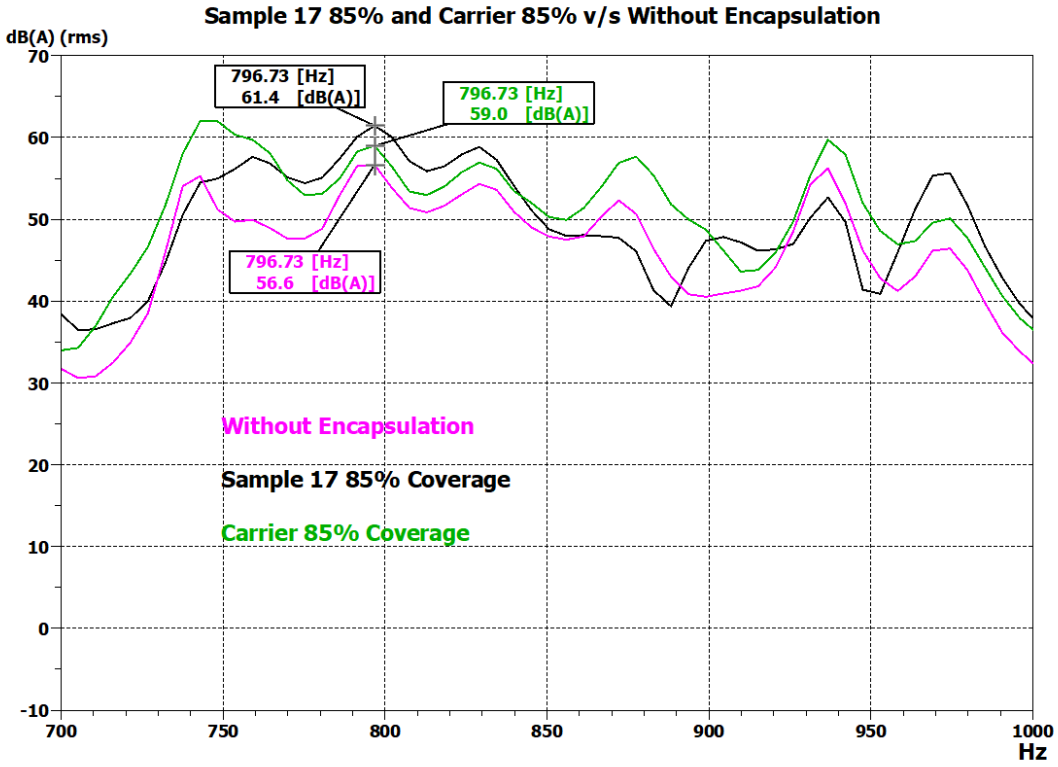


**Figure 4.30:** Sample 17 & Carrier at 1/1 Octave 1kHz - 85 % Coverages

Because there is an amplification at these two frequencies for these particular encapsulations, it is being observed at the 1 kHz peak in the 1/1 Octave bands. This is because of the fact that both 797 Hz and 937 Hz lie in the upper and lower limit of the 1 kHz 1/1 Octave peak which is from 707 Hz to 1414 Hz. As all the levels are added up, this amplification too is getting added up.

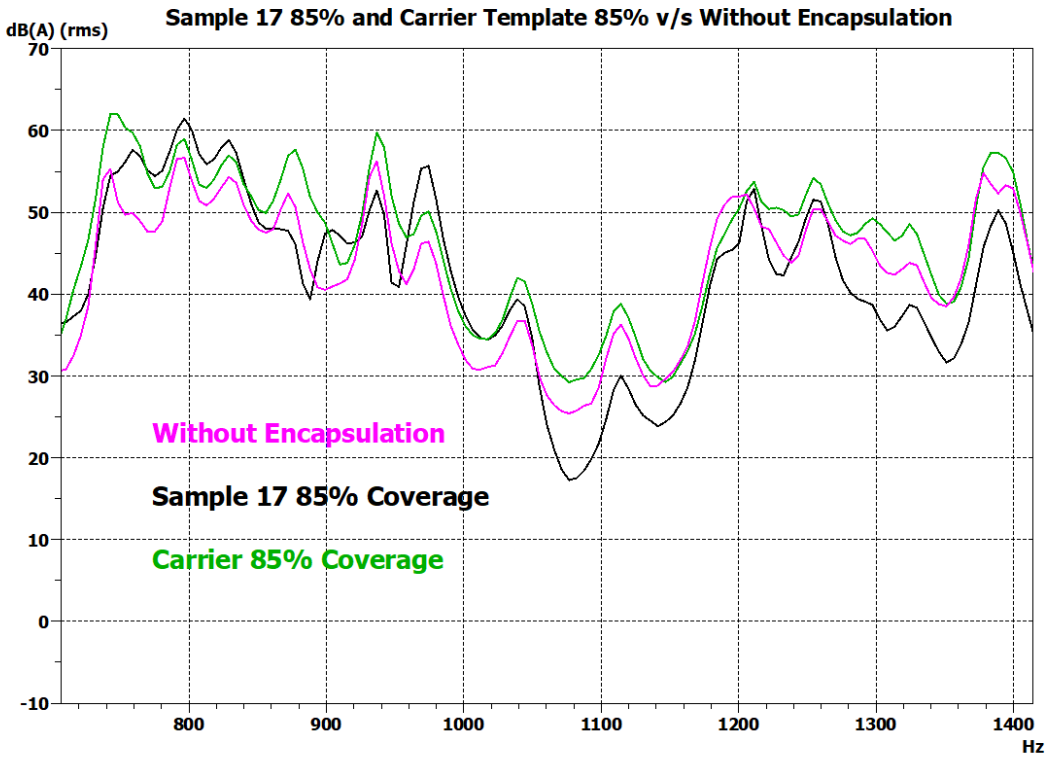


**Figure 4.31:** Sample 17 & Carrier in Narrow Band - 85 % Coverages

The Figure 4.31 shows the 1 kHz Octave range in which it can be seen that the SPL for without encapsulation is not so dominant throughout the range which again explains the amplification of levels in the 1/1 Octave bands. The SPL and the insertion loss values for all the encapsulations at different coverage types (along with the weight) is summarized in the Figure 4.32.

| 100% Coverage | *Base Measurement* | Wt. 2851 in gms | IL in dB | Wt. 3475,4 in gms | IL in dB | Wt. 5753,9 in gms | IL in dB | Wt.1686,9 ingms | IL in dB | Wt.3004,1 in gms | IL in dB |
|---|---|---|---|---|---|---|---|---|---|---|---|
| Frequency in Hz | *Without Encaps* | Sample17 | IL sample17 | Sample24 | IL sample24 | Sample30 | IL sample30 | Carrier 10mm | IL Carrier 10mm | Special Sample1 | IL Special Samples1 |
| 1000 | *67,8* | 61,3 | 6,5 | 60,9 | 6,9 | 57,1 | 10,7 | 67,7 | 0,1 | 57,4 | 10,4 |
| 2000 | *67,7* | 55,3 | 12,4 | 54,9 | 12,8 | 50,2 | 17,5 | 61,7 | 6 | 50,1 | 17,6 |
| 4000 | *75,6* | 57,7 | 17,9 | 55 | 20,6 | 53,2 | 22,4 | 66,1 | 9,5 | 50,7 | 24,9 |
| 95%Coverage | | Wt. 2699,9 | | Wt. 3324 | | Wt. 5410,8 | | Wt. 1596,9 | | | |
| Frequency | *Without Encaps* | Sample17 | IL sample17 | Sample24 | IL sample24 | Sample30 | IL sample30 | Carrier 10mm | | Wt. 2845 | |
| 1000 | *67,8* | 67,9 | -0,1 | 62,3 | 5,5 | 59,3 | 8,5 | 69,5 | -1,7 | 60,5 | 7,3 |
| 2000 | *67,7* | 57 | 10,7 | 59 | 8,7 | 53,6 | 14,1 | 68,5 | -0,8 | 52,9 | 14,8 |
| 4000 | *75,6* | 61,2 | 14,4 | 66,5 | 9,1 | 60,2 | 15,4 | 72,9 | 2,7 | 55,4 | 20,2 |
| 90%Coverage | | Wt. 2563,5 | | Wt. 3133,6 | | Wt. 5090,5 | | Wt. 1502,6 | | | |
| Frequency | *Without Encaps* | Sample17 | IL sample17 | Sample24 | IL sample24 | Sample30 | IL sample30 | Carrier 10mm | | Wt.2673,2 | |
| 1000 | *67,8* | 69,7 | -1,9 | 64,8 | 3 | 62,1 | 5,7 | 71,7 | -3,9 | 64,6 | 3,2 |
| 2000 | *67,7* | 62 | 5,7 | 60,8 | 6,9 | 58,3 | 9,4 | 70 | -2,3 | 57 | 10,7 |
| 4000 | *75,6* | 69,8 | 5,8 | 66,9 | 8,7 | 62,6 | 13 | 74,7 | 0,9 | 60,9 | 14,7 |
| 85%Coverage | | Wt. 2412 | | Wt. 2939,1 | | Wt. 4965,4 | | Wt. 1396,6 | | | |
| Frequency | *Without Encaps* | Sample17 | IL sample17 | Sample24 | IL sample24 | Sample30 | IL sample30 | Carrier 10mm | | Wt. 2537,8 | |
| 1000 | *67,8* | 71,5 | -3,7 | 66,4 | 1,4 | 64,6 | 3,2 | 71,8 | -4 | 66,7 | 1,1 |
| 2000 | *67,7* | 63,3 | 4,4 | 66,3 | 1,4 | 59,8 | 7,9 | 70,9 | -3,2 | 58,7 | 9 |
| 4000 | *75,6* | 71,1 | 4,5 | 68 | 7,6 | 62,7 | 12,9 | 76,2 | -0,6 | 62,4 | 13,2 |

**Figure 4.32:** Insertion Loss Values in 1/1 Octave.

The insertion loss values mentioned in the Figure 4.32 will now be made use of to build the final prediction model. Along with these, the absorption coefficient and transmission loss values were also calculated in 1/1 Octave bands using the impedance tube results. They are shown in the Figure 4.33.

| TL | Sample 17 | Sample 24 | Sample 30 | Carrier 10mm | SS1 |
|---|---|---|---|---|---|
| 1000 | 22 | 36 | 35 | 32 | 45 |
| 2000 | 26 | 43 | 42 | 35 | 50 |
| 4000 | 30 | 51 | 52 | 42 | 63 |
| | | | | | |
| **Alpha** | **Sample 17** | **Sample 24** | **Sample 30** | **Carrier 10mm** | **SS1** |
| 1000 | 0,19 | 0,16 | 0,3 | 0,02 | 0,43 |
| 2000 | 0,64 | 0,39 | 0,67 | 0,05 | 0,77 |
| 4000 | 0,66 | 0,81 | 0,97 | 0,23 | 0,88 |

**Figure 4.33:** Impedance Tube Results in Octave Bands.

Insertion loss values using the theoretical formula is in general evaluated using ratio of sound power radiated with and without the isolation as mentioned in the theory section of insertion loss. Below we have evaluated the insertion loss for one of the cases for validation and understanding of the closeness of our results with theoretical calculation.
Sound power for without encapsulation data and all the other samples was calculated using equation 2.46 and the insertion loss is calculated using equation 2.44 and is summarised in the table below:

| 100% Coverage | IL Theory | IL Level difference | IL Theory | IL Level difference | IL Theory | IL Level difference | IL Theory | IL Level difference | IL Theory | IL Level difference |
|---|---|---|---|---|---|---|---|---|---|---|
| Frequency in Hz | IL sample17 | IL sample17 | IL sample24 | IL sample24 | IL sample30 | IL sample30 | IL Carrier 10mm | IL Carrier 10mm | IL Special Samples1 | IL Special Samples1 |
| 1000 | -0,4 | 6,5 | -0,4 | 6,9 | -0,7 | 10,7 | 0,0 | 0,1 | -0,6 | 10,4 |
| 2000 | -0,8 | 12,4 | -0,8 | 12,8 | -1,1 | 17,5 | -0,4 | 6 | -1,1 | 17,6 |
| 4000 | -1,0 | 17,9 | -1,2 | 20,6 | -1,4 | 22,4 | -0,5 | 9,5 | -1,5 | 24,9 |
| 95%Coverage | | | | | | | | | | |
| Frequency | IL sample17 | IL sample17 | IL sample24 | IL sample24 | IL sample30 | IL sample30 | IL Carrier 10mm | | IL Special Samples1 | |
| 1000 | 0,0 | -0,1 | -0,3 | 5,5 | -0,5 | 8,5 | 0,1 | -1,7 | -0,4 | 7,3 |
| 2000 | -0,7 | 10,7 | -0,5 | 8,7 | -0,9 | 14,1 | 0,0 | -0,8 | -0,9 | 14,8 |
| 4000 | -0,8 | 14,4 | -0,5 | 9,1 | -0,9 | 15,4 | -0,1 | 2,7 | -1,2 | 20,2 |
| 90%Coverage | | | | | | | | | | |
| Frequency | IL sample17 | IL sample17 | IL sample24 | IL sample24 | IL sample30 | IL sample30 | IL Carrier 10mm | | IL Special Samples1 | |
| 1000 | 0,1 | -1,9 | -0,2 | 3 | -0,3 | 5,7 | 0,2 | -3,9 | -0,2 | 3,2 |
| 2000 | -0,3 | 5,7 | -0,4 | 6,9 | -0,6 | 9,4 | 0,1 | -2,3 | -0,7 | 10,7 |
| 4000 | -0,3 | 5,8 | -0,5 | 8,7 | -0,7 | 13 | 0,0 | 0,9 | -0,8 | 14,7 |
| 85%Coverage | | | | | | | | | | |
| Frequency | ` | IL sample17 | IL sample24 | IL sample24 | IL sample30 | IL sample30 | IL Carrier 10mm | | IL Special Samples1 | |
| 1000 | 0,2 | -3,7 | -0,1 | 1,4 | -0,2 | 3,2 | 0,2 | -4 | -0,1 | 1,1 |
| 2000 | -0,3 | 4,4 | -0,1 | 1,4 | -0,5 | 7,9 | 0,2 | -3,2 | -0,5 | 9 |
| 4000 | -0,2 | 4,5 | -0,4 | 7,6 | -0,7 | 12,9 | 0,0 | -0,6 | -0,7 | 13,2 |

**Figure 4.34:** IL values according theoretical calculation compared with the IL values obtained from the measurements.

In the Figure 4.34, is a summary of insertion loss of all samples, at all coverage's is shown calculated using sound power from the ISO 3745 and eventually calculating the theoretical insertion loss value and using the direct level difference. While calculating the sound power levels the constants in equation 2.46 are considered to be zero for convenience. As seen, the insertion loss values calculated using the theoretical formula are very less compared to the direct level difference calculated. But they represent correctly where there is a amplification and when there is a reduction. In the case where insertion loss is theoretically calculated, negative values indicate a reduction and a positive value indicates a amplification.

# 5

# Model Building and Prediction

## 5.1 Linear Regression Analysis

Linear regression analysis is carried out to determine whether there is a statistical relationship between between the output variable and the other input variables. In this thesis work, the output variable is 'Insertion Loss (dB)' and the input variables are 'Sound Absorption coefficient', 'Sound Transmission Loss (dB)' and 'Percentage Coverage'. Along with the aim of building a model for prediction of the insertion loss, the magnitude of contribution by each of the control parameters was also one of the important findings to be made.
Minitab software was used to obtain the regression model and to carry out all other statistical analysis. The linear regression analysis model was made by using the insertion loss values mentioned in Figure 4.32 along with the sound absorption coefficient and transmission loss values mentioned in the Figure 4.34. The values for IL and transmission loss were in dB scale. The residual squared or the 'R-squared' for the model is 90.52%. This represents the proportion of the variance for the output variable that is explained by all the input variables. This is pretty significant as it can be also interpreted as the efficiency of the regression model obtained. The model summary as given by the software is shown in the Figure 5.1.

Model Summary

| S | R-sq | R-sq(adj) | R-sq(pred) |
|---|---|---|---|
| 2,22284 | 90,52% | 90,02% | 89,23% |

**Figure 5.1:** Linear Regression Analysis - Model Summary

The equation 5.1 represents the regression equation for Insertion Loss prediction.

$$\text{IL(dB)} = \beta_0 + \beta_1 \cdot (\alpha) + \beta_2 \cdot (TL(dB)) + \beta_3 \cdot (\%\ Coverage) + \epsilon \quad (5.1)$$

The terms $\beta_1$, $\beta_2$ and $\beta_3$ represent the three coefficients corresponding to the sound absorption coefficient, sound transmission loss in dB and percentage of coverage respectively. The constants $\beta_0$ and $\epsilon$ balance the overall equation. The original or

the obtained values for all the coefficients and the constants are not disclosed as it was transferred to Volvo Car Corporation as a proprietary information.

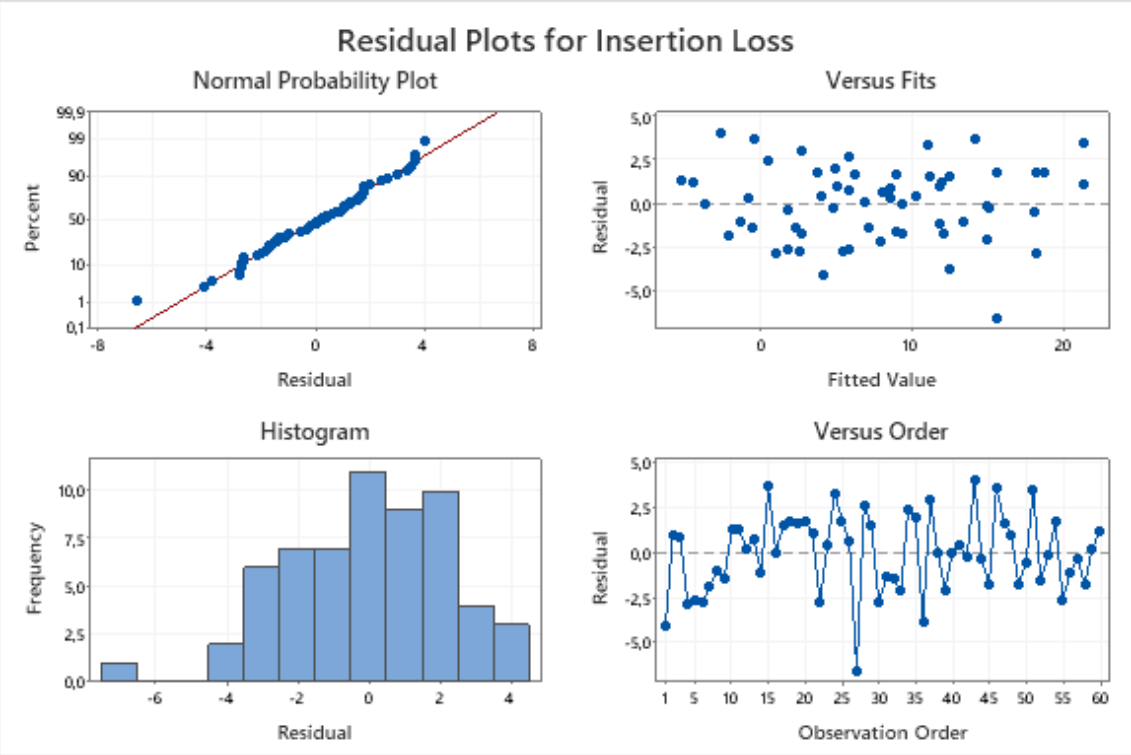


**Figure 5.2:** Residual Plots for the Linear Regression Analysis

The Figure 5.2 shows the residual plots for the model. The most important are the fitted value plot and the histogram. The fitted value plot shows all the data points from the model which are scattered all across the plot. Statistically speaking, the data points in the fitted value plot should be totally randomly distributed with no patterns. This holds good for the obtained fitted value plot which validates that the model is solid and reliable. On the other hand, the histogram shows the normal distribution of the insertion loss values which is one more point for model validation. However, the spacing between the values might be logarithmic as the insertion loss values are in dB scale.

## 5.2 Key Deductions

After deriving a strong and highly accurate prediction model, there were some more important relationships observed between the input and output variables.

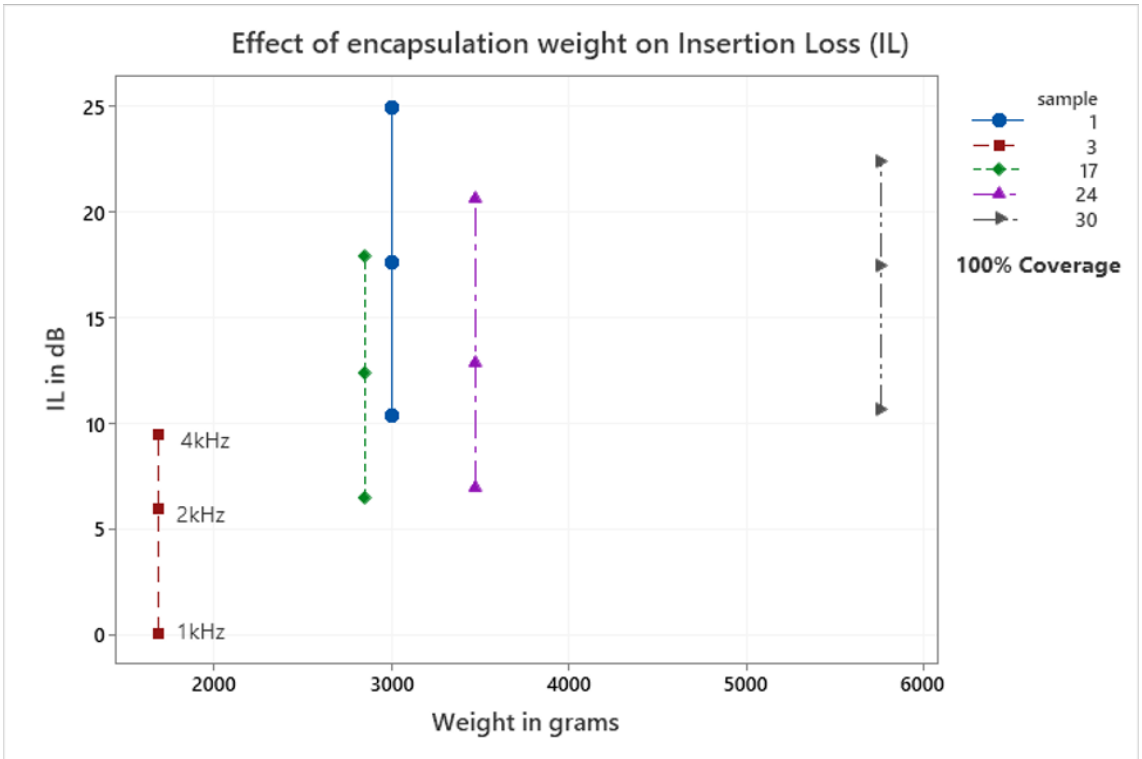


**Figure 5.3:** IL vs Weight

The Figure 5.3 shows the effect of encapsulation weight on the insertion loss. The blue dots are for the special sample 1 which show the highest insertion loss especially at 4 kHz and equal to sample 30 at 2 kHz. But, sample 30 is the heaviest encapsulation and now it is clear that merely increasing the weight does not necessarily increase insertion loss. Special sample 1 shows higher insertion loss than sample 30 despite having lower weight as it does not include any mass layer. It is a bit clear from here that absorption somehow controls the insertion loss even though it is not mixed with a mass layer.

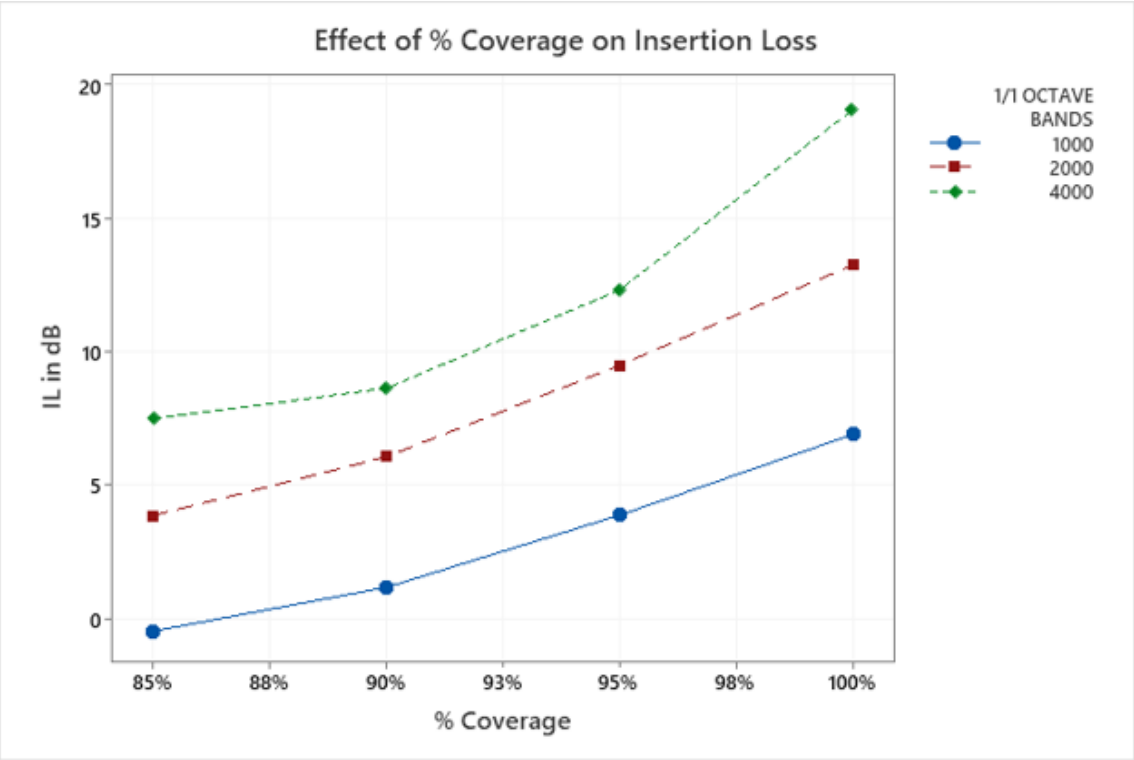


**Figure 5.4:** IL vs Coverage

The Figure 5.4 shows the effect of coverage variation on the insertion loss. It is very clear that the insertion loss increases as the coverage area of the encapsulation increases. This is shown for the 1/1 Octave bands of 1 kHz, 2 kHz and 4 kHz.

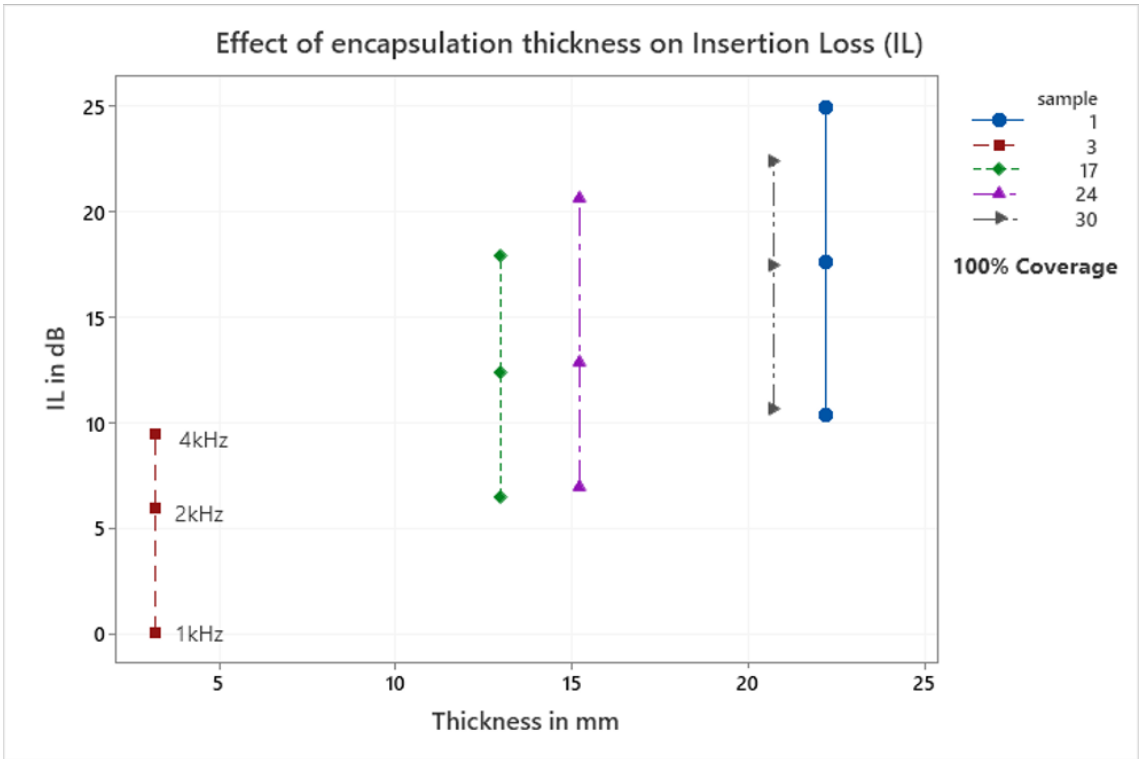


**Figure 5.5:** IL vs Thickness

The Figure 5.5 shows the effect of encapsulation thickness on the insertion loss. It is clear that the insertion loss increases as the thickness of the encapsulation increases. The important thing here is, the special sample - 1 (blue dots) does not have any mass layer but is thicker than sample 30. This increased thickness is due to the two layers of foam which seem to be contributing more to the insertion loss. So, it is essential for the NVH engineers to carefully decide on which layer's thickness to be increased as it could be either of the mass layer or the absorptive layer.

## 5.3 Model Validation

In this section one of the special samples i.e. special sample 2 - which has a combination of two different types of foam layers and carrier layer has been used for model validation. Using the empirical formula the insertion loss values at three different 1/1 octave band frequencies, is predicted for three different coverages - 100%, 95% and 90%. It was finally measured on the EDU by building its encapsulation and comparing its measured and predicted values.

We can see that the prediction model works well and is somehow an under-estimator which is good in a way. The maximum deviation is ± 6 dB approximately from the original value, which is quite good considering the methodology adopted. Figure 5.6 shows a summary of the results.

| Special Sample 2: 9mm Nitto (EPDM foam) + 10mm Sundquist foam + 3.2mm Carrier | | | | |
|---|---|---|---|---|
| %Coverage | Frequency in Hz(1/1 octave band) | Measured IL in dB | Predicted IL in dB | Error in dB ± |
| 100% | 1k | 10,30 | 8,18 | 2,12 |
| | 2k | 15,10 | 13,99 | 1,11 |
| | 4k | 23,60 | 17,78 | 5,82 |
| | | | | |
| 95% | 1k | 6,90 | 5,03 | 1,87 |
| | 2k | 13,00 | 10,84 | 2,16 |
| | 4k | 15,10 | 14,63 | 0,47 |
| | | | | |
| 90% | 1k | 1,90 | 1,88 | 0,02 |
| | 2k | 10,50 | 7,69 | 2,81 |
| | 4k | 14,40 | 11,48 | 2,92 |

**Figure 5.6:** Measured Vs predicted Insertion Loss values for Special Sample 2

# 6
# Conclusion

Based on the above discussion of results and complete experimental work, we can conclude by first addressing the aim of the topic. It is possible to build a empirical model using absorption coefficient, transmission loss and percentage coverage as estimation parameters to predict insertion loss of a encapsulation. Figure 6.1 shows the dependency of insertion loss (IL) on these individual parameters as a summary. It can be said that coverage plays an important role in the encapsulation design and based on the work any coverage below 85% may not be very effective, as it almost matches with the without encapsulation data. Also as coverage increases as seen in figure 5.4 from section 5 from model building, the insertion loss increases in all frequency bands. Transmission loss and absorption coefficient have a direct effect on the insertion loss however absorption coefficient is major contributor. As the entire work has been a experimental approach there are uncertainties in measurement and hence performing repeatability study in every aspect of the testing has helped in mitigating errors and produce reliable results.

Insertion loss also increases if the weight of the encapsulation increases refer figure 5.3 from section 5 on model building, but based on the results from special sample 1 which has no mass layer, it can be said that it is not mandatory to have a heavy encapsulation to get good IL. An encapsulation with right combination of materials can also give a good insertion loss. Thickness of the encapsulation has a direct effect on the insertion loss and it increases if the thickness of the encapsulation increases refer figure 5.5 from section 5 on model building , however the thickness can be of a absorption layer or a mass layer.

To conclude finally it can be said that depending on the frequency range of interest and practical constraints, the control parameters - transmission loss, absorption coefficient and coverage can be tuned using our prediction tool to give an optimized encapsulation. And be a reference for future design engineers to estimate the IL performance.

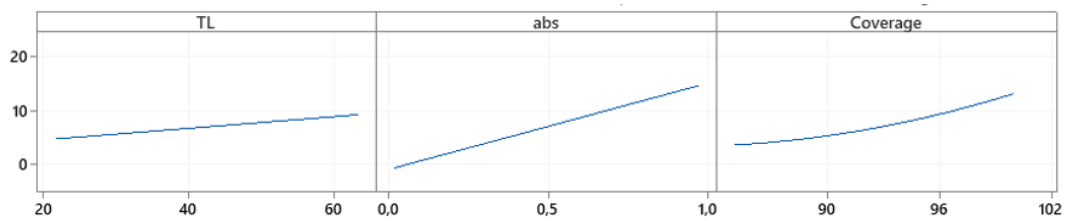


**Figure 6.1:** Measured Vs predicted Insertion Loss values for one of the samples

# 7

# Future Scope for Study

Based on the conclusion of the work, below are listed some future scope activities which could bring more insights into the topic :-

- More material configurations lighter and efficient could be investigated along with more coverage variation.
- A new model could be built to check the effects below 85% coverage.
- Similar study could be performed on actual test rig to understand the limitations and get an idea of how the encapsulations behave in operating conditions.
- CAE study can be performed by setting up model with sufficient information of material BIOT parameters and to estimate the effect of radiated levels from the encapsulation using boundary element method (BEM) or finite element method (FEM).
- A tool for prediction could be built with more data and study for design engineers to get an estimation of performance.

# Bibliography


[1] Frisk, D. (2018) A Chalmers University of Technology Master's thesis template for LaTeX. Unpublished.

[2] PCB Data sheet `https://www.pcb.com/products?m=378B02`

[3] David Lennström (2014) Volvo Cars, HF Source Characterization

[4] NVH Design Guideline for ENCAPSULATIONS - Proprietary Information, Volvo Car Corporation.

[5] Driver `http://www.bmsspeakers.com/index.php?id=bms_4590_coaxial`

[6] Siemens Webinar on Troubleshooting torsional vibration challenges with rotating machinery

[7] Product Data - Brüel Kjær Sound Vibration Measurement A/S, Denmark (2019),
Impedance Tube Kit (50 Hz – 6.4 kHz) Type 4206
Impedance Tube Kit (100 Hz – 3.2 kHz) Type 4206-A
Transmission Loss Tube Kit (50 Hz – 6.4 kHz) Type 4206-T.

[8] ISO 10354-2 - Acoustics - Determination of sound absorption coefficient and impedance in impedance tubes (November 1998).

[9] Measurement of the Acoustic Absorption Coefficient by Impedance Tube - Research Papers Faculty of Materials Science and Technology in Trnava.

[10] What is Design of Experiments (DOE)? - American Society for Quality. https://asq.org/quality-resources/design-of-experiments

[11] Optimization of the Polishing Efficiency and Torque by Using Taguchi Method and ANOVA in Robotic Polishing - Imran Mohsin, Kai He, Zheng Li, Feifei Zhang and Ruxu Du.

[12] Design of Experiments (DOE) Using the Taguchi Approach - Nutek, Inc. Bloomfield Hills, MI. USA. Tel: 1-248-540-4827,Support@Nutek-us.com, www.Nutek-us.com.

[13] Taguchi Orthogonal Arrays - John M. Cimbala, Penn State University, 2014.

[14] Determining Sound Absorbing and Transmission Loss Properties of Rubbers Used in Automotive Industries - IConTES 2018, International Conference on Technology, Engineering and Science - Osman IPEK, Murat KORU, Orhan SERCE, Huseyin KARABULUT and Mehtap HIDIROGLU.

[15] Holes prevent sound from passing through plate - physics world, Hamish Johnston, Sep 2008.

URL:https://physicsworld.com/a/holes-prevent-sound-from-passing-through-plate/

[16] D.W. Herrin, PhD, PE, University of Kentucky, Mechanical Engineering Department.
[17] Martin Wolkesson (2013), Master Thesis, Evaluation of impedance tube methods - A two microphone in-situ method for road surfaces and the three microphone transfer function method for porous materials.
[18] Impedance Tube Measurements, Vibroacoustics consortium (June 11, 2020), University of Kentucky.
[19] Sound intensity mapping of 2 stroke Engine by using hemispherical surface coordinate arrangement, M S M Sani, et al 2019, IOP conference, Ser.: Mater. Sci. Eng.506 012060.
[20] Technical Acoustics 1, Wolfgang Kropp (2015), Propagation and radiation of strucutre borne sound.
[21] Audio Technology and acoustics, VTA137, Absorbers(Lecture Notes), Astrid Pieringer.
[22] Audio Technology and acoustics, VTA137, Sound insulation(Lecture Notes), Astrid Pieringer.
[23] Audio Technology and acoustics, VTA137, Basic acoustic concepts 3(Lecture Notes), Astrid Pieringer and Jens Ahrens.
[24] Audio Technology and acoustics, VTA137, Basic acoustic concepts 2(Lecture Notes), Astrid Pieringer and Jens Ahrens.
[25] Electric motor encapsulation design for improved NVH: a CAE-based approach (2019) Federico Di Marco, Roberto D'Amico, Francesca Ronzio Autonuem Management AG Schlosstalstrasse 43, Winterthur 8406, Switzerland.
[26] Multiphysics Modelling to Simulate the Noise of an Automotive Electric Motor, Jean-Baptiste DUPONT and Pascal BOUVET, 2012, e-ISSN: 2688-3627.
[27] Master Thesis Work: Simulation and optimization of airborne radiated sound from electric machines, Mohit Singhal, 2020, RWTH Aachen, 390092.
[28] Design Guidelines, Fibre Encapsulation, Proprietary information of Volvo cars corporation.
[29] International Standard, ISO 3745:2012(E), Acoustics — Determination of sound power levels and sound energy levels of noise sources using sound pressure — Precision methods for anechoic rooms and hemi-anechoic rooms.

# A

# Appendix - Data Sheets

Appendices contain material that is too detailed to include in the main report, such as long mathematical derivations or calculations, detailed technical drawings, or tables of raw data. ... each appendix must be referred to by number (or letter) at the relevant point in the text

Data sheet PSN 152

# AcuBlok

## Description

A reinforced-foil faced, robust and hard-wearing, high-density noise barrier material. It is able to withstand the normal daily demands of the working environment.

## Applications

**Noise control measures in:**

- *Building*
- *Engineering*
- *Factory*
- *Automotive*

## Availability

- *Sheets*
- *Pads*
- *Rolls*
- *Bonded to other materials e.g. foam*
- *Self-adhesive*

## Composition

### Facing

- *Foil - aluminium*
- *Reinforcing - bi-directional glass-fibre - 16/100 mm (MD), 16/100 mm (XD)*

### Noise Barrier

- *High-performance mineralised vinyl (pvc)*

## Typical properties

### Facing

**Thickness** ..... 12.7 µm

### Noise-barrier

**Weight** .....5.0 ± 10 % kg

**Thickness** .....2.5 ± 10 % mm

**Width** .....1000 ± 10 % mm

**Roll length** .....50 m

**Colour** .....charcoal

**Fire rating (ISO 3795)** .....Self-extinguishing

### Noise-barrier

**Tensile strength (min)**

Length.....4.0 $Nmm^{-2}$

Width .....4.0 $Nmm^{-2}$

**Acoustic performance**

***Typical noise-barrier transmission loss***

| Frequency - Hz | 125 | 250 | 500 | 1000 | 2000 | 4000 |
|---|---|---|---|---|---|---|
| Transmission loss - dB | 18 | 17.9 | 22.4 | 28.4 | 34.1 | 38.6 |

***Typical noise-barrier weighted sound reduction index (BS5821:1984)***

.....27 dB

**Note**

Product performance can be affected by adverse conditions e.g. contamination. Contact Pritex for advice.

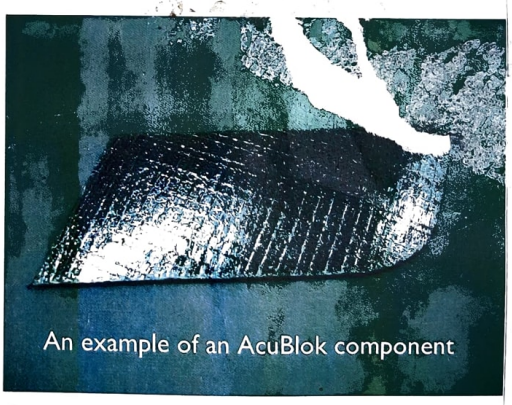

An example of an AcuBlok component

The company reserves the right to alter specifications

Authorised.....

**Pritex Limited**
Wellington Somerset TA21 8NN England
TELEPHONE +44 (0)1823 664271 FACSIMILE +44 (0)1823 660023
www.pritex.co.uk enquiries@pritex.co.uk

Issue.....1..... Date.....24/11/05

**Figure A.1:** Acublok - Mass Layer.

## Applications


Door mirror


Window dam rubber


Rear combination lamp


Outdoor unit of air-conditioners


Car air-conditioners


Housing materials


Construction parts


Refrigerators

## Features

- Exceptionally good heat resistance, weather resistance, chemical resistance (acid, alkaline), etc. for general-purpose rubber material are made possible by the use of EPDM rubber as the main ingredient.
- Foaming control range of 3-30 fold expansion achieved by advanced foaming process.
- Variety of cell structures, from closed and semi-closed cell to open cell, are made available by Nitto Denko's extensive foaming process technology.

### Foaming control and adhesive technology

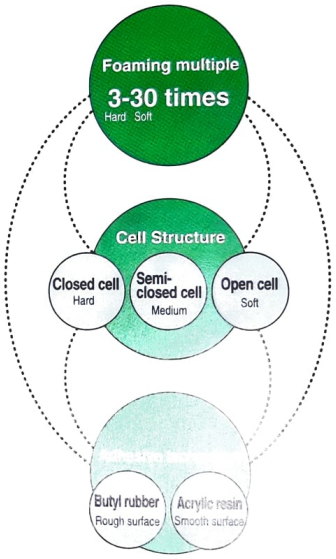


Nitto Denko's advanced foaming and adhesive technology permits diverse combinations.

## Product List

| Product name | Color | Adhesive | Cell structure | Foam Properties | | Standard size | | |
|---|---|---|---|---|---|---|---|---|
| | | | | Specific gravity | 25% Compresive hardness(N/cm²) | Thickness(mm) | Width(mm) | Length(m) |
| No.6800 | Black | —— | Closed cell | 0.12 | 1.8~2.0 | 2~14 | 900 | 2 |
| No.6801 | Black | Acrylic resin | | | | | | |
| No.680 | Black | Butyl rubber | | | | | | |
| No.685 | Black | —— | Semi-closed cell | 0.14 | 0.4~0.5 | 3~35 | | |
| No.686 | Black | Acrylic resin | | | | | | |
| No.687 | Black | Butyl rubber | | | | | | |
| No.686G | Gray | Acrylic resin | | 0.15 | | 3~30 | | |
| No.686H | White | Acrylic resin | | 0.14 | | | | |
| EE-1000 | Black | —— | | 0.10 | 0.2~0.3 | 3~35 | | |
| EE-1010 | Black | Acrylic resin | | | | | | |
| EE-1040 | Black | Butyl rubber | | | | | | |
| EE-700FR* | Black | —— | | 0.11 | | 3~20 | | |
| EE-710FR* | Black | Acrylic resin | | | | | | |

*Flame-retardant

## Construction

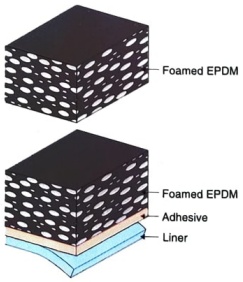


**Figure A.2:** Nitto - Foam.

PCB PIEZOTRONICS
AN MTS COMPANY

MODEL 378B02

# 1/2" PREPOLARIZED FREE-FIELD MICROPHONE

- Sensitivity: 50 mV/Pa (± 1.5 dB)
- Frequency: 3.75 Hz – 20 kHz (± 2 dB)
- Dynamic range: 15.5 dB(A) – 146 dB

## TYPICAL APPLICATIONS

- Precision sound level measurements
- Transfer path analysis
- Environmental noise monitoring
- White goods tests in anechoic chambers

## STANDARDS COMPLIANCE

- IEC 61094-4 WS2F compliant, and designed to be used in an IEC 61672 Class 1 compliant system for sound level meter use
- Calibration reference microphone traceable to NIST, PTB or DFM National Labs
- PCB calibration service accredited to ISO 17025, ANSI-Z540.3 by A2LA or ILAC

## USE OF MODEL 378B02

Model 378B02 is a 1/2 in (12 mm) prepolarized microphone and preamplifier combination for applications where the audible range frequencies need to be accurately measured in areas free of reflective surfaces. The high sensitivity allows for low amplitudes to 15.5 dB(A) to be tested. The 378B02 is suited for a wide variety of auto, aerospace, and R & D applications making it one of the best selling microphones.

Acoustic pressure waves may be altered by objects in the sound field including the microphone itself. The 378B02 corrects for its own presence, providing more accurate measurements within a free-field.

## POLARIZATION VOLTAGE – ICP® (0V) PREPOLARIZED

PCB® is the inventor of ICP® sensor power technology. All manufacturers of IEC 61094-4 compliant prepolarized (0V) microphones use the technology that PCB developed. Prepolarized microphones operate on 2-20 mA constant current supply and use coaxial cables resulting in significant per channel cost savings over the PCB 200V models. Other ICP® compatible sensors such as accelerometers, force, strain, and pressure sensors use the same power supplies and cables as prepolarized microphones, further reducing set-up time and initial investment costs.

pcb.com | 1 800 828 8840

**Figure A.3:** Microphone Datasheet [2]

## PCB® QUALITY COMMITMENT

PCB is uniquely equipped with a state of the art, CNC machining facility, allowing control over quality, pricing, and delivery. Investments in clean rooms, anechoic, and environmental test chambers, combined with our rigorous testing and aging process, ensures our products will survive in demanding environmental conditions. PCB has the industry's best 5-year warranty with a "Total Customer Satisfaction" policy.

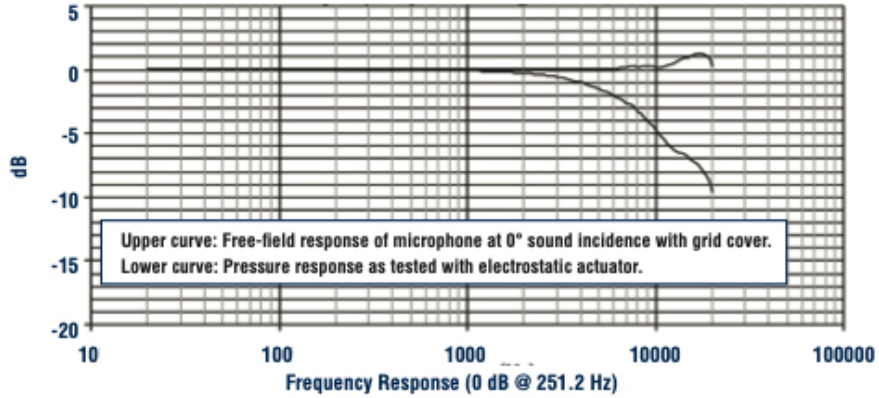


| 378B02 PREPOLARIZED FREE-FIELD MICROPHONE SYSTEM | | |
|---|---|---|
| Nominal Microphone Diameter | in (mm) | 1/2 (12) |
| Sensitivity at 250 Hz (± 1.5 dB) | mV/Pa (dB re 1 V/Pa) | 50 (-26) |
| Frequency Range (± 2 dB) | Hz | 3.75 - 20,000 |
| Frequency Range (± 1 dB) | Hz | 7 - 10,000 |
| Cartridge Thermal Noise (Microphone) | dB[A] re 20 µPa | 15 |
| Inherent Noise with 426E01 Preamp | dB[A] re 20 µPa | 15.5 |
| Harmonic Distortion Limit: 3% | dB re 20 µPa | 147 |
| Distortion Limit with 426E01 Preamp | dB re 20 µPa | 137 |
| **Environmental Specifications** | | |
| Operating Temperature Range Microphone | °F (°C) | -40 to +302 (-40 to +150) |
| Operating Temp. with 426E01 Preamp | °F (°C) | -40 to +176 (-40 to +80) |
| Operating Temp. with HT426E01 Preamp | °F (°C) | -40 to +257 (-40 to +125) |
| **Electrical Specifications** | | |
| Polarization Voltage | V | 0 |
| Constant Current Excitation | mA | 2 - 20 |
| **Physical Specifications** | | |
| Size (Diameter x Length with Grid) | in (mm) | 0.52 x 3.62 (13.2 x 91.9) |
| Connector | Coaxial | BNC Jack |

* all specifications typical unless otherwise noted

## OPTIONAL ACCESSORIES

- **426A10** – 1/2" preamplifier with 20 Hz high pass filter
- **426A11** – 1/2" preamplifier with gain and filter switches
- **HT426E01** – 1/2" preamplifier, high temperature (125° C)
- **079A06** – 1/2" microphone windscreen
- **079A11** – 1/2" microphone holder
- **079A15** – tripod microphone stand with boom arm
- **079B16** – miniature microphone stand
- **079A18** – clamp on flexible extension arm
- **079B21** – 1/2" nose cone
- **079C23** – microphone holder with swivel mount
- **CAL200** – handheld calibrator
- **ACS-63** – microphone system calibration

**Figure A.4:** Microphone Frequency Response [2]

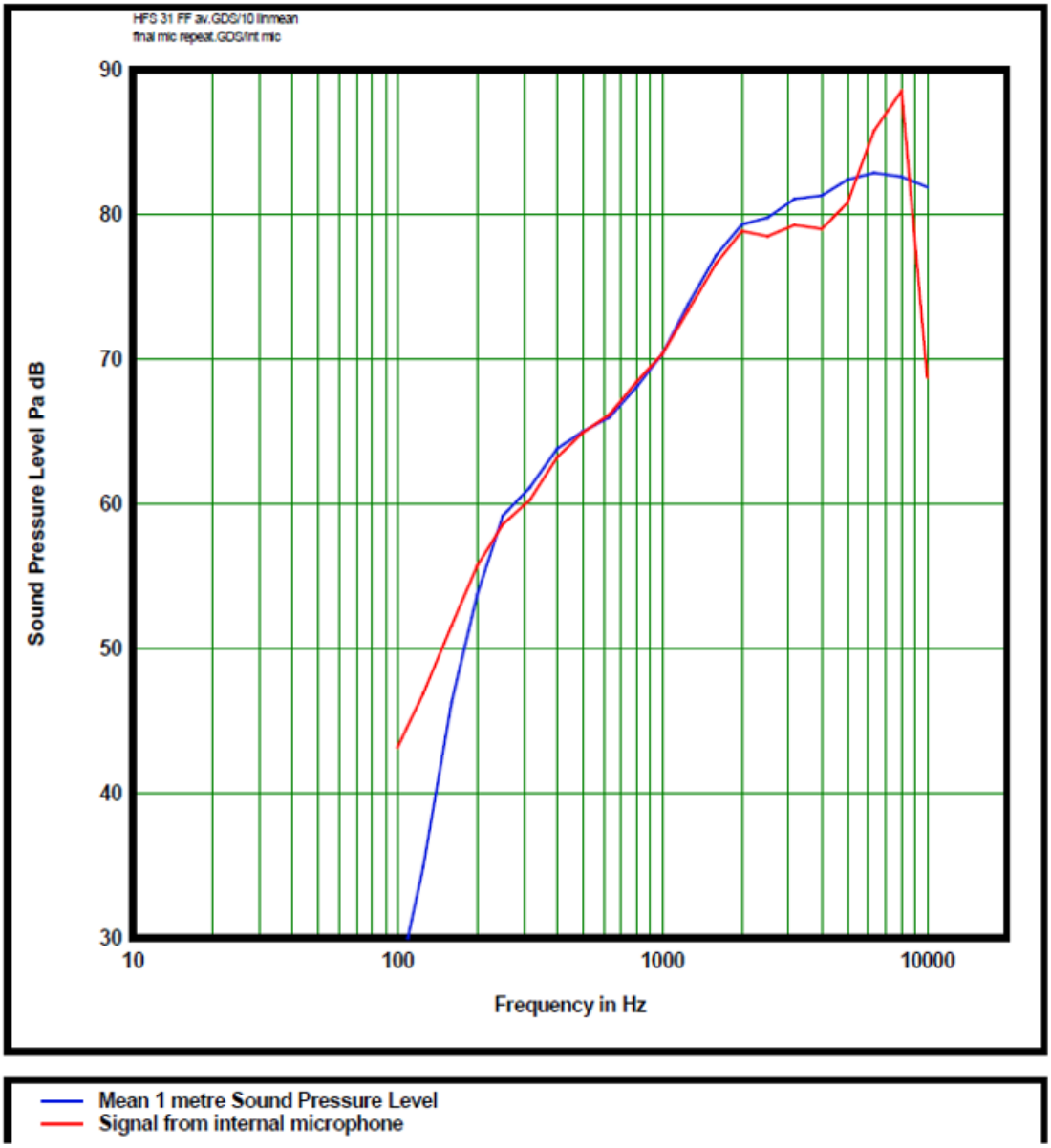


**Figure A.5:** Driver Characterization - Spectrum of source [3]

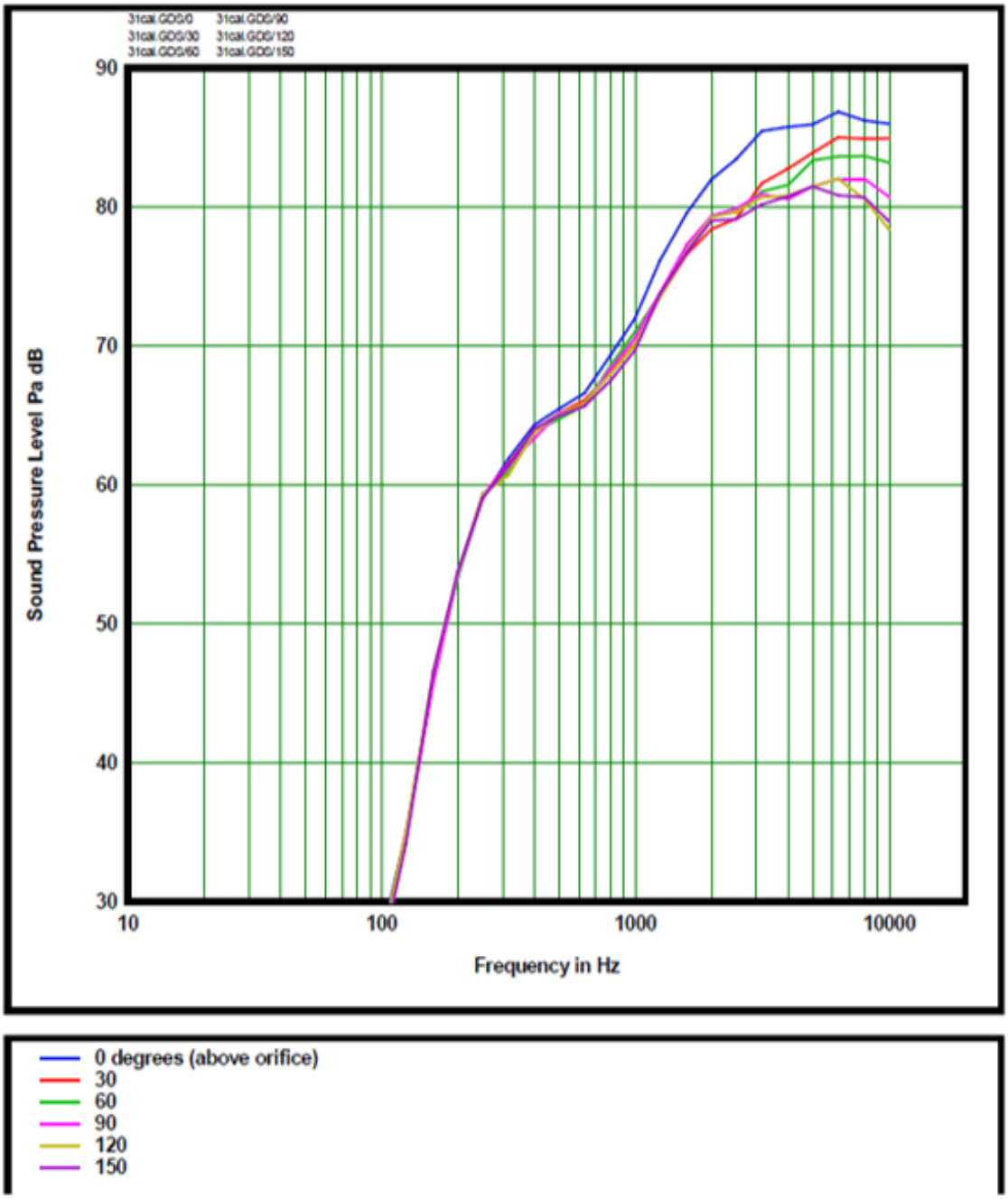


**Figure A.6:** Driver Characterization - Directivity of source [3]

## 4590 / 4590P

2" Coaxial compression driver

## 2" Coaxial Compression Drivers

BMS

**Features:**

- Extended bandwidth (300 - 22000 Hz)
- Point source sound reproduction
- Excellent phase coherence
- With two subsystems in one, each driver covers a smaller frequency range for increased power handling, high dynamic and extremely low distortion
- Perfect time alignment without problems of multi-source interference

In a conventional full range compression driver the phase plug must be located extremely close to the diaphragm, excursion of the diaphragm is limited and middle frequency performance is compromised. A typical 2" dome compression driver has a limited high frequency response. Over 8 kHz the dome diaphragm breaks up causing resonance and harsh, metallic sound.

The BMS annular midrange diaphragm covers the frequency range between 400 and 7000 Hz with a smooth, linear response. The large diaphragm excursion of max. +/-0.8 mm results in high output and increased power handling up to 1300 W peak. The ultra light annular diaphragm for the high range offers exceptional transient response with very high efficiency from 6 to 22 kHz.

Coaxial Compression Drivers

## SPECIFICATIONS

| | |
|---|---|
| Throat diameter | 2" (50.8 mm) |
| Nominal impedance | 8 or 16 Ohm |
| Power capacity | |
| Middle range (AES) | 150 W AES above 400 Hz |
| peak | 1000 W peak above 500 Hz |
| High range (AES) | 80 W |
| peak | 450 W |
| Sensitivity 1W/1m | 118 dB on 2242 Horn |
| Frequency range (Hz) | 300 - 22000 |
| Recommended crossover | 300 Hz |
| Middle frequency range | 300 - 7000 Hz |
| High frequency range | 6000 - 22000 Hz |
| Middle/High crossover | 6300Hz |
| Voice coil high-range | 1.75" (44.4 mm) |
| Voice coil mid-range | 3.5" (90 mm) |
| Magnet material | Ferrite |
| Flux density (Tesla) | 1.95 (mid), 2.1 (high) |
| Efficency | 35% (300 - 5000 Hz) |
| Voice coil material | Copper Clad Aluminum |
| | (2Layers in and outside of the VC) |
| Voice coil former | Kapton™ |
| Diaphragm material | Polyester |
| **Mounting information** | |
| Overall Diameter | 182 mm (+/- 3 mm) |
| Depth | 129 mm |
| Net weight | 9 kg |
| 4x M6 holes, 90° on | 101.6 mm, 4" diameter |

BMS4590, 90°x60° Horn, 1W/1m, 4V RMS

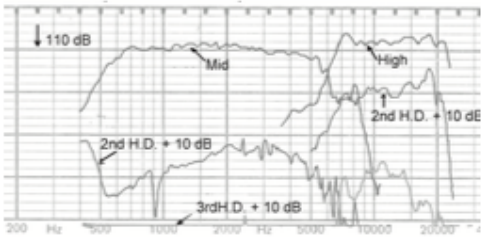


BMS4590, 90°x60° Horn, 1W/1m, 4V RMS

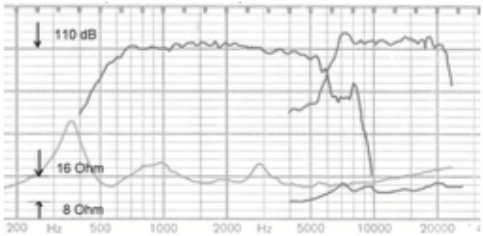


BMS 4590P, including passive crossover, SPL 1W / 1m

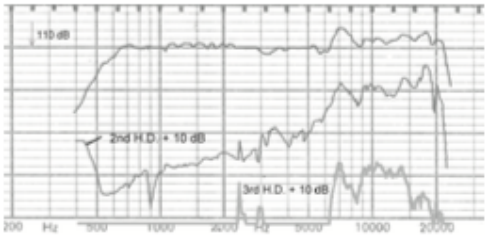


**Figure A.7:** Driver [5]